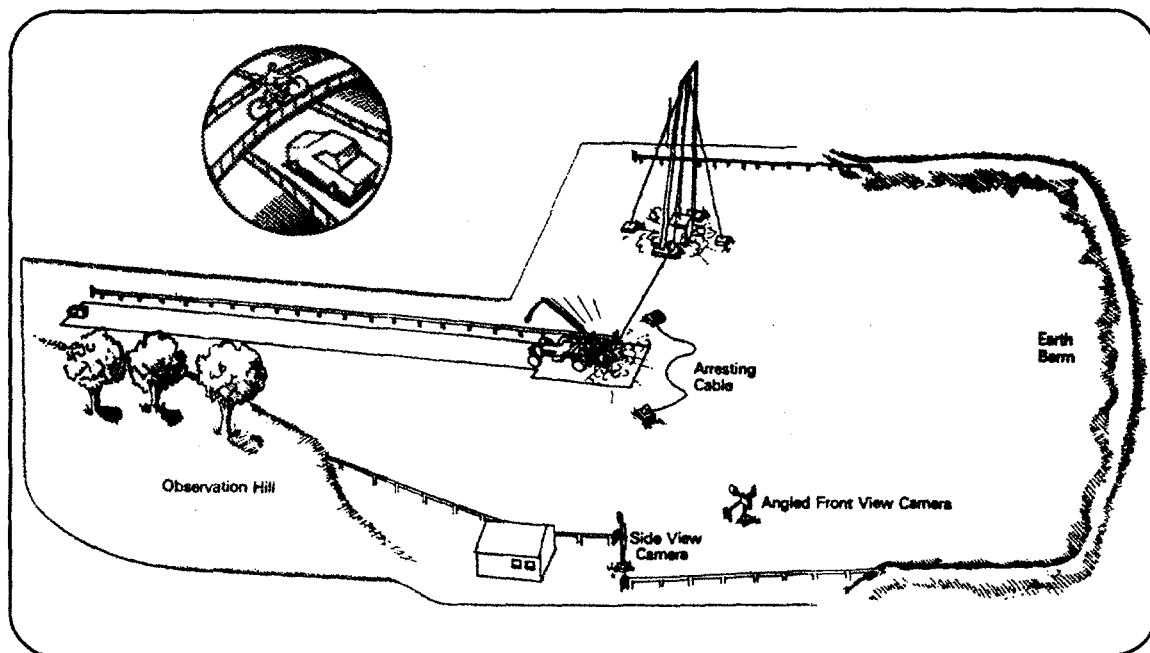

Dynamic Testing of Steel W-Beam Guardrail Elements Using the FOIL 2000P Pendulum: FOIL Test Numbers 00P007 Through 00P017

PUBLICATION NO. FHWA-RD-01-045

MARCH 2001



FOIL



U.S. Department of Transportation
Federal Highway Administration

Research, Development, and Technology
Turner-Fairbank Highway Research Center
6300 Georgetown Pike
McLean, VA 22101-2296

FOREWORD

This report documents the results from 10 pendulum crash tests between the FOIL 2000P pendulum and a four-post w-beam guardrail semi-rigidly anchored at both ends. The Federal Highway Administration's (FHWA) Federal Outdoor Impact Laboratory (FOIL) conducted these tests as part of an ongoing research project to collect baseline dynamic properties of a steel w-beam guardrail. The data from these crash tests may be used to develop a test procedure and a minimum impact test for guardrail beam elements fabricated using composite materials. The developed impact test would not serve as a certification test for the guardrail design but rather as a starting point for roadside safety hardware designers. The dynamic test could be used to show the prototype rail's ability to withstand a minimal energy level before proceeding to the final design. The nominal test speeds for these tests varied and ranged from 15 km/h to 40 km/h. The nominal weight of the new FOIL pendulum mass was 2000 kg (actual mass was 2032 kg).

This report (FHWA-RD-01-045) contains test data, photographs, and a data summary of the test results.

This report will be of interest to all State departments of transportation; FHWA headquarters; region and division personnel; and highway safety researchers interested in the crashworthiness of roadside safety hardware.



Michael Trentacoste, Director
Office of Safety and Traffic
Operations Research and Development

NOTICE

This document is disseminated under the sponsorship of the Department of Transportation in the interest of information exchange. The United States Government assumes no liability for its contents or use thereof. This report does not constitute a standard, specification, or regulation.

The United States Government does not endorse products or manufacturers. Trade and manufacturers' names appear in this report only because they are considered essential to the object of the document.

1. Report No. FHWA-RD-01-045	2. Government Accession No.	3. Recipient's Catalog No.	
4. Title and Subtitle DYNAMIC TESTING OF STEEL W-BEAM GUARDRAIL ELEMENTS USING THE FOIL 2000P PENDULUM: FOIL TEST NUMBERS 00P007 THROUGH 00P017		5. Report Date	
		6. Performing Organization Code	
7. Author(s) Christopher M. Brown		8. Performing Organization Report No.	
9. Performing Organization Name and Address MiTech Incorporated 8484 Georgia Avenue, Suite 950 Silver Spring, MD 20910		10. Work Unit No. (TRAIS) 3A5f3142	
		11. Contract or Grant No. DTFH61-99-F-00104	
12. Sponsoring Agency Name and Address Office of Safety and Traffic Operations R&D Federal Highway Administration 6300 Georgetown Pike McLean, VA 22101-2296		13. Type of Report and Period Covered Final Report, February 2000 to April 2000	
		14. Sponsoring Agency Code	
15. Supplementary Notes - Contracting Officer's Technical Representative (COTR) - Charlie McDevitt			
16. Abstract This report contains the test procedures followed and test results from 10 crash tests between the FOIL 2000P pendulum and a four-post steel w-beam guardrail. The tests were conducted at the Federal Highway Administration's (FHWA) Federal Outdoor Impact Laboratory (FOIL) located at the Turner-Fairbank Highway Research Center (TFHRC) in McLean, Virginia. The target test speeds for these tests ranged from 15 km/h to 40 km/h. The target test inertial weight of the pendulum was 2000 kg (actual was 2032 kg). The 2000P pendulum was configured with a rigid nose assembled using an oak nose-piece mounted to a steel frame. The four-post steel w-beam guardrail was semi-rigidly anchored using standard 20-mm guardrail wire-rope anchor cables. The two interior posts were standard G4(1s) steel strong posts. The tests were conducted to provide baseline dynamic material properties of w-beam guardrail. The data will be used to establish a possible test procedure and minimal test requirement for prototype guardrail beam elements fabricated from composite materials. The tests also were conducted to ensure that the new concrete and steel pendulum mass and its associated rigging and other accessories were structurally sound and practical. The results indicate that the new pendulum was both structurally sound and compatible with the pendulum facility. The test data provided a baseline response of the steel w-beam. The steel w-beam splice failed at a test speed of 40 km/h. The 35-km/h 2000P pendulum impact test could serve as a minimum energy level that a composite rail prototype ought to withstand before being considered as an alternative.			
17. Key Words 2000P pendulum, acceleration, FOIL, w-beam guardrail, composite materials, strain gauge, energy, dynamic material properties.		18. Distribution Statement No restrictions. This document is available to the public through the National Technical Information Service, Springfield, VA 22161.	
19. Security Classif (of this report) Unclassified	20. Security Classif. (of this page) Unclassified	21. No. of Pages 93	22. Price

SI* (MODERN METRIC) CONVERSION FACTORS

APPROXIMATE CONVERSIONS TO SI UNITS

Symbol	When You Know	Multiply By	To Find	Symbol
LENGTH				
in	inches	25.4	millimeters	mm
ft	feet	0.305	meters	m
yd	yards	0.914	meters	m
mi	miles	1.61	kilometers	km
AREA				
in ²	square inches	645.2	square millimeters	mm ²
ft ²	square feet	0.093	square meters	m ²
yd ²	square yards	0.836	square meters	m ²
ac	acres	0.405	hectares	ha
mi ²	square miles	2.59	square kilometers	km ²
VOLUME				
fl oz	fluid ounces	29.57	milliliters	mL
gal	gallons	3.785	liters	L
ft ³	cubic feet	0.028	cubic meters	m ³
yd ³	cubic yards	0.765	cubic meters	m ³
MASS				
oz	ounces	28.35	grams	g
lb	pounds	0.454	kilograms	kg
T	short tons (2000 lb)	0.907	megagrams (or "metric ton")	Mg (or "t")
TEMPERATURE (exact)				
°F	Fahrenheit temperature	5(F-32)/9 or (F-32)/1.8	Celcius temperature	°C
ILLUMINATION				
fc	foot-candles	10.76	lux	lx
fl	foot-Lamberts	3.426	candela/m ²	cd/m ²
FORCE and PRESSURE or STRESS				
lbf	poundforce	4.45	newtons	N
lbf/in ²	poundforce per square inch	6.89	kilopascals	kPa

APPROXIMATE CONVERSIONS FROM SI UNITS

Symbol	When You Know	Multiply By	To Find	Symbol
LENGTH				
mm	millimeters	0.039	inches	in
m	meters	3.28	feet	ft
m	meters	1.09	yards	yd
km	kilometers	0.621	miles	mi
AREA				
mm ²	square millimeters	0.0016	square inches	in ²
m ²	square meters	10.764	square feet	ft ²
m ²	square meters	1.195	square yards	yd ²
ha	hectares	2.47	acres	ac
km ²	square kilometers	0.386	square miles	mi ²
VOLUME				
mL	milliliters	0.034	fluid ounces	fl oz
L	liters	0.264	gallons	gal
m ³	cubic meters	35.71	cubic feet	ft ³
m ³	cubic meters	1.307	cubic yards	yd ³
MASS				
g	grams	0.035	ounces	oz
kg	kilograms	2.202	pounds	lb
Mg	megagrams (or "metric ton")	1.103	short tons (2000 lb)	T
TEMPERATURE (exact)				
°C	Celcius temperature	1.8C + 32	Fahrenheit temperature	°F
ILLUMINATION				
lx	lux	0.0929	foot-candles	fc
cd/m ²	candela/m ²	0.2919	foot-Lamberts	fl
FORCE and PRESSURE or STRESS				
N	newtons	0.225	poundforce	lbf
kPa	kilopascals	0.145	poundforce per square inch	lbf/in ²

* SI is the symbol for the International System of Units. Appropriate rounding should be made to comply with Section 4 of ASTM E380.

Table of Contents

BACKGROUND	1
SCOPE	2
TEST MATRIX	2
PENDULUM	4
TEST ARTICLES	5
INSTRUMENTATION AND DATA ACQUISITION	10
Speed trap	10
Accelerometers	10
Strain gauges	13
High-speed photography	13
DATA ANALYSIS	16
Speed trap	16
Accelerometers and strain gauges	16
High-speed photography	17
RESULTS	17
Tests 00P007 through 00P010	18
Tests 00P011, 00P012, 00P014, and 00P015	18
Tests 00P016 and 00P017.	19
CONCLUSIONS	21
APPENDIX A: POST-TEST PHOTOGRAPHS FROM EACH PENDULUM TEST	23
APPENDIX B: DATA PLOTS OF DATA OBTAINED FROM PENDULUM ACCELEROMETERS	42
REFERENCES	87

List of Figures

<u>Figure</u>	<u>Page</u>
1. Sketch of the FOIL 2000-kg pendulum (nose assembly and ballast not shown)	6
2. Photographs of new pendulum mass with rigid nose	7
3. Sketch of pendulum nose	8
4. Pre-test photographs of a typical guardrail for tests 00P007 through 00P015.	11
5. Pre-test photographs of a typical guardrail for tests 00P016 and 00P017	12
6. Sketch of w-beam specimen and strain gauge locations	14
7. Plan view of test layout and high-speed camera locations	15
8. Post-test photographs, test 00P007	23
9. Post-test photographs, test 00P007 (continued)	24
10. Post-test photographs, test 00P008	25
11. Post-test photographs, test 00P008 (continued)	26
12. Post-test photographs, test 00P009	27
13. Post-test photographs, test 00P009 (continued)	28
14. Post-test photographs, test 00P011	29
15. Post-test photographs, test 00P011 (continued)	30
16. Post-test photographs, test 00P012	31
17. Post-test photographs, test 00P012 (continued)	32
18. Post-test photographs, test 00P014	33
19. Post-test photographs, test 00P014 (continued)	34
20. Post-test photographs, test 00P015	35
21. Post-test photographs, test 00P015 (continued)	36
22. Post-test photographs, test 00P016	37
23. Post-test photographs, test 00P016 (continued)	38
24. Post-test photographs, test 00P017	39
25. Post-test photographs, test 00P017 (continued)	40
26. Additional post-test photographs, test 00P017	41
27. Acceleration vs. time (class 60 data), test 00P007	42
28. Velocity vs. time, test 00P007	43
29. Displacement vs. time, test 00P007	44
30. Force vs. displacement, test 00P007	45
31. Energy vs. displacement, test 00P007	46
32. Acceleration vs. time (class 60 data), test 00P008	47
33. Velocity vs. time, test 00P008	48
34. Displacement vs. time, test 00P008	49
35. Force vs. displacement, test 00P008	50
36. Energy vs. displacement, test 00P008	51
37. Acceleration vs. time (class 60 data), test 00P010	52
38. Velocity vs. time, test 00P010	53

List of Tables

<u>Table</u>	<u>Page</u>
1. Energy comparison between 820C and 2000P pendulums	3
2. Test matrix for 2000-kg pendulum testing of a four-post w-beam guardrail	4
3. Camera configuration and placement	13
4. Summary of pendulum testing of four-post w-beam rail . .	20

BACKGROUND

The Federal Highway Administration (FHWA) has been evaluating the viability of using advanced composite materials in lieu of conventional materials for applications in the construction of roadside safety hardware. One application for advanced composite materials is as an alternative to steel w-beam used in most guardrail designs. A test method to measure baseline data on the dynamic properties of standard steel w-beam was needed to develop a design envelope for a composite rail element. The test developed could then be used to test the new composite rail to determine whether it was suitable for use in an actual roadside barrier. The test would not serve as an acceptance test, but rather as a relative performance test to compare a candidate composite rail's dynamic properties to that of steel w-beam. To replicate the full range of steel w-beam, an ideal test method would be to fail the steel w-beam rail element either by tearing the w-beam or failing the splice joint.

The FHWA's Federal Outdoor Impact Laboratory's (FOIL) 820-kg pendulum facility was used to conduct six dynamic impact tests on a four-post w-beam rail configuration. The w-beam rail consisted of three 1,905-mm sections spliced together and semi-rigidly attached at each end using standard 20-mm wire rope anchor cables. Standard steel I-section guardrail posts (strong posts) and off-set blocks were installed at the two interior post locations. The interior strong posts fit inside two box-sections at the groundline rigidly securing the base of the strong posts. The 820-kg pendulum was fitted with a rigid nose made from oak blocks glued together, cut to shape, and then bolted to a steel weldment that attached to the pendulum mass. The rigid nose and secured strong posts allowed for complete energy absorption by the w-beam rail, cable anchors, and bending of the strong posts. Energy dissipation from vehicle deformation and soil buckling was not a variable in these tests. The results from these pendulum tests are presented in the report *Pendulum Testing of Fixed-End W-Beam Guardrail: FOIL Test Numbers 96P001, 96P002, 96P003, 96P004, 96P005, and 96P006.*⁽¹⁾ One conclusion drawn from these six tests was that the energy from an 820-kg (actual mass was 912 kg) pendulum traveling at 35 km/h was not enough to load the steel w-beam guardrail to failure. A larger pendulum was needed in order to measure the upper limits of the w-beam rail element. A larger 2000P pendulum was constructed and installed in the FOIL's pendulum frame and suspended using larger wire rope cables.

The following test report summarizes the data collected during a series of 10 pendulum impact tests of standard steel w-beam using a 2000-kg pendulum with a rigid nose.

SCOPE

This report documents the test procedures followed and test results from a series of ten pendulum crash tests between the FOIL 2000P pendulum and a 5.7-m w-beam guardrail specimen. The pendulum tests were conducted at FHWA's FOIL facility located at the Turner-Fairbank Highway Research Center (TFHRC) in McLean, Virginia. The tests were conducted on steel w-beam rail elements rigidly anchored at both ends (a four-post configuration). The tests were conducted as part of an ongoing research effort to obtain baseline dynamic response data for standard w-beam guardrail. The pendulum struck the w-beam rail element at 90°, the major axis of the pendulum mass was perpendicular to the major axis of the guardrail barrier. The nominal weight of the FOIL pendulum with a rigid nose assembly was 2000 kg (actual mass, 2032 kg). The test speed varied from 15 km/h to 40 km/h. The first tests were conducted at 15 km/h and 20 km/h to ensure that the new pendulum mass and rigging were structurally sound. The test speed was increased incrementally up to the speed (energy) level necessary to achieve w-beam failure. The target increment was 2.5 km/h in an attempt to closely monitor and determine the actual energy level required to fail the w-beam rail element.

The 90° orientation and a 2000-kg pendulum impact speed of 40 km/h roughly approximates test designation 3-11 outlined in the National Cooperative Research Program Report 350 (NCHRP 350).⁽²⁾ Test 3-11 is a test level 3 test used to certify longitudinal barriers for use on the National Highway System (NHS). The test calls for a longitudinal barrier to be tested using a 2000P vehicle (pick up truck) traveling at 100 km/h and striking the barrier at 25°. The normal velocity to the barrier face during a 3-11 test is a vector component of the initial velocity;

$$V_n \text{ km/h} = \sin(25^\circ) * 100 \text{ km/h} = 42 \text{ km/h}$$

Thus the pendulum test scenario is roughly approximating the impact energy of the NCHRP 350 3-11 test. This is important because it is reasonable to test any candidate composite rail element in an environment similar to real world (or compliance test) conditions.

TEST MATRIX

The FOIL w-beam guardrail inventory was sufficient enough to conduct a maximum of 10 pendulum tests using the 2000P pendulum. The first two tests were conducted at 15 km/h and 20 km/h. These

two tests were conducted as a precaution to ensure the new pendulum mass and rigging were structurally sound. The speed was then increased incrementally up to the energy required to rupture the guardrail.

Table 1 shows kinetic energy values for different speeds for each pendulum mass at the FOIL. The highest energy level imparted on a guardrail in the FOIL test fixture to date was by the 820-kg pendulum traveling at 35 km/h (43,102 J). This energy level was the next 2000-kg pendulum test conducted. To produce the same energy, the 2000-kg pendulum was accelerated to 23.4 km/h. This level was the next logical test to ensure that this energy level wasn't the borderline energy between guardrail failure and not failing. It served as a good starting point for testing with the new larger pendulum. Two tests were conducted at this level because of a data acquisition system trigger failure. No sensor data were recorded during the first 23.4-km/h test. Because there were no anomalies or failures during these first four tests, the testing proceeded to the next energy levels. The test speed was increased incrementally up to 40 km/h. The target increment was 2.5 km/h. However, due to guardrail inventory, decisions were made during testing to increment the speed between tests as needed to ensure the maximum speed of 40 km/h was reached if needed to rupture the w-beam guardrail system. The final test matrix conducted is listed in table 2.

Table 1. Energy comparison between 820C and 2000P pendulums.			
Speed (km/h)	Speed (m/s)	820C Energy (N•m) *	2000P Energy (N•m) **
10	2.78	3,519	7,852
15	4.17	7,917	17,667
20	5.56	14,074	31,408
23.4	6.51	19,325	43,102
25	6.94	21,991	48,934
30	8.33	31,667	70,499
35	9.72	43,102	95,990
40	11.11	56,296	125,407
*The actual mass of the 820C pendulum was 912 kg.			
**The actual mass of the 2000P pendulum was 2032 kg.			

Table 2. Test matrix for 2000-kg pendulum testing of a four-post w-beam guardrail.

Test Number	Test speed (km/h)	Impact location
00P007	15.0	center of w-beam rail
00P008	20.0	center of w-beam rail
00P009	23.4	center of w-beam rail
00P010	23.4	center of w-beam rail
00P011	25.0	center of w-beam rail
00P012	27.5	center of w-beam rail
00P014	30.0	center of w-beam rail
00P015	35.0	center of w-beam rail
00P016	35.0	center of w-beam rail
00P017	40.0	center of w-beam rail

PENDULUM

The FOIL 820C (820-kg mass) pendulum facility was upgraded to include a new 2000-kg swinging mass (2000P pendulum). A new concrete and steel pendulum mass was fabricated. The design and construction technique used was similar to that used during construction of the 820-kg pendulum. An attempt was made to use the same ratio of concrete and steel as in the 820-kg pendulum. In addition to the new mass, the A-frame structure needed to be upgraded. New 20-mm suspension cables were purchased, installed, and tested. The new larger cables were needed to support the larger swinging mass.

The 2000P pendulum consists of a reinforced concrete mass with steel end-plates suspended from a steel structure by four 20-mm steel cables. The pendulum setup used a rigid, solid oak nose. This was done so that the four-post w-beam guardrail specimen would be subjected to all of the pendulum's kinetic energy with no energy dissipation by deformation of the nose. Within the concrete mass are two aluminum guide sleeves; the wood nose is attached to two aluminum guide tubes that are inserted into the guide sleeves. Five oak spacers (total length of 250 mm) were to be placed between the nose assembly and the pendulum mass. The spacers were necessary to allow for optimal contact between the w-beam specimen and the pendulum nose before the

pendulum passes completely through bottom dead center and begins to rise. The smaller pendulum used 325 mm of oak spacers. However, the new pendulum is longer than the old 820-kg pendulum; therefore, fewer spacers were required to achieve the same contact stroke. A thin rubber mat was nailed to the pendulum nose to reduce the high frequency ring and inertial spike associated with contact between two rigid objects. The vertical center of the pendulum mass was set 533 mm above ground. The pendulum centerline was aligned with the height of the center of the w-beam guardrail being tested. The pendulum was configured in the same manner for each test. The following summarizes the 2000-kg pendulum configuration:

- Pendulum mass: actual 2032 kg (nose, weight plates, etc.).
- Pendulum vertical center: aligned with vertical center of guardrail.
- Oak nose shaved to a larger radius than 820-kg pendulum (305 mm).
- Fewer oak spacers than 820-kg but same contact stroke.
- Rubber mat fastened to front to dampen ring effect.
- No sweeper plate.

Figure 1 shows the 2000-kg pendulum mechanical design drawings. Figure 2 contains photographs of the new pendulum mass and nose. Figure 3 is a sketch of the pendulum nose.

TEST ARTICLES

The standard steel w-beam guardrail specimens tested consisted of three 1,905-mm w-beam sections spliced end-to-end and bolted to standard guardrail strong posts (I-section) and blockouts. The post spacing between posts was 1,905 mm, which is standard for strong-post guardrail systems. The blockout-to-post connections were made using standard bolts in the same pattern that is in use on the NHS. Standard post and rail heights of 710 mm and 685 mm, respectively, were used to set up the four-post w-beam systems. The FOIL pendulum foundation's rigid anchor stanchions served as the two end posts. The two interior guardrail posts were rigidly clamped at ground level. Thus, no energy dissipation could be contributed to the posts' "plowing" or moving through soil as is typical in an actual highway installation. Because of this and the pendulum's use of a rigid nose, all of the pendulum's kinetic energy will be absorbed solely by the guardrail sections, posts, and cables through bending, torsional loading, and tension loading. Each end of the three-panel system was semi-rigidly anchored using standard 20-mm-diameter wire rope cable. The cables were fastened to the w-beam using standard cable anchor brackets used in typical guardrail systems. The outer ends of the cable brackets were notched to

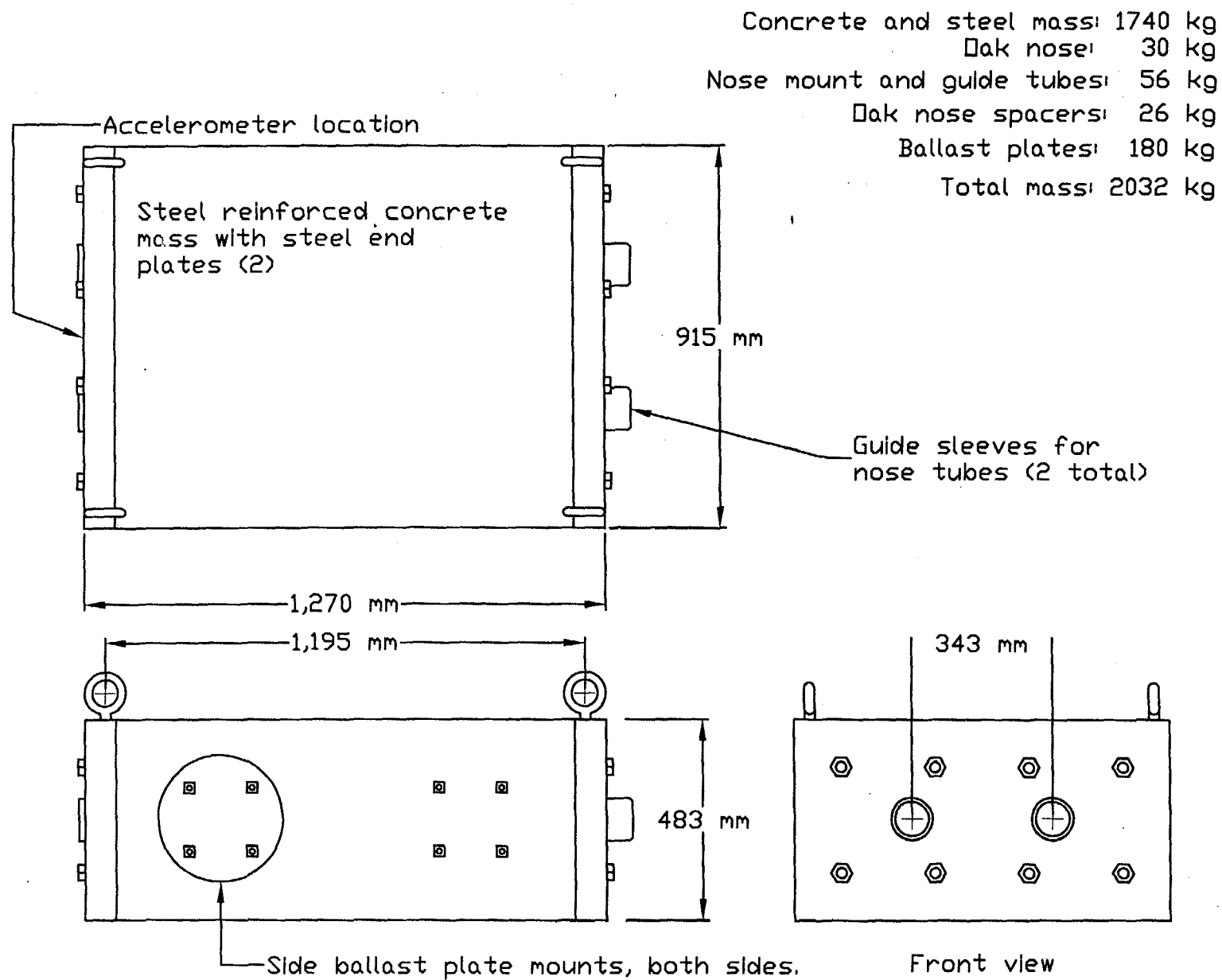


Figure 1. Sketch of the FOIL 2000P pendulum (nose assembly and ballast not shown).



Figure 2. Photographs of new pendulum mass with rigid nose.

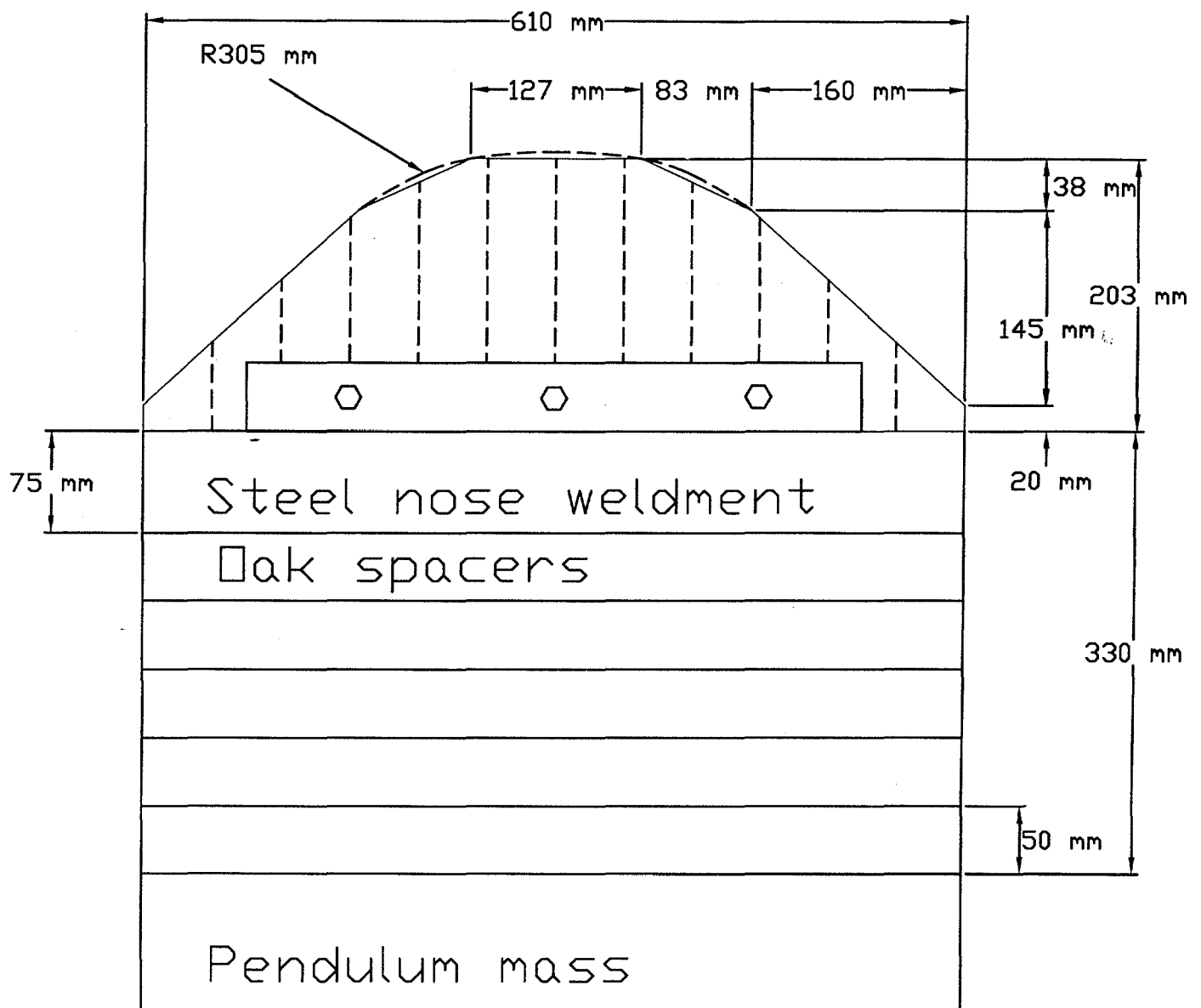


Figure 3. Sketch of pendulum nose.

prevent cutting action that can result as the rail is pushed back and the cables bear against the interior edges of the cable brackets. The other end of the cables were passed through the two rigid anchor stanchions (one at each end) and fastened with a 20-mm cable nut and washer. Standard rail-to-post bolts with one square washer were used to fasten the ends of the w-beam to the anchor stanchions. Standard bolts without washers were used for the rail-to-blockout connections on the two interior posts. Tension was applied to the four-post w-beam systems prior to testing by tightening the anchor cables. An attempt was made to apply the same amount of rail tension to each tested rail. This was accomplished by monitoring the voltage output from two strain gauges bonded to the front valley of the w-beam guardrail. One gauge from each side (left and right) of the specimen was monitored. Each threaded end of the anchor cables was lubricated with a greaseless lubricant. The cables were tightened until the voltage output was approximately equal to the voltage outputs recorded during previous 820-kg pendulum tests of w-beam guardrail. The following summarizes the guardrail setup:

- Three spliced 1.9-m panels.
- Splices overlapped as in real world, on the NHS.
- Two standard posts and blockouts.
- Base of posts rigidly clamped.
- Post height: 710 mm.
- Rail height: 685 mm.
- Both ends semi-rigidly anchored using 20-mm cables and notched cable brackets.
- Specimen pretension set to previous value used during an earlier test series. Set to same for each test.
- New hardware, including the anchor cables, was used for each test (except cable anchor brackets).
- One square washer under each bolt head at each end anchor.
- No washers under head of interior post-to-rail bolts.

The guardrail system described above was used in the majority of the tests and is shown in figure 4. However, during test 00P015 the rail-to-post connection at the end stanchion posts failed. The bolts began to tear through the w-beam then sheared. The connection failure caused a significant load transfer to the anchor cables. The load caused the left anchor cable to fail. The cable failed in tension at the cable-stud swage joint. The failure was not due to guardrail failure but rather to a flaw in the end-anchorage technique used. To prevent this from occurring in the remaining tests, a 305-mm steel w-beam backer plate and a high-strength bolt were installed at each end of the guardrail system. The backer plate reinforced the single w-beam, effectively doubling the cross section. This was done to limit the amount of bearing failure at the bolt slot. The high-strength bolt was added to prevent bolt shear as the bolt slot

bore against the anchor bolt. This guardrail configuration is shown in figure 5.

INSTRUMENTATION AND DATA ACQUISITION

For each pendulum test, speed trap, accelerometer, strain gauge, and high-speed film data were collected to measure the steel w-beam's dynamic properties. Strain gauges were placed on the w-beam rail elements to set the guardrail element pretension prior to each test. The strain gauge data were essentially useless after the first 160 mm of deflection. At that point, the gauges indicated that the guardrail had exceeded the elastic range. The following summarizes the instrumentation and method of acquisition:

Speed trap. The speed trap consisted of a set of four light emitting diode (LED) infrared emitter/receiver pairs fastened on opposite sides of the pendulum's swing path at 150-mm intervals. The scanner pairs were positioned before the impact area to measure the speed of the pendulum just prior to contact with the w-beam. Signals from the sensors were recorded on a Honeywell model 5600E analog tape recorder. The signals were stored on analog tape for future analysis.

Accelerometers. Two longitudinal (x-axis) 100-g accelerometers were mounted at the center of the rear face of the pendulum. This location corresponded to vertical and lateral center-of-gravity (c.g.).

For tests 00P007 through 00P009, the data from the two accelerometers were recorded by a single data acquisition system, the FOIL's TDAS PRO. The TDAS PRO system is a fully self-contained data system. The TDAS PRO supplies each sensor with a user-specified excitation voltage. The signals from each sensor are digitally sampled at a user-specified sample rate, conditioned, and stored in the system's memory for download to a laptop computer. The signals from the accelerometers were digitally sampled at 12,500 Hz and pre-filtered with a low-pass filter set at 3,000 Hz.

During test 00P009, a malfunction occurred in the trigger circuit of the TDAS PRO system. No accelerometer data were recorded during 00P009. A second data cable was fabricated to interface one accelerometer with the FOIL analog data system. This enabled the data to be recorded by two independent systems. The FOIL analog system uses a rack of signal conditioning amplifiers to supply the transducer with excitation voltage, signal conditioning, and the interface to a Honeywell model 5600E analog tape recorder. The accelerometer's signal was recorded on



Figure 4. Pre-test photographs of a typical guardrail for tests 00P007 through 00P015.



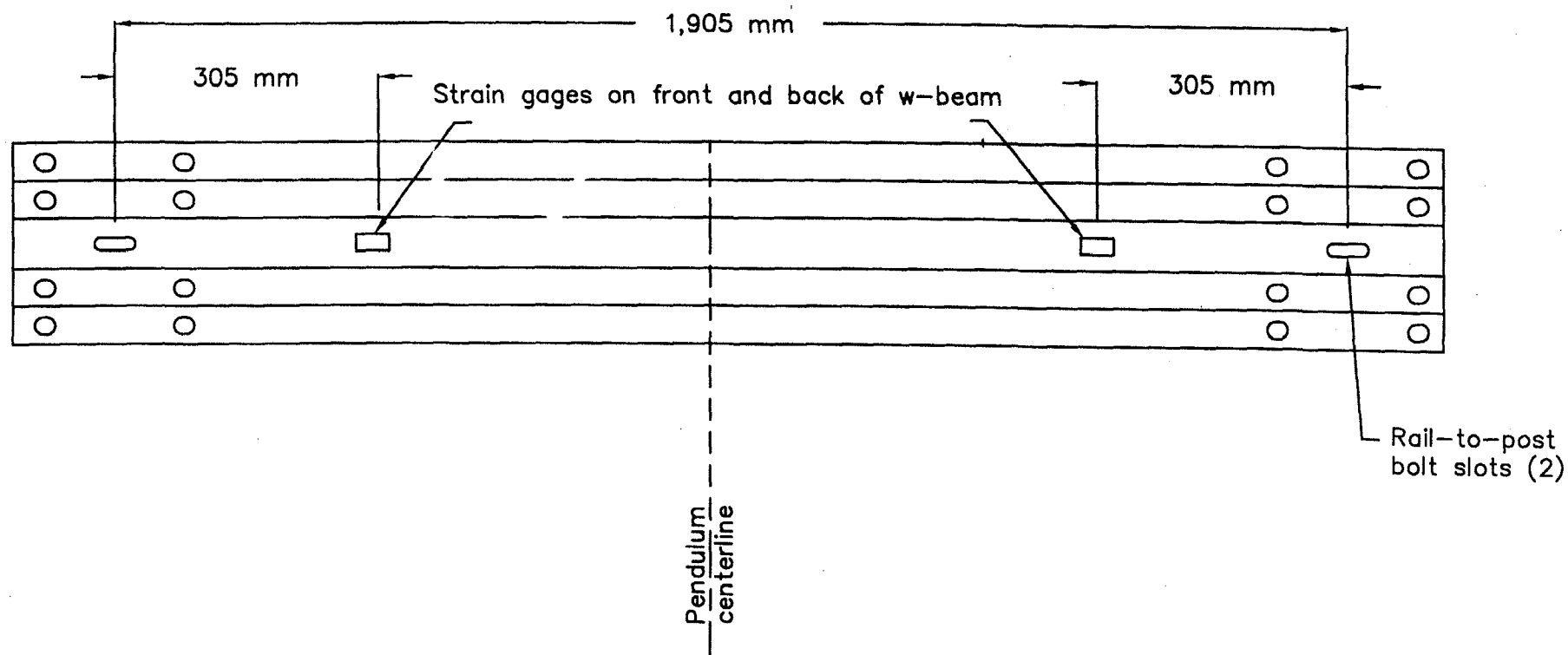
Figure 5. Pre-test photographs of a typical guardrail for tests 00P016 and 00P017.

the analog tape for analysis after the test. The analog signals were played back through an anti-aliasing filter set to 3000 Hz then input to an analog-to-digital converter with a sample rate set to 12,500 Hz. The digital data were stored on a hard drive for future analysis.

Strain gauges. Eight 350-ohm single-gauge strain gauges were bonded to each steel w-beam specimen. The gauge axes of sensitivity were oriented longitudinally along the guardrail element's major axis. Two gauges were affixed 305 mm from each interior steel post toward the pendulum (four gauges on the front). Gauges were also placed at the same location on the back side of the guardrail (four gauges on the back side). The two gauges at each location were placed side-by-side to collect redundant data between the two FOIL data acquisition systems (analog tape and TDAS PRO). The gauges' primary function was to set the pretension in the guardrail specimens. Once the strain recorded surpassed the yield level for steel the data became useless. Figure 6 is a sketch that depicts the strain gauge locations.

High-speed photography. Each pendulum test was photographed using five high-speed cameras, one real-time camera, and two 35-mm still cameras. The high-speed cameras were loaded with Kodak 2253 color daylight film and the real-time camera was loaded with Kodak 7239 color film. One 35-mm camera was loaded with black and white print film and the other with color slide film. The configuration and placement of each camera is summarized in table 3. Figure 7 is a plan view of the test layout. Included in the figure are the camera numbers listed below depicting the camera locations.

Table 3. Camera configuration and placement.				
Camera Number	Type	Film Speed (frames/s)	Lens (mm)	Location
1	Locam II	500	50	90° to impact rt. side
2	Locam II	500	25	45° to impact rt. side
3	Locam II	500	50	180° to impact
4	Locam II	500	25	45° to impact left side
5	Locam II	500	25	overhead
6	Bolex	24	zoom	documentary
7	Canon A-1 (prints)	still	zoom	documentary
8	Canon A-1 (slides)	still	zoom	documentary



Steel w-beam test specimen strain gage locations.
Front of rail pictured.

Figure 6. Sketch of w-beam specimen and strain gauge locations.

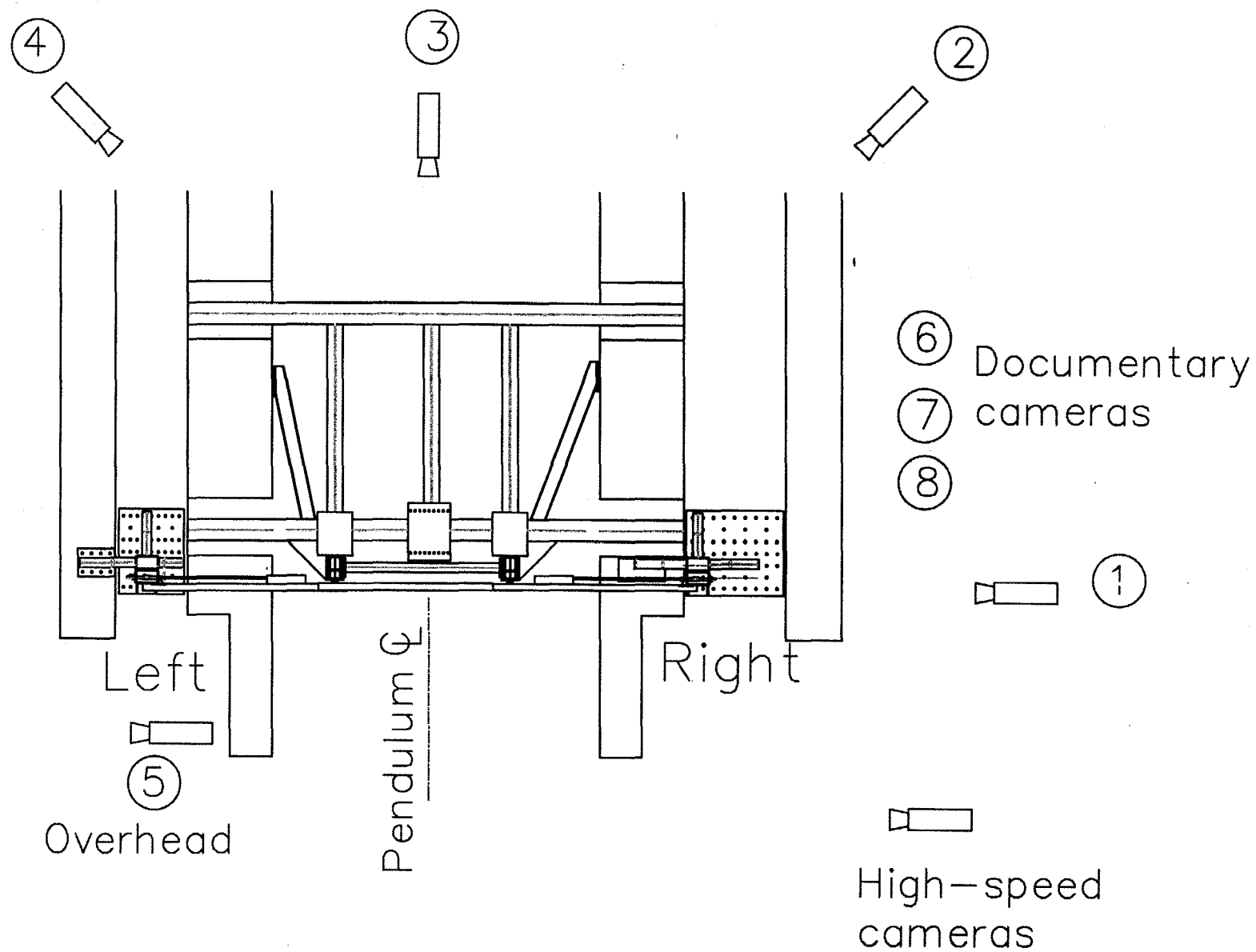


Figure 7. Plan view of test layout and high-speed camera locations.

DATA ANALYSIS

For each pendulum test, a speed trap, accelerometers, strain gauges, and high-speed film were used for data collection. All electronic data were originally recorded or converted to digital. The files were then converted to the ASCII format. The data were analyzed (zero bias removed and digitally filtered to the appropriate frequency class) and archived. The high-speed film was developed and edited into one master film. The film was analyzed to find the pendulum initial speed and other pertinent data and then was transferred to video tape.

Speed trap. The speed trap consisted of a set of four LED infrared emitter/receiver pairs fastened on opposite sides of the pendulum's swing path at 150-mm intervals just prior to the w-beam specimen. As the pendulum passed through the infrared scanners, electronic pulses were recorded on analog tape. The tape was played back through a Data Translation analog-to-digital converter (ADC), and the time between pulses was determined. Time-displacement data were entered into a computer spreadsheet and a linear regression was performed on the data to determine the pendulum speed.

Accelerometers and strain gauges. The data from the accelerometers and strain gauges were digitally recorded and converted to the ASCII format. The digital sampling rate was set to 12,500 Hz for all electronic data. The ASCII files were processed, which included removal of zero-bias, storing the region of interest, and digitally filtering the data to 300 Hz (Class 180). This cut-off frequency is specified by SAE J211 for integration of vehicle accelerations to determine vehicle velocity. For determining peak accelerations, SAE J211 specified frequency class 60. The data were filtered a second time to class 60, which calls for a cut-off frequency of 100 Hz. The data were imported into a spreadsheet for plotting and analysis. Acceleration-time histories were created and integrated to produce velocity- and displacement-time histories. The displacement-time history is a record of the pendulum mass movement after contact. Because the pendulum and guardrail were in contact, this history was used as the dynamic guardrail deflection profile. The acceleration-time history was multiplied by the mass (2032 kg) of the pendulum to obtain a force-time history. The force data were plotted with the guardrail deflection or displacement trace. This data trace shows the force level for a given amount of system deformation. It conveys an approximation of which system component may be attributed to the opposing load (w-beam flattening, w-beam bending, torsional bending of posts and blockouts, failure of end bolts, tension loading of rail and/or anchor cables). The force-deflection history was integrated to produce an energy trace. The energy

trace shows the energy loss for a given deflection level. No energy is lost to pendulum deformation or soil plow; therefore, the energy values shown on the energy trace may be attributed entirely to the guardrail structure. As with the force-deflection history, the energy trace can be used to help determine which structures and events absorb the most energy. The strain gauge data were plotted against time and displacement (rail deflection). These plots proved useless given that the yield strain for steel was exceeded early in the impact event. After that point, calculations of the longitudinal tension in the rail are not accurate using Euler's equation.

High-speed photography. The crash event was recorded on 16-mm film by five high-speed cameras. Primarily, the perpendicular and overhead camera were the only cameras used for high-speed film analysis. Analysis of the crash event was performed using an NAC Film Motion Analyzer model 160-F in conjunction with a desktop PC. The motion analyzer digitized the 16-mm film, reducing the image to Cartesian coordinates. Using the Cartesian coordinate data, a time-displacement history of the test was obtained. The time-displacement data were then imported into a computer spreadsheet and a linear regression was performed to determine the impact velocity of the pendulum. Using the Cartesian coordinate data, the deflection of the rail could be measured directly. Film analysis data would have been used to obtain continuous velocity and acceleration data in the event of electronic data acquisition system failure. The time-displacement data could be differentiated to find the pendulum velocity and acceleration. The high-speed film initial velocity measurement served as a redundant measuring system, the inferred speed trap system data was used as the primary measurement for initial velocity.

RESULTS

For each test, the pendulum was accelerated to within ± 0.5 km/h prior to striking the w-beam guardrail specimen. Due to the consistent swing plane, the pendulum struck each guardrail specimen at the intended impact location (same location for each test). The intended pendulum test matrix called for increasing the pendulum impact velocity by 2.5 km/h each test. However, due to the limited inventory of 1.9-m w-beam specimens, the matrix was modified as necessary to ensure that the maximum energy level (40 km/h) could be achieved during this series of tests. Table 4 summarizes the results from the 10 pendulum tests conducted. Appendix A contains post-test environment photographs for all 10 pendulum tests. Data plots generated from analysis of the pendulum accelerometers are located in Appendix B.

Tests 00P007 through 00P010. The purpose of these tests was to evaluate the new pendulum mass, new oak nose radius, suspension cables, and other structures before proceeding to energy levels higher than previously achieved. This was done by gradually increasing the initial impact velocity (energy) from 15 km/h to 23.5 km/h. The 23.5-km/h energy level is equivalent to the highest energy level achieved using the FOIL's 820C (912 kg actual mass) pendulum during a previous w-beam test program. Test 00P010 was a retest of test 00P009 due to a data acquisition system trigger failure (no electronic data) during test 00P009. During test 00P007, the pendulum struck the guardrail and deformed the w-beam shape. The rail deformation was not severe, the end anchorage bolts held, and no rotation or buckling was observed in the two interior steel posts or blockouts. This deflection pattern and lack of a second peak in the acceleration-time history indicate that the w-beam rail was loaded with little or no load transfer to the anchor cables. The maximum deflection and deformation to the interior posts increased with the increase in pendulum speed (energy) during 00P008. However, the end anchor bolts held as in 00P007, which would indicate the majority of the load was absorbed by the rail with some load transfer to the anchor cables. The two tests at 23.5 km/h (00P009 and 00P010) demonstrated good repeatability in performance of the w-beam rail (visual observations and static deflection). During each of these tests, the rail deflection increased as expected along with the buckling and torsional failure of the interior posts. However, during the tests the two end anchor bolt connections failed. The bolts began to shear through the w-beam until the bolts either sheared or pulled through the bolt slot. The release of the end anchor bolts allowed for the remaining load to be transferred to the anchor cables and center section of w-beam. Inspection of the rail after the test revealed movement of the rail elements at the splice joints and cable anchor bracket. At this time, no attempt was made to prevent the end anchor bolts from failing.

Inspection of the pendulum mass, nose assembly, and support structure and rigging revealed that all mechanical systems remained sound. The deflection pattern of the guardrail was different from that observed during the 820C pendulum testing. This was due to the increased radius of the 2000P pendulum nose. The guardrail anchorage system and the specimens themselves showed no sign of impending failure or fatigue. The testing proceeded to the higher energy levels.

Tests 00P011, 00P012, 00P014, and 00P015. In each test the guardrail deflection, bending, and torsional buckling of the standard posts increased as the impact energy increased. The two end rail-to-post bolts either sheared or pulled through the bolt slot. During test 00P014, the rail disconnected from the two inner posts due to severe torsional buckling in the posts. The

pendulum continued to push the rail as it began to rise in its upswing. The w-beam rail element showed no sign of failure. Because the inventory of steel w-beam was limited, the velocity for the next energy level was increased by 5 km/h to 35 km/h (00P015). The deflection and deformation to the guardrail system was similar to that of test 00P014. However, due to increase in residual energy and the direction of load in the cables, the left anchor cable ruptured. The cable bent around the swaged connection and snapped. The pendulum continued through the impact area then fell backward. The pendulum swung back and forth until it came to rest. Because the rail was not loaded to failure, testing continued. Modifications were made to the end anchorage technique. A 305-mm backer plate was added to each end, effectively doubling the w-beam cross section. This was done to prevent bearing failure of the bolt slot. High-grade steel bolts were used to fasten the backer plate and w-beam to the end anchor stanchions. The stronger bolts were used to prevent bolt shear. The next test repeated the energy level of test 00P015.

Tests 00P016 and 00P017. The nominal test speed for test 00P016 was 35 km/h. The end anchor rail-to-post connection was reinforced with a 305-mm backer plate and a high-strength bolt. The pendulum struck the guardrail and deformed the rail w-shape and began to buckle the inner posts. The loading of the w-beam continued and the ends of the rail began to pull inward. However, the extra rail thickness provided by the backer plate and the extra shear strength of the bolt prevented the end anchor rail-to-post connection from failing. The bearing failure at the bolt slot was limited to 50 mm. The bolt did not tear all the way through nor did it pull through the slot. The energy was dissipated by the rail deformation, bearing failure, inner-post buckling, rail tension, and cable tension. Typical damage to the rail resulted after the test. However, it was noted that the bolts located at the splice joints were on the verge of either tearing through the bolt holes (bearing failure) or pulling out of the holes. The next test was conducted at 40 km/h (00P017), the maximum speed (energy) that the FOIL pendulum could produce. The pendulum struck the rail and deformed the w-shape and then the posts. The end anchorage rail-to-post bolts began to tear through the w-beam at the bolt slot. Approximately 75 mm of bearing failure resulted but the connection held. The pendulum continued to load the rail and the left splice joint failed. The bolts in the splice joint either pulled out of the hole or ripped through the guardrail. Each bolt hole showed signs of bearing failure. The holes tore open enough for the bolt heads to pass through the hole. As the splice failed, the blockout twisted around and the two blockout-to-post bolts sheared. The blockout remained fastened to the middle section of w-beam.

Table 4. Summary of pendulum testing of four-post w-beam rail.

Test Number	Speed (km/h)		E _i (kJ)	Rail Pre-tension (μE)		Peaks (class 60 data)		Rail Deflection (mm)			Work F•d (kJ)
	Trap	Film		Left guage	Right guage	g's	Force (1000 N)	Accel	Film	Static	
00P007	14.9	14.8	17.10	103	107	4.7	94.3	287	303	205	17.0
00P008	----	19.9	30.96	91	89	6.3	125.1	450	482	409	30.9
00P009	23.4	23.4	42.93	118	129	----	----	----	688	515	----
00P010	23.5	23.4	43.06	92	111	6.1	121.2	620	693	527	42.9
00P011	25.0	25.0	49.08	113	104	7.2	143.4	630	710	535	49.0
00P012	27.3	27.5	59.30	105	106	7.1	140.6	730	818	611	59.2
00P014	29.7	30.2	71.52	112	98	8.8	175.4	800	800	700	71.4
00P015	35.4	35.1	96.58	132	108	9.4	189.4	770	745	CABLE FAILED	76.0
00P016	34.8	35.1	96.60	88	96	11.4	227.0	860	864	741	96.2
00P017	39.3	40.6	129.20	112	99	11.7	233.4	890	876	SPLICE FAILED	102.2

CONCLUSIONS

The FOIL 2000P pendulum system was structurally sound and was compatible with the 820C pendulum accessories (nose, rigid and honeycomb, speed trap system, data systems, etc.). The new rigging and suspension components were easily adjusted and were readily interchangeable to accommodate either pendulum mass.

The energy from the 2000P pendulum traveling at 40 km/h produced enough load to rupture a splice joint in a semi-rigidly anchored guardrail system comprised of 3 1.9-m steel w-beam rails. The w-beam element itself showed no sign of impending failure or wear. The w-shape was flattened out a width equivalent to the pendulum nose radius spreading the load over larger contact area than that seen in the 820C pendulum test program. The load required to rupture the splice joint was approximately 233 kN (class 60 data). To determine whether this load would consistently result in failure of the guardrail system and whether a 40 km/h initial velocity is necessary to rupture the guardrail additional testing would be required. The increase in energy from the 35-km/h test to the 40-km/h test was roughly 30 percent. The actual energy required to rupture the steel w-beam may fall between that of a 35-km/h pendulum and a 40-km/h pendulum. Additional testing to energy level between those is needed to more closely identify the actual energy needed to rupture the splice.

When using a rigidly fixed end test configuration it is important to ensure that the ends of the rail are in fact rigid. If the connection fails, the sudden loading of the anchor cables can result in cable failure without maximum loading of the guardrail element being tested.

Within the first several (6 mm) mm of rail deflection, the strain gauges affixed to the w-beam register strain values higher than the yield strain for steel from which the standard w-beam was manufactured. For typical guardrail steel the actual yield point is approximately $1936 \mu\epsilon$ as determined by Ray and Wright.⁽³⁾ Because the useful range of Euler's equation was exceeded, the strain gauges were useful for setting guardrail pretension but not in measuring the maximum tension or longitudinal loading of the w-beam during impact.

The steel w-beam guardrail failed at a splice during the 40-km/h pendulum test yet was able to withstand a 35-km/h strike. Although these test conditions are more severe than real-world conditions, given no energy dissipation through soil buckling or vehicle deformation, it is a dynamic measurement of the steel w-beam's load-carrying capacity. If the steel w-beam system cannot withstand a 40-km/h 2000P pendulum strike and it is the most

widely used material for guardrail applications on the NHS today, then a candidate alternative rail element fabricated from composite materials should perform as well if not better than did the steel w-beam given similar test conditions. The 35-km/h 2000P pendulum test could be used as a baseline dynamic response test for the viability of using alternative composite rail elements. This test could not serve as a method of certifying the composite rail elements for use in NHS applications. Other important factors would have to be addressed and tested to *NCHRP Report 350* standards before a candidate guardrail element could be used in real-world applications. The test would serve as an initial step in designing a guardrail element before a prototype guardrail system could be certified.

APPENDIX A: POST-TEST PHOTOGRAPHS FROM EACH PENDULUM TEST

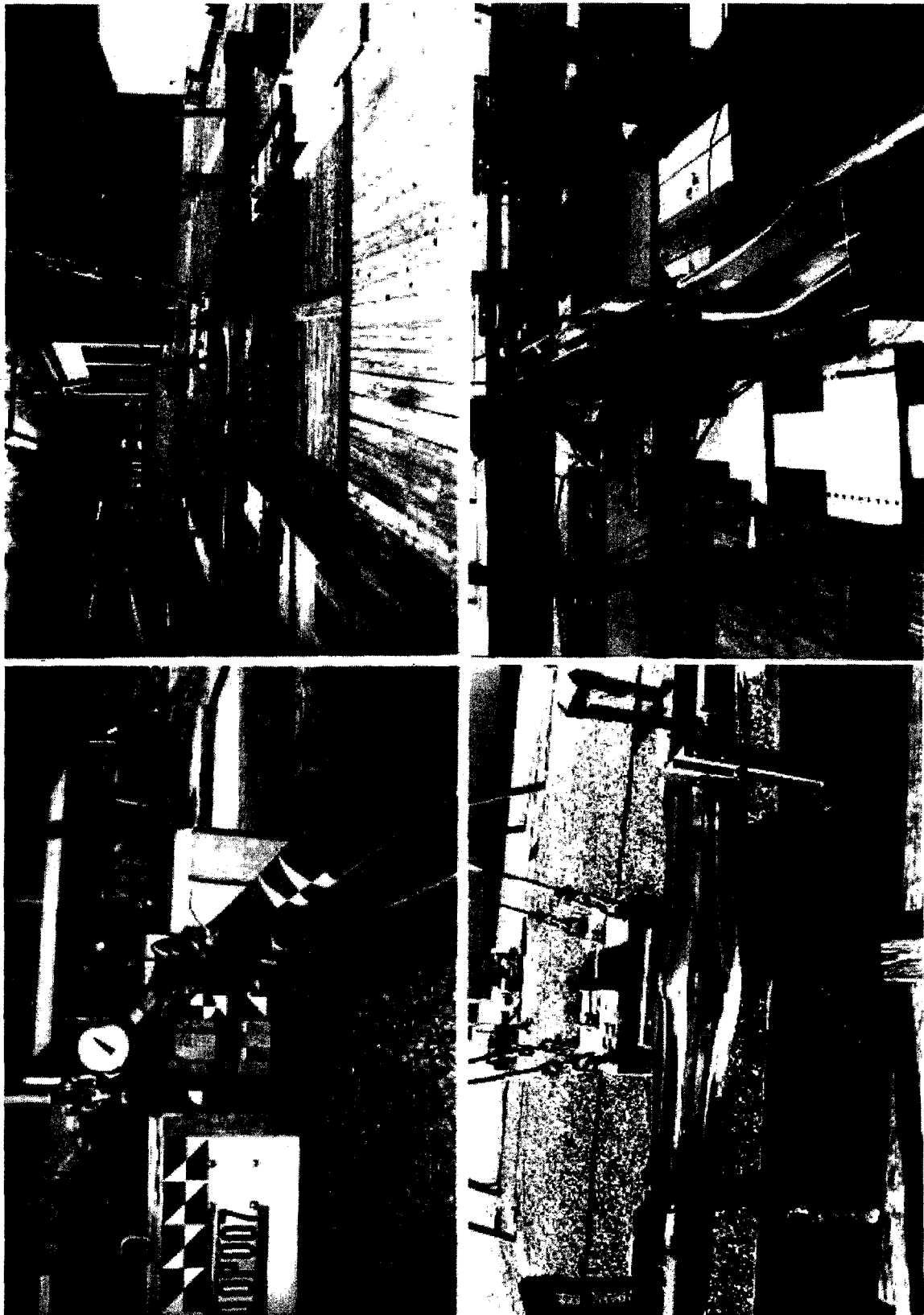


Figure 8. Post-test photographs, test 00P007.

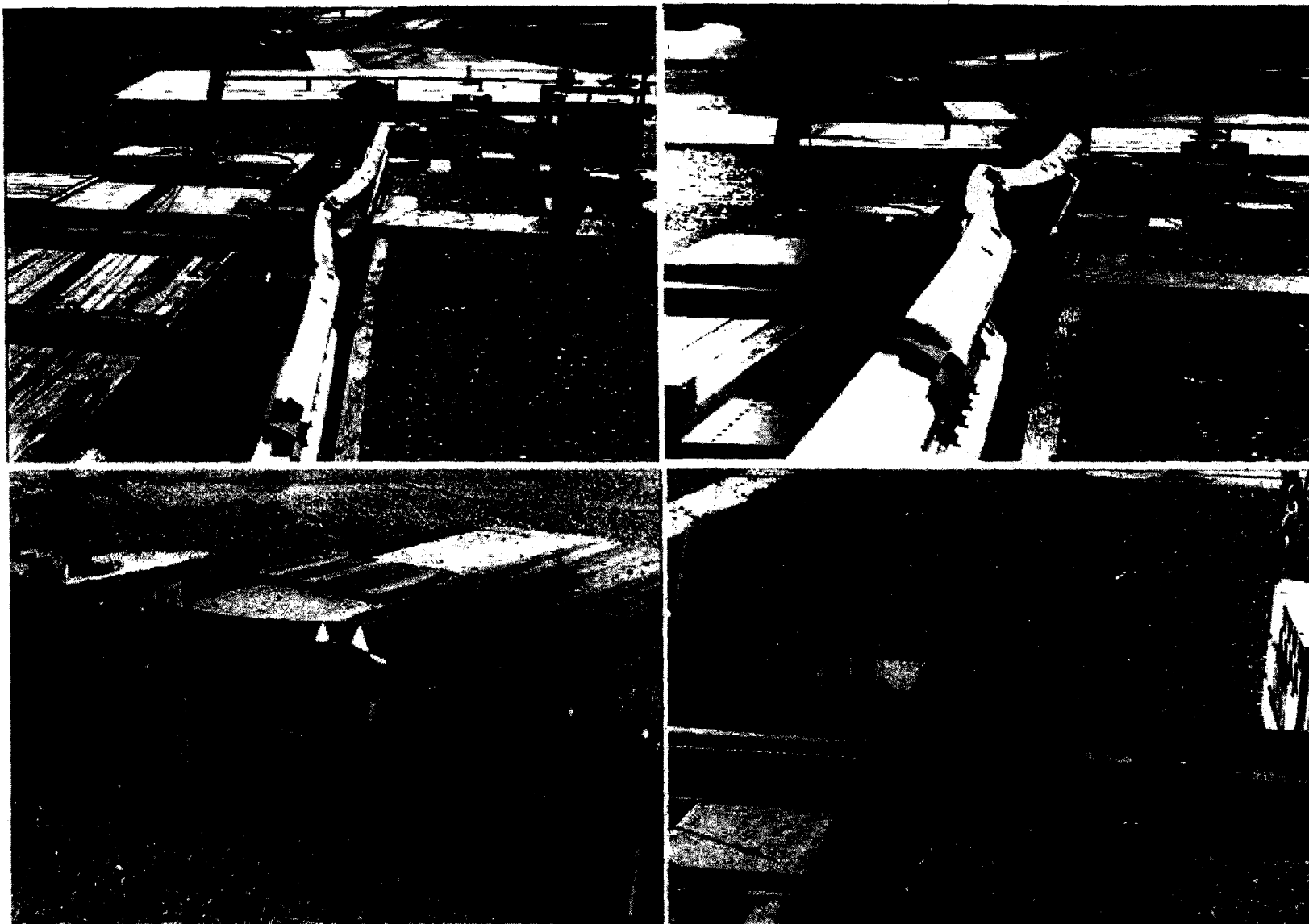


Figure 9. Post-test photographs, test 00P007 (continued).

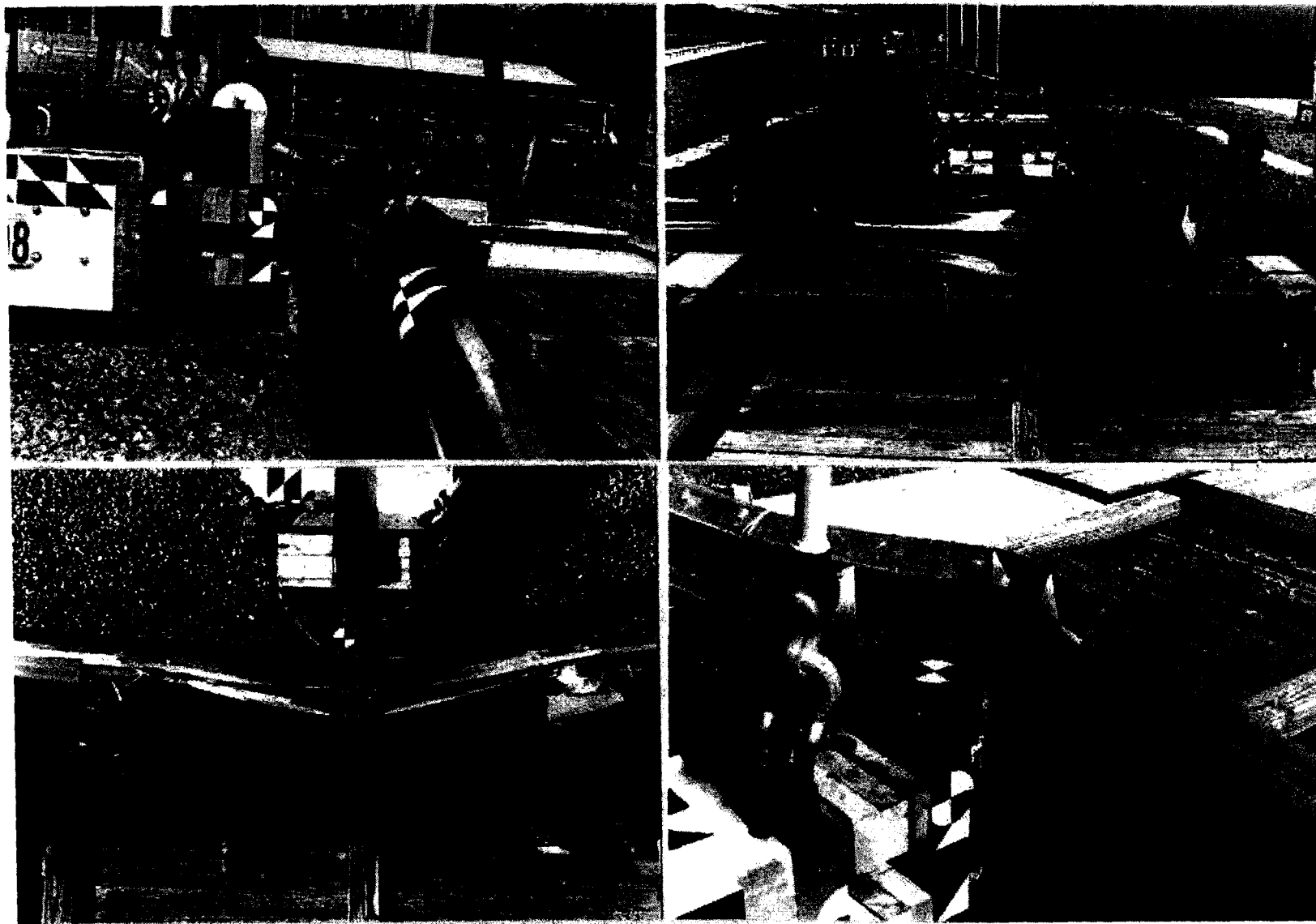


Figure 10. Post-test photographs, test 00P008.

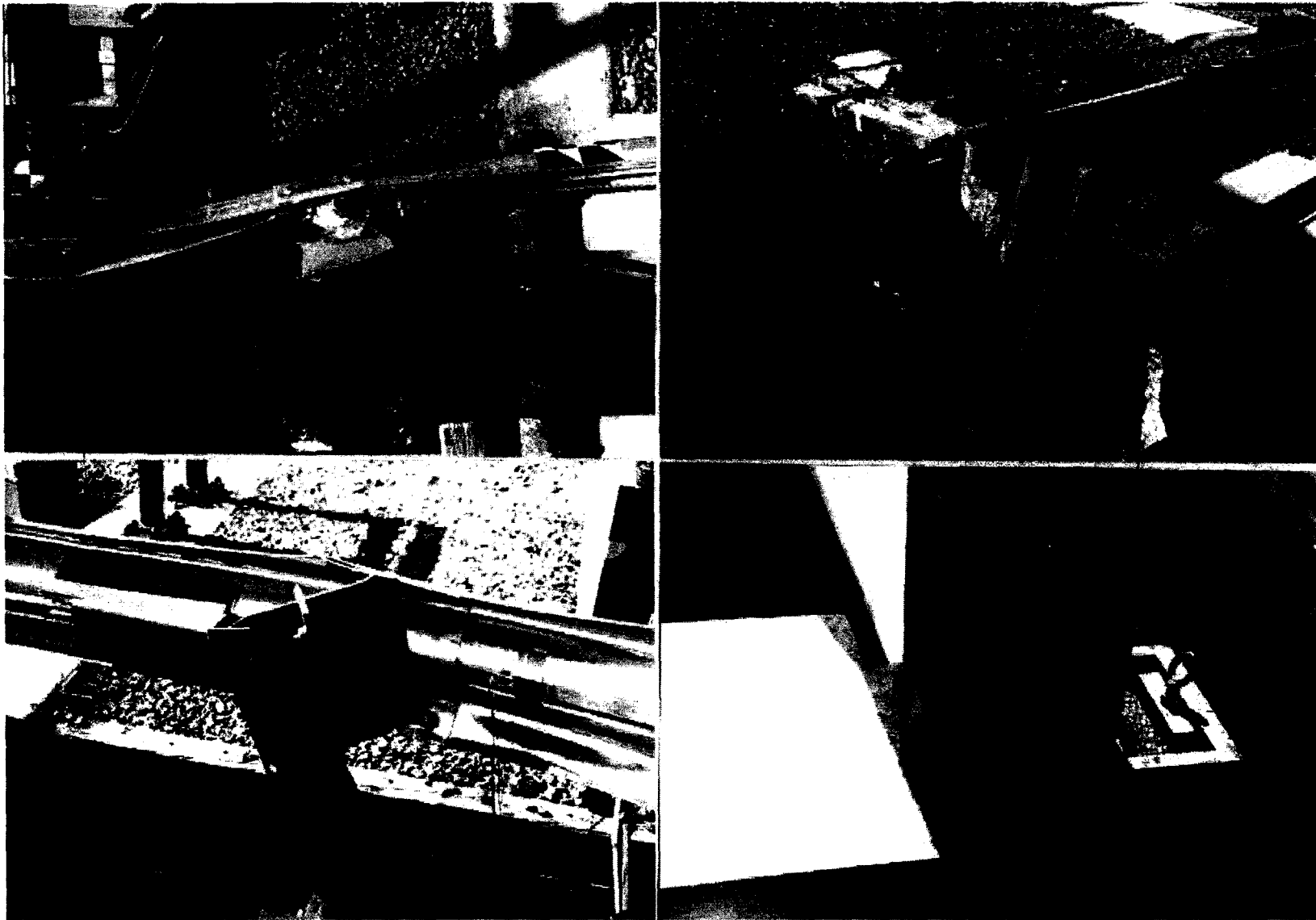


Figure 11. Post-test photographs, test 00P008 (continued).



Figure 12. Post-test photographs, test 00P009.



Figure 13. Post-test photographs, test 00P009 (continued).

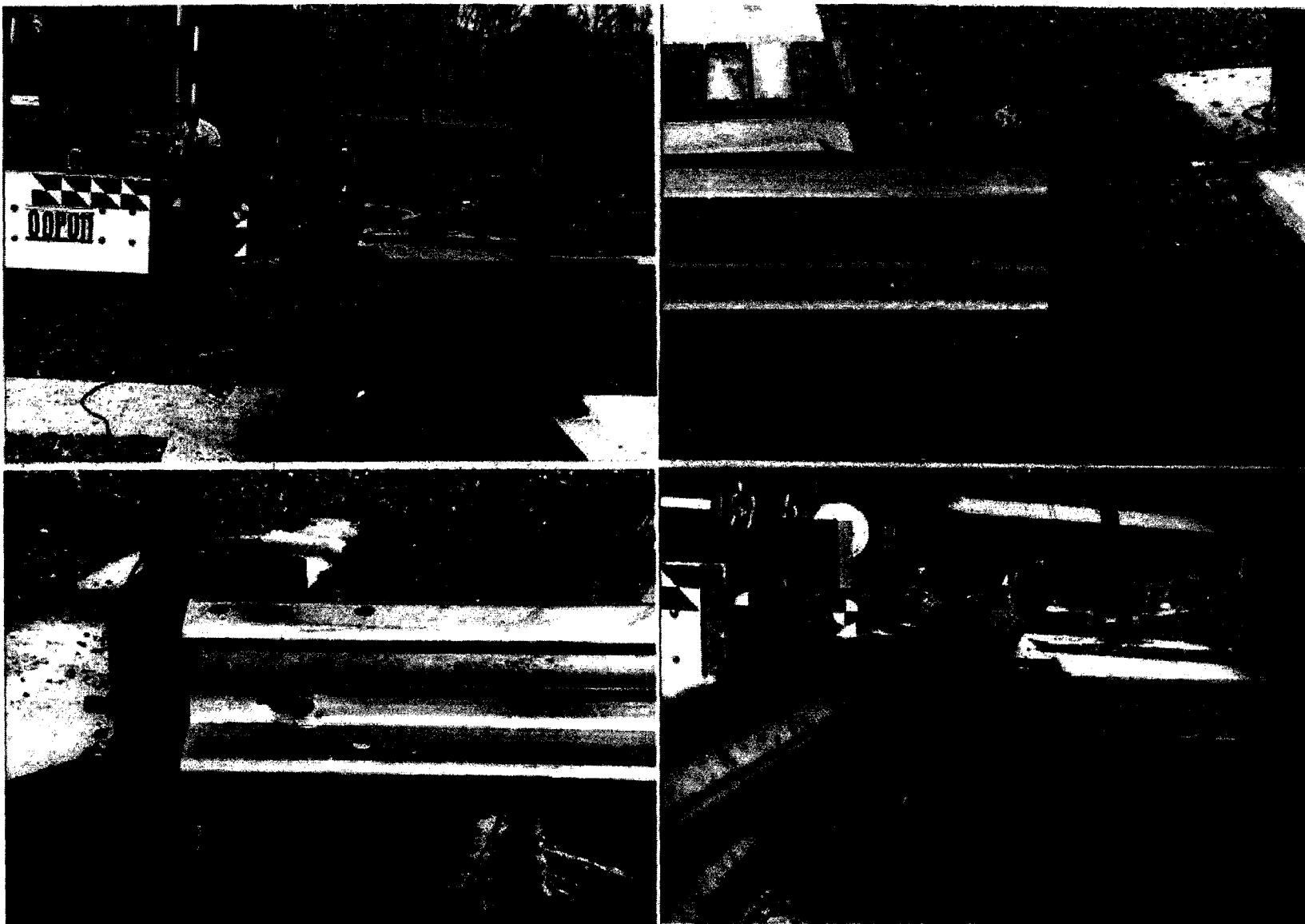


Figure 14. Post-test photographs, test 00P011.

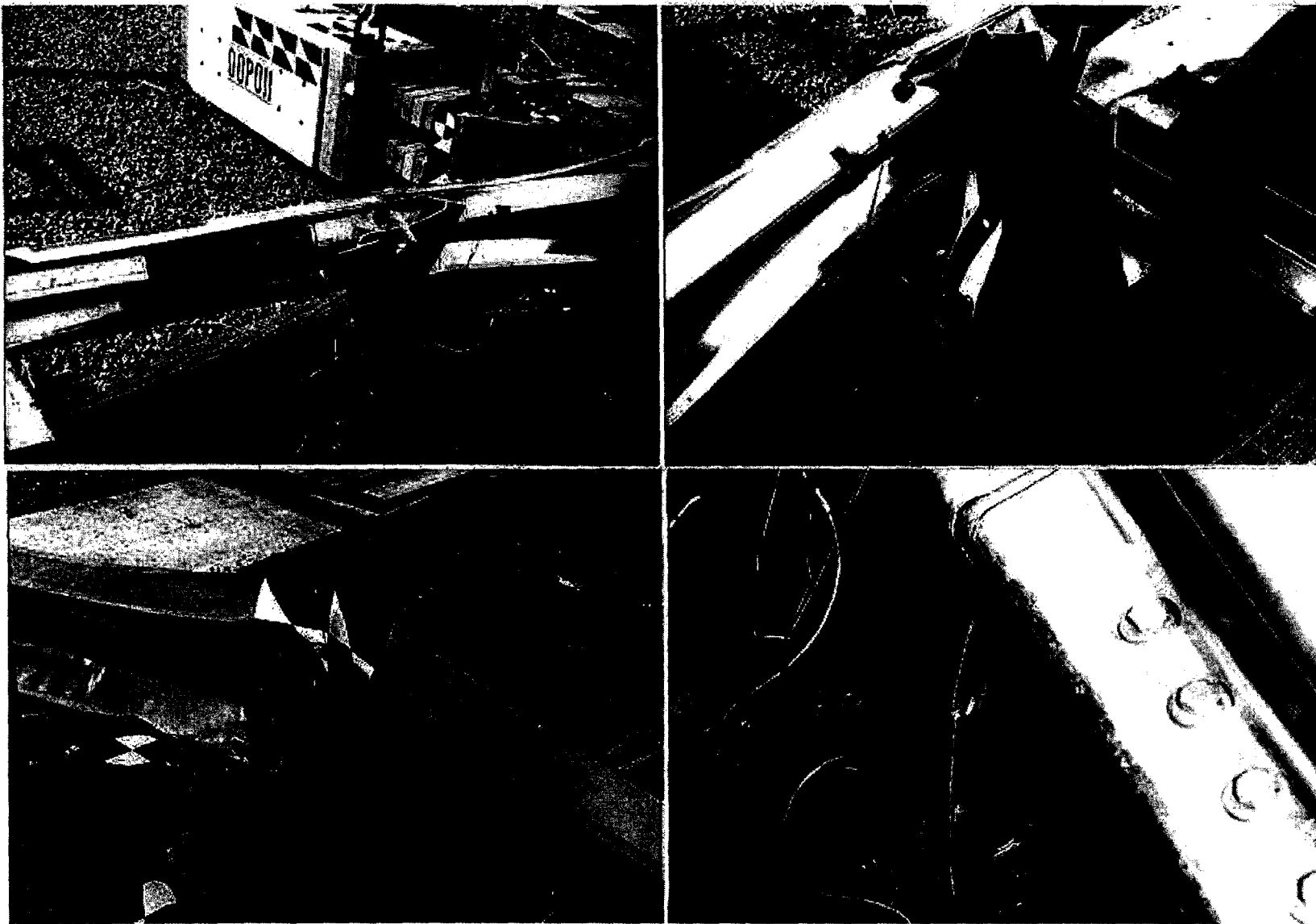


Figure 15. Post-test photographs, test 00P011 (continued).

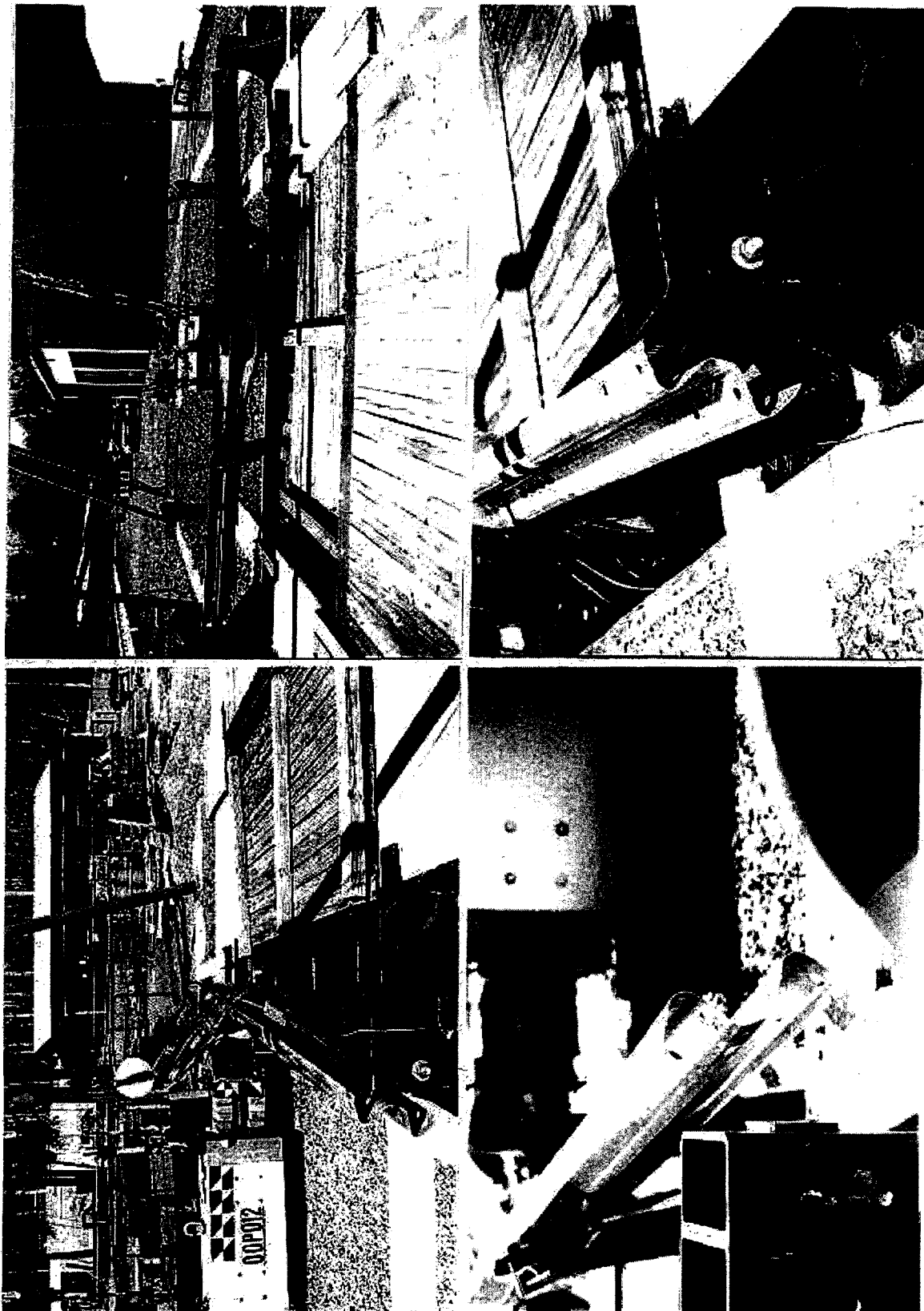


Figure 16. Post-test photographs, test 00P012.

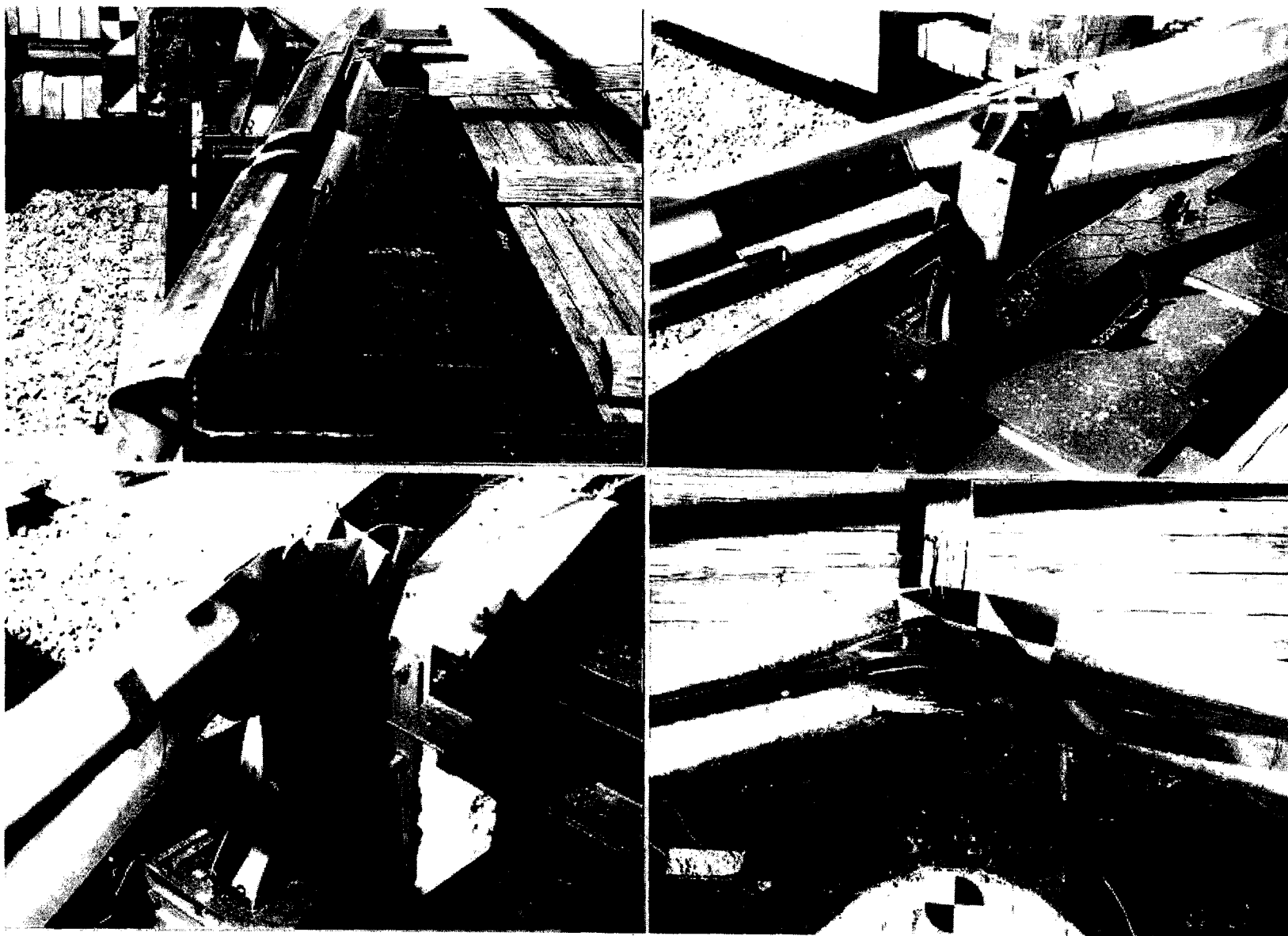


Figure 17. Post-test photographs, test 00P012 (continued).

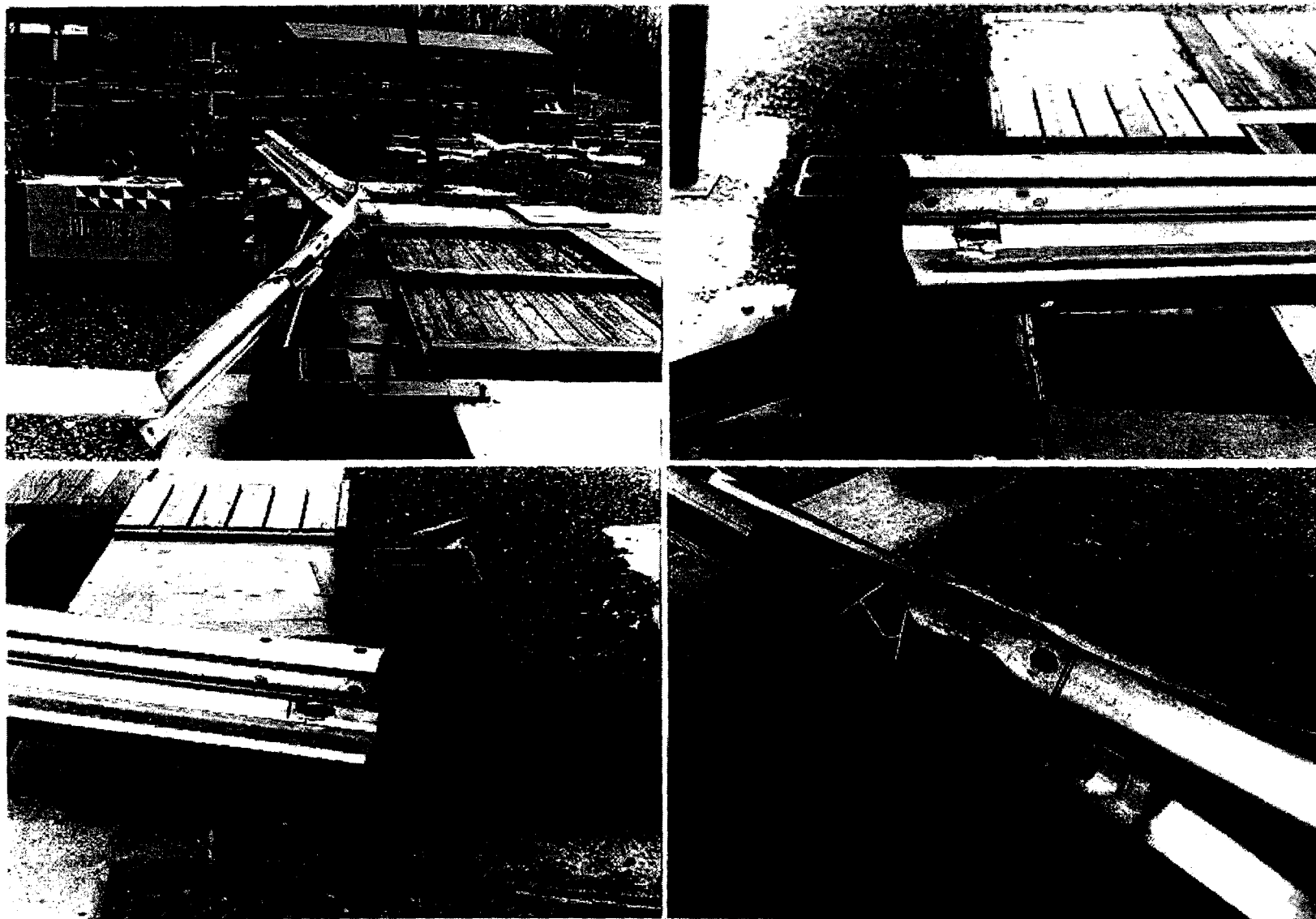


Figure 18. Post-test photographs, test 00P014.

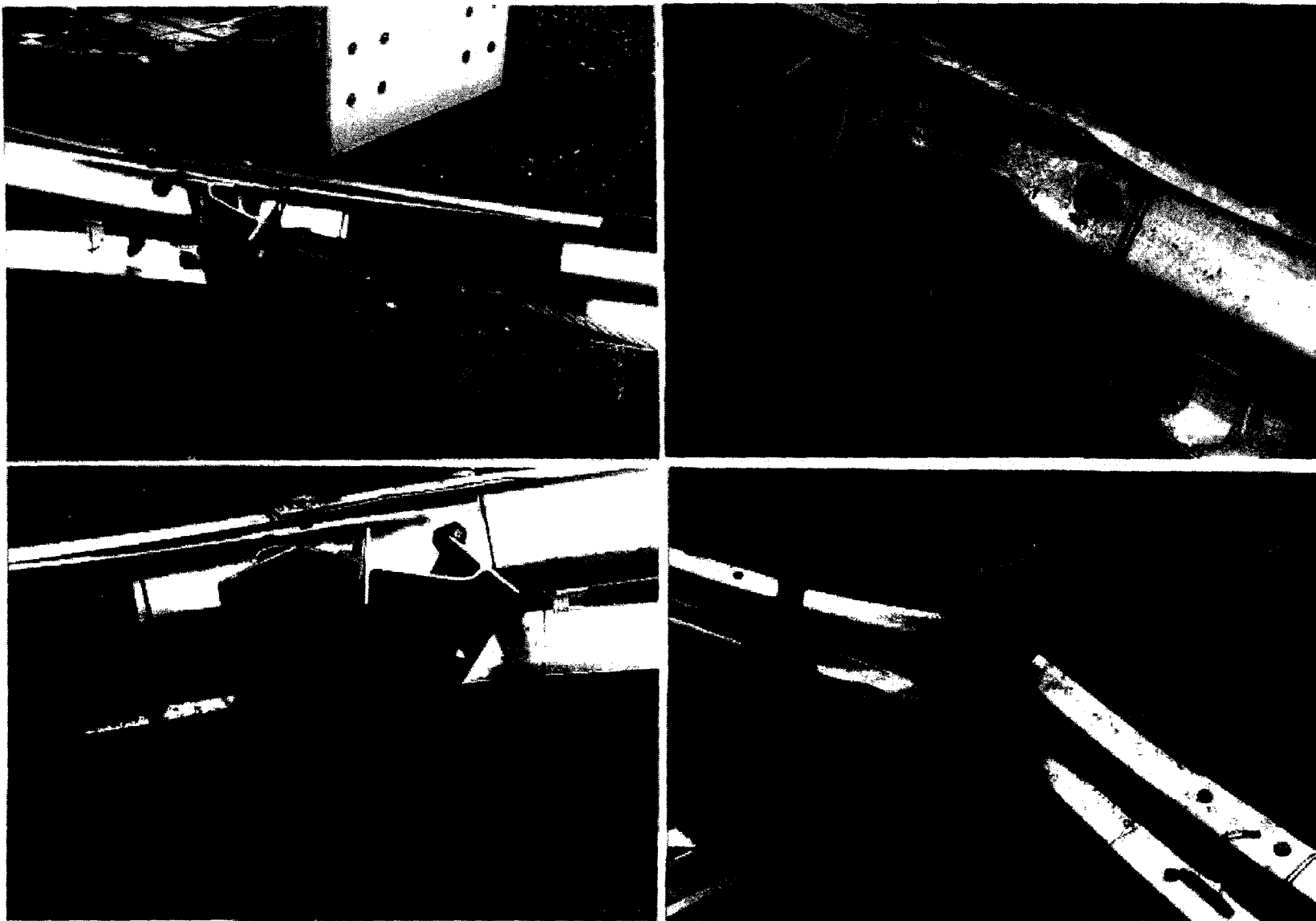


Figure 19. Post-test photographs, test 00P014 (continued).



Figure 20. Post-test photographs, test 00P015.

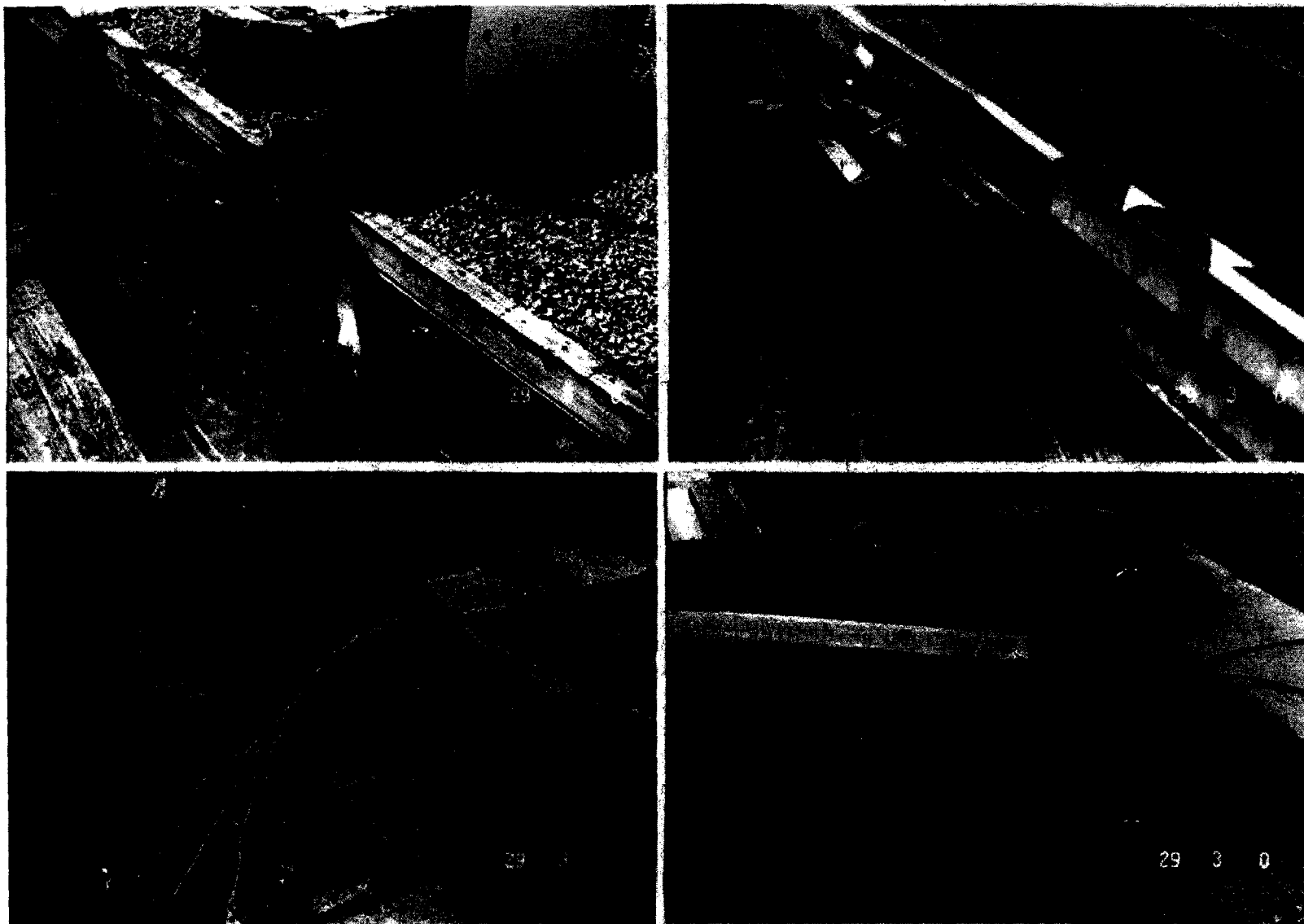


Figure 21. Post-test photographs, test 00P015 (continued).

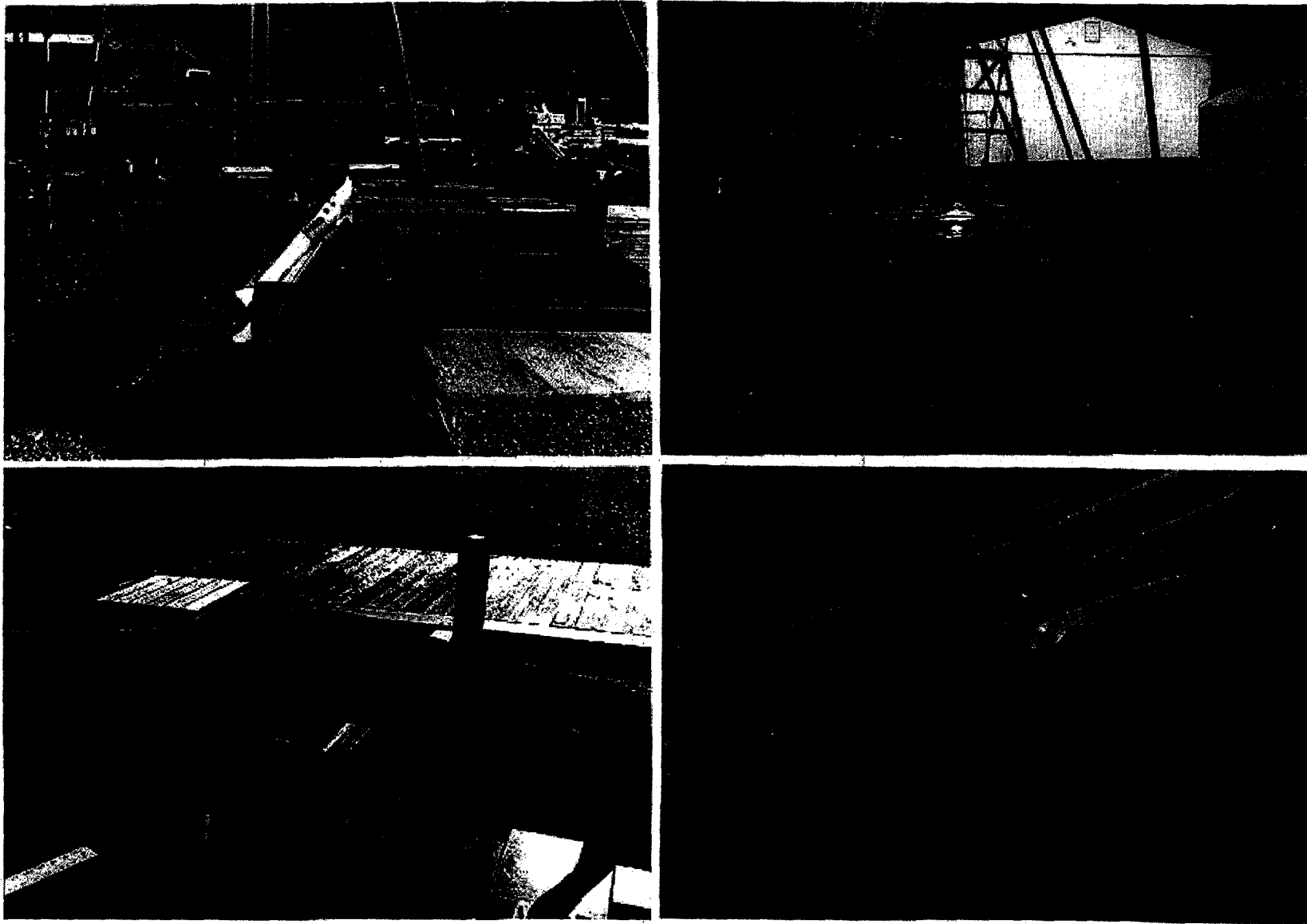


Figure 22. Post-test photographs, test 00P016.

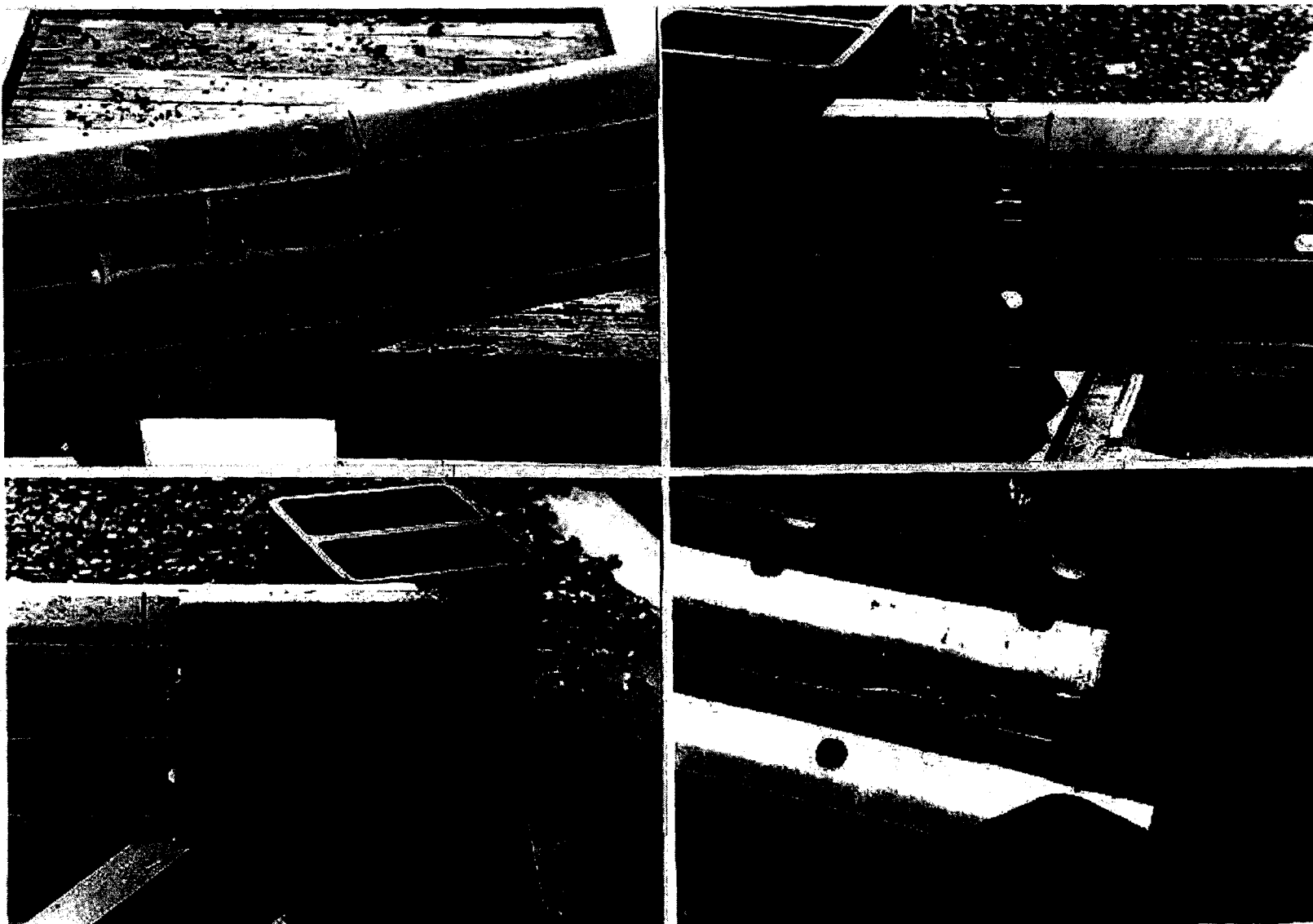


Figure 23. Post-test photographs, test 00P016 (continued).

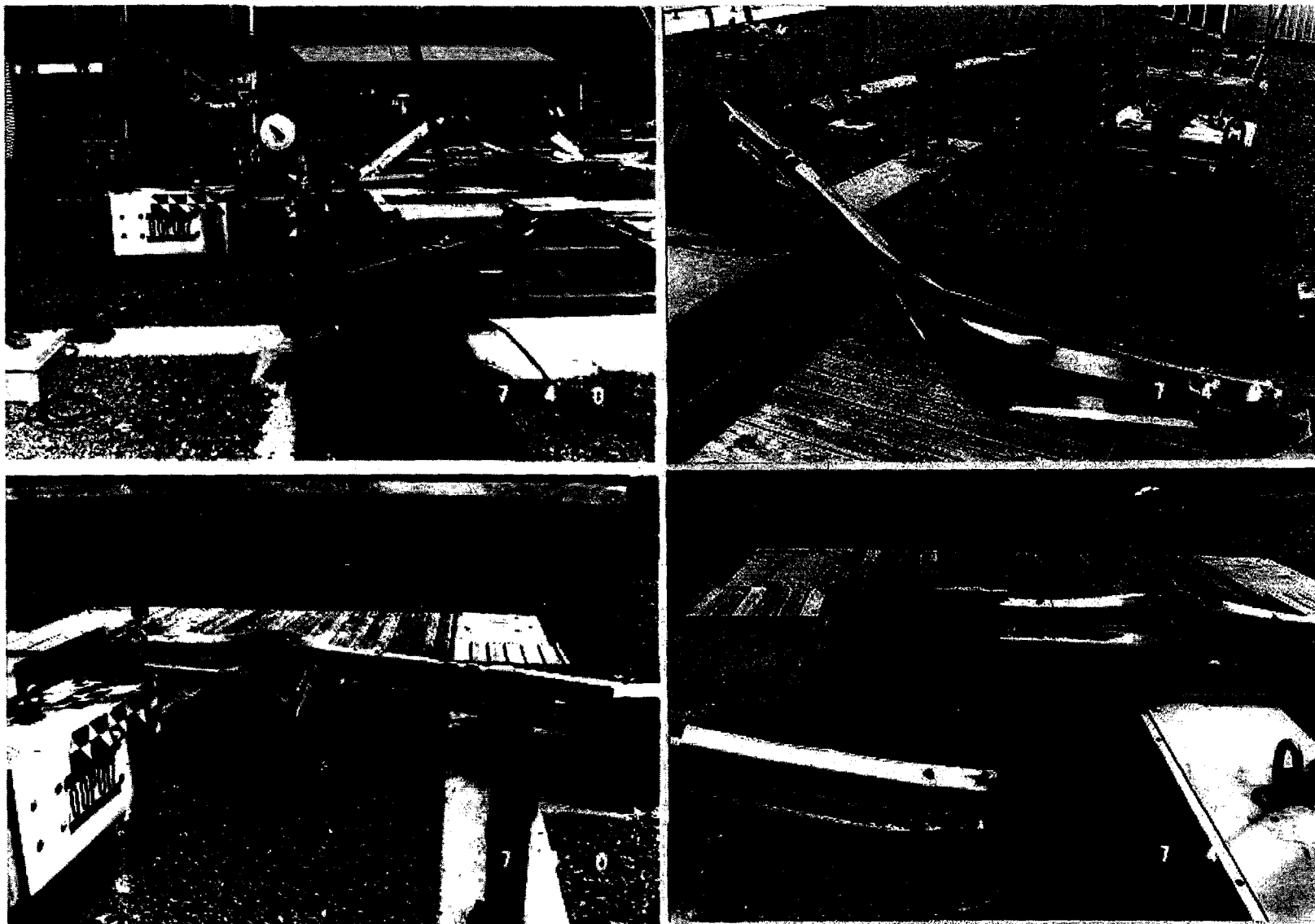


Figure 24. Post-test photographs, test 00P017.

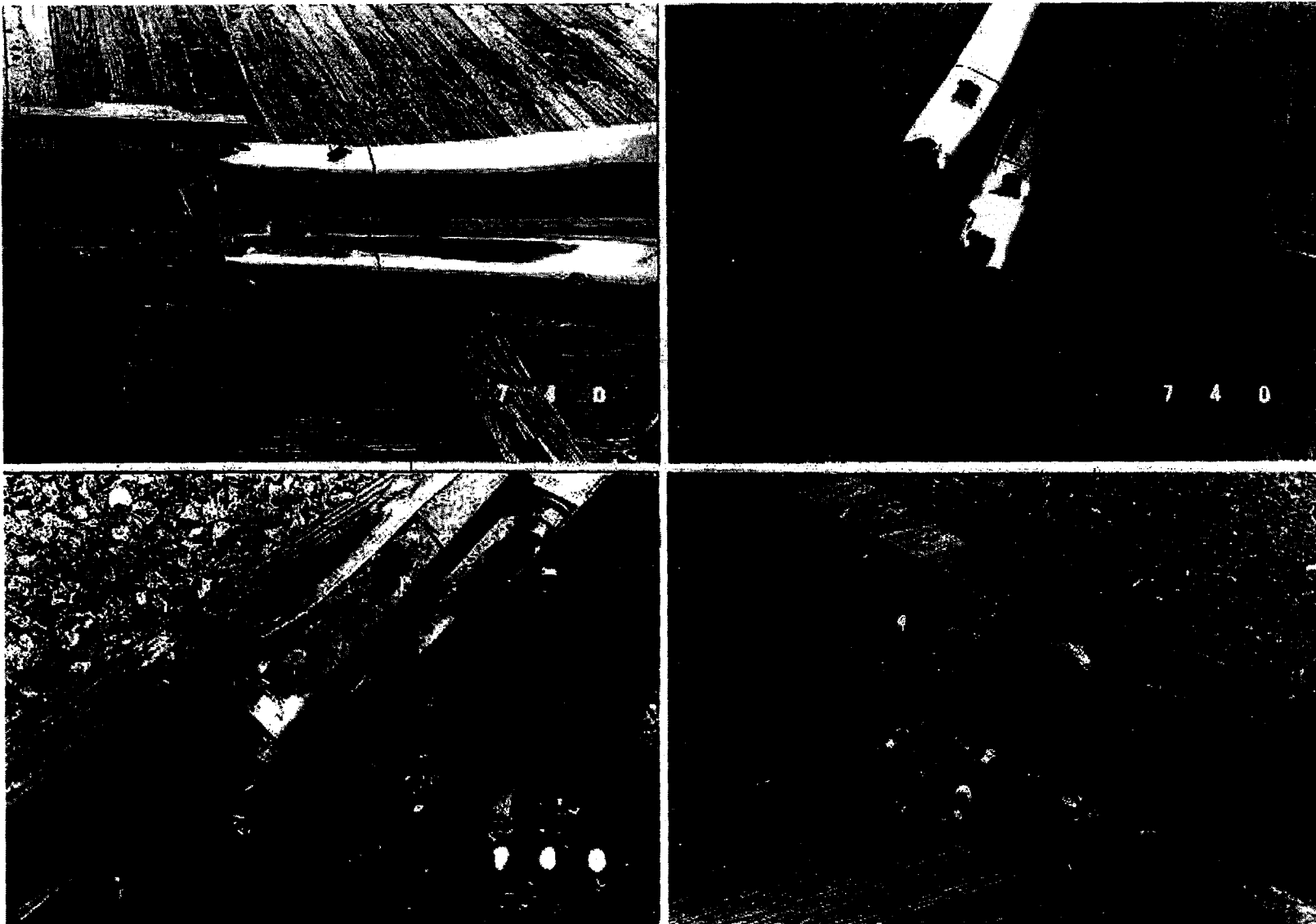


Figure 25. Post-test photographs, test 00P017 (continued).

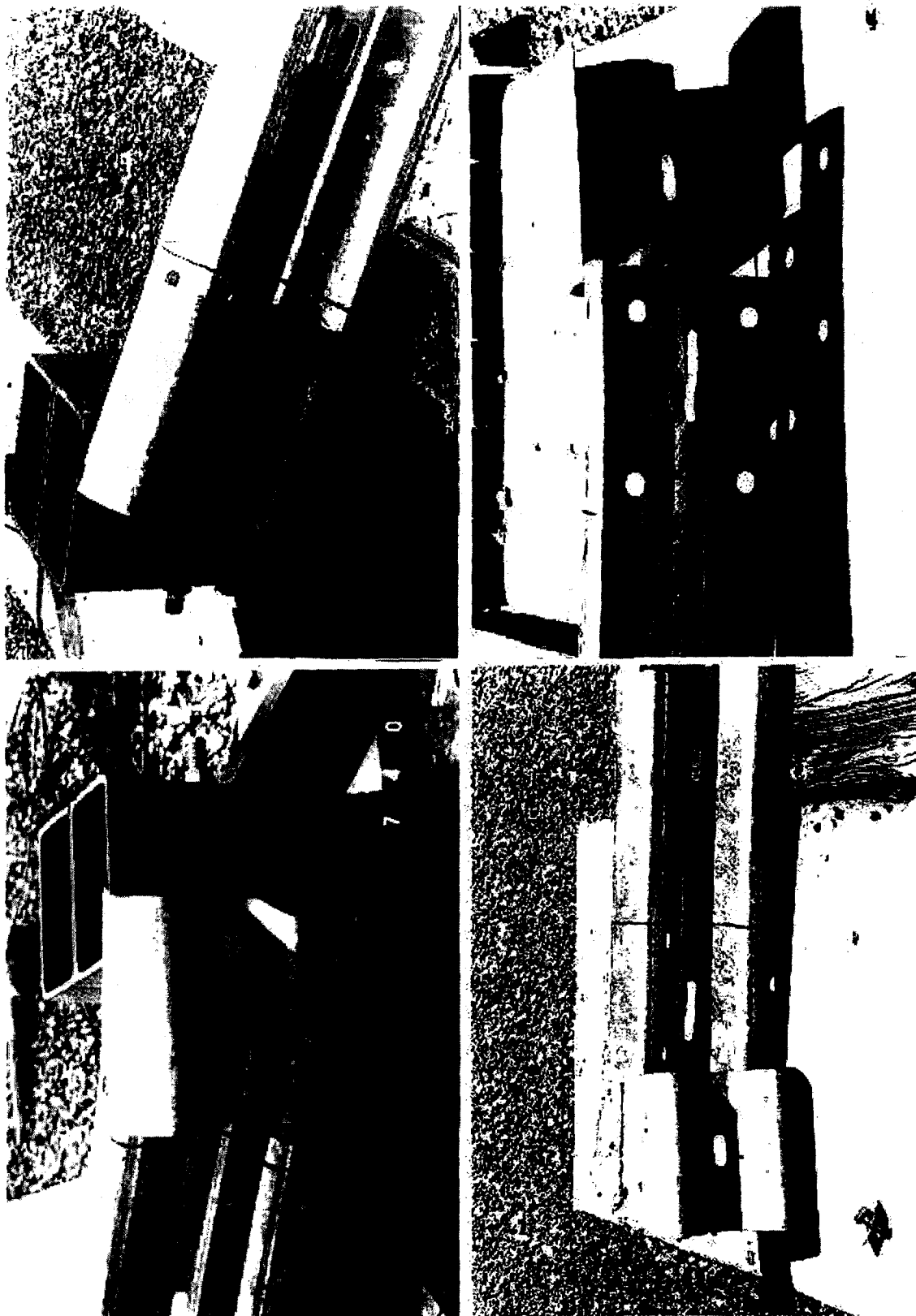


Figure 26. Additional post-test photographs, test 00P017.

APPENDIX B: DATA PLOTS OF DATA OBTAINED FROM PENDULUM
ACCELEROMETERS

Test No. 00P007

Acceleration vs. time (class 60 data)

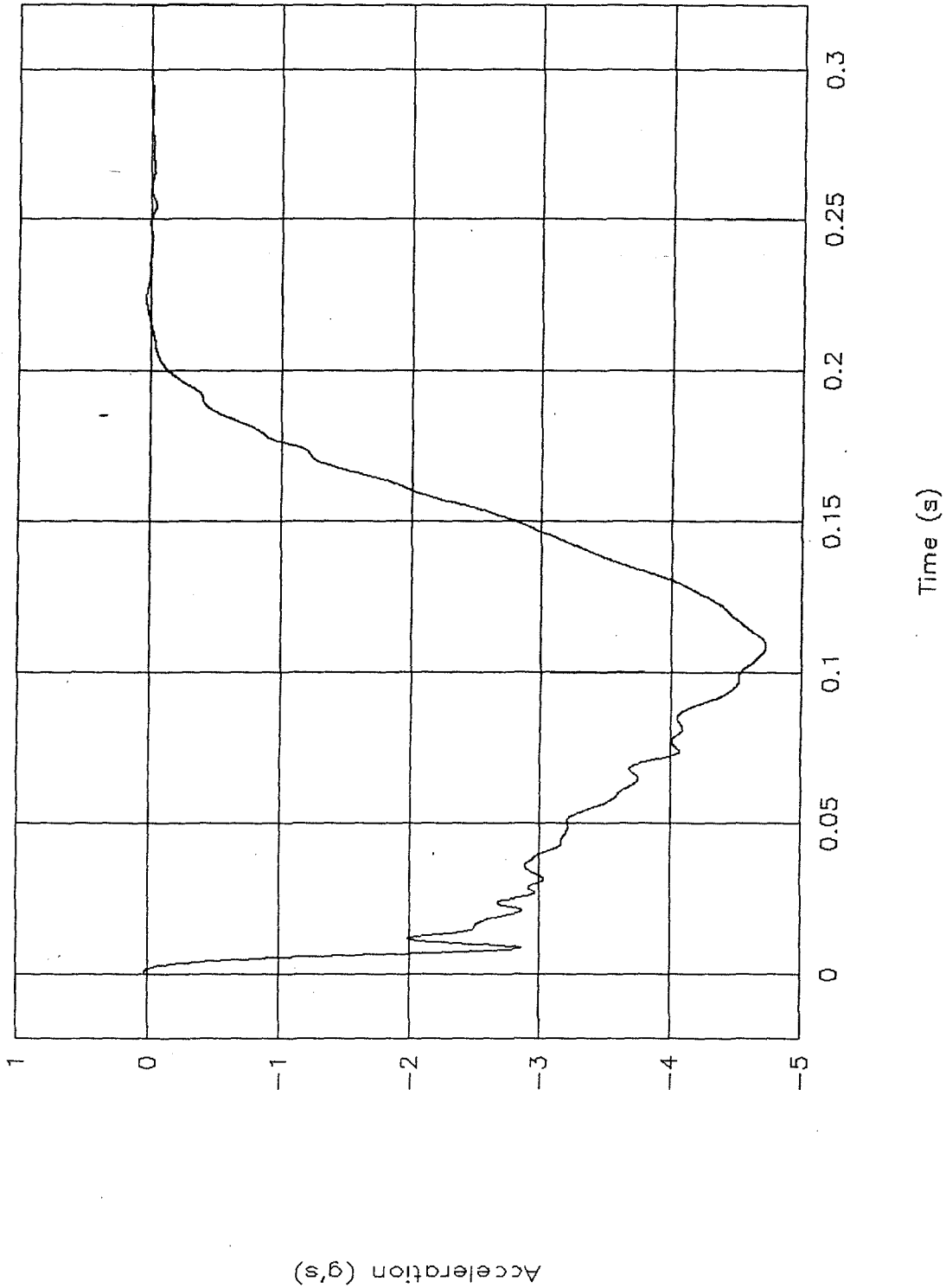


Figure 27. Acceleration vs. time (class 60 data), test 00P007.

Test No. 00P007

Velocity vs. time

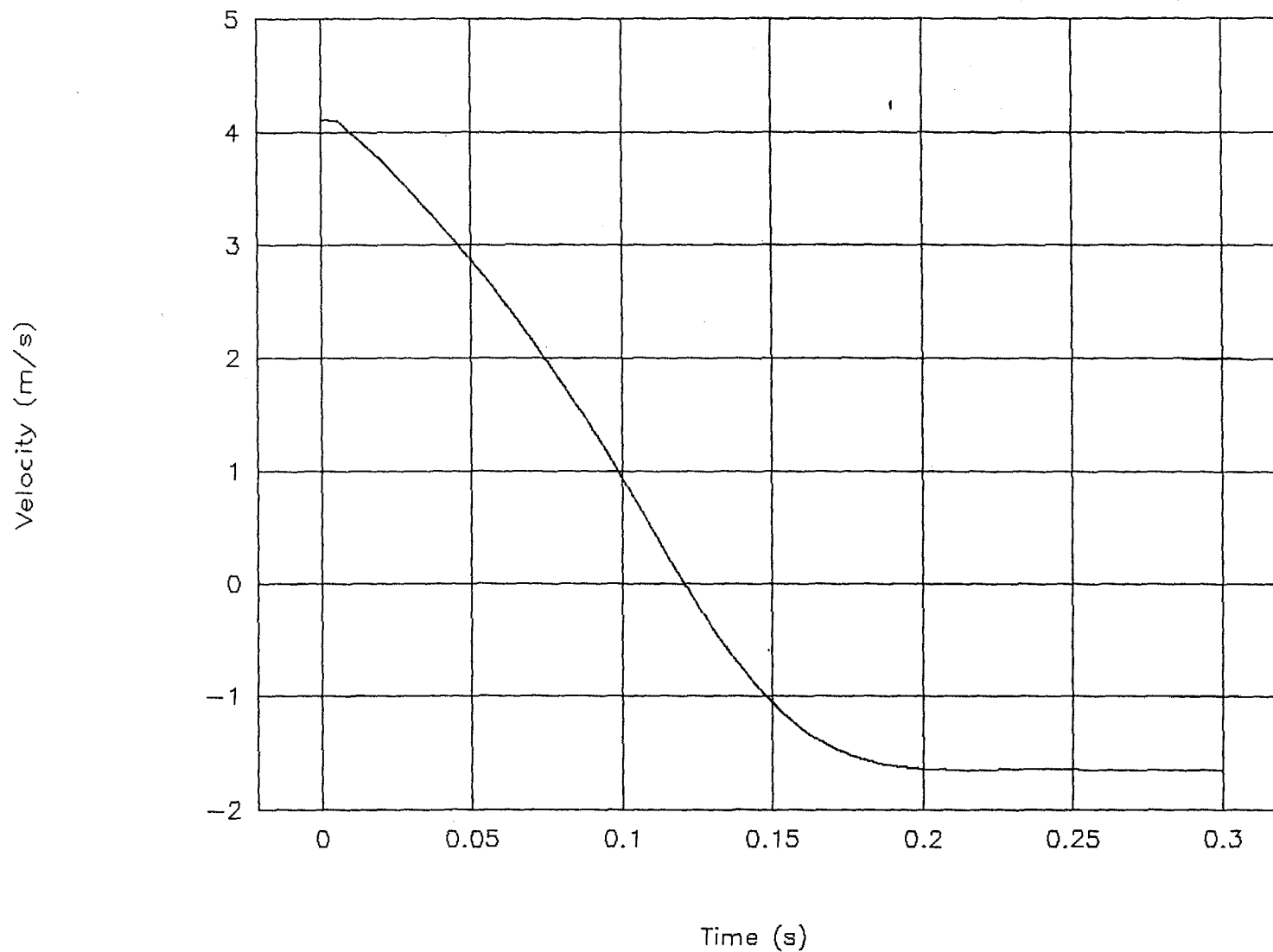


Figure 28. Velocity vs. time, test 00P007.

Test No. 00P007

Displacement vs. time

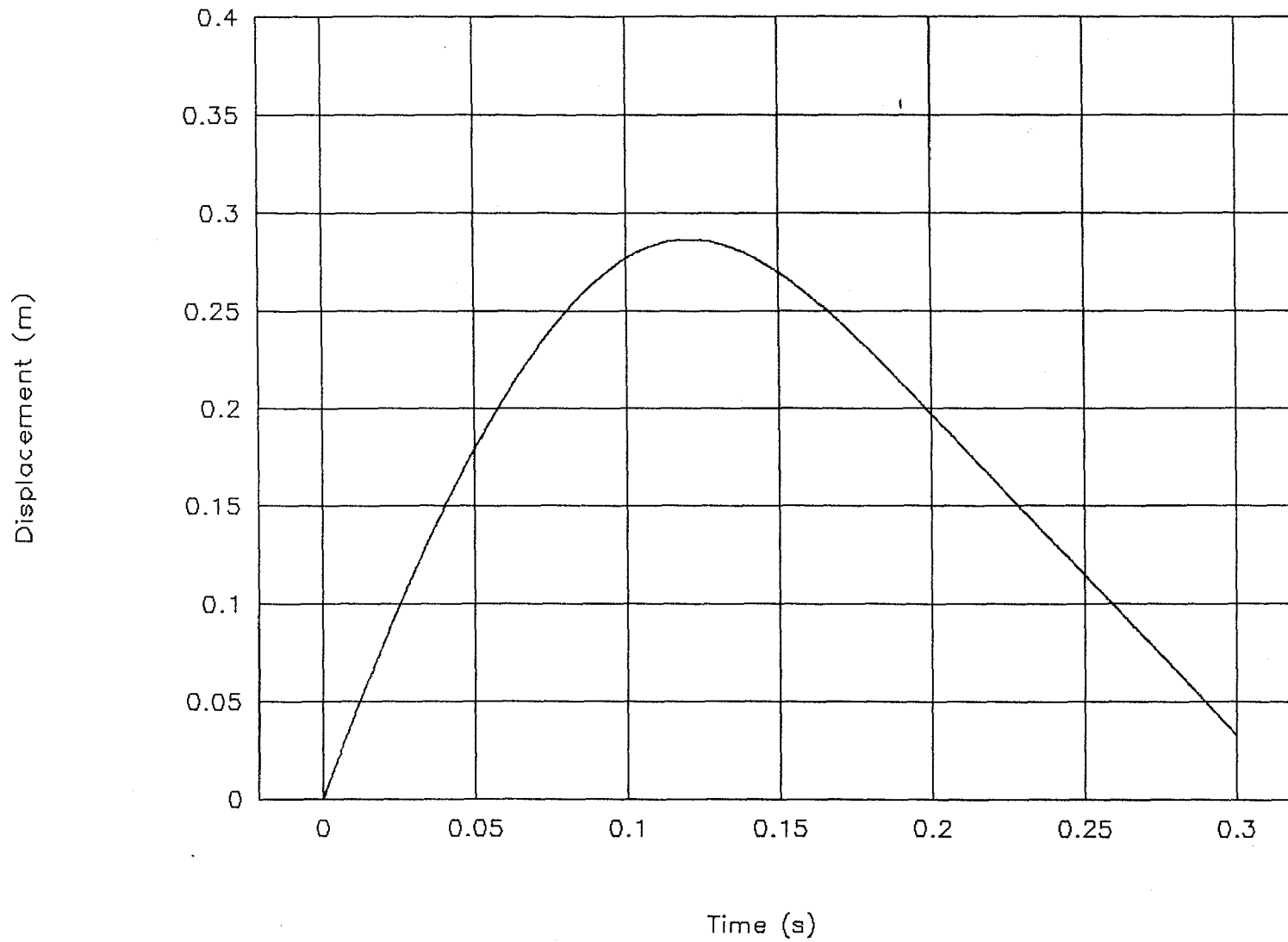


Figure 29. Displacement vs. time, test 00P007.

Test No. 00P007

Force vs. displacement

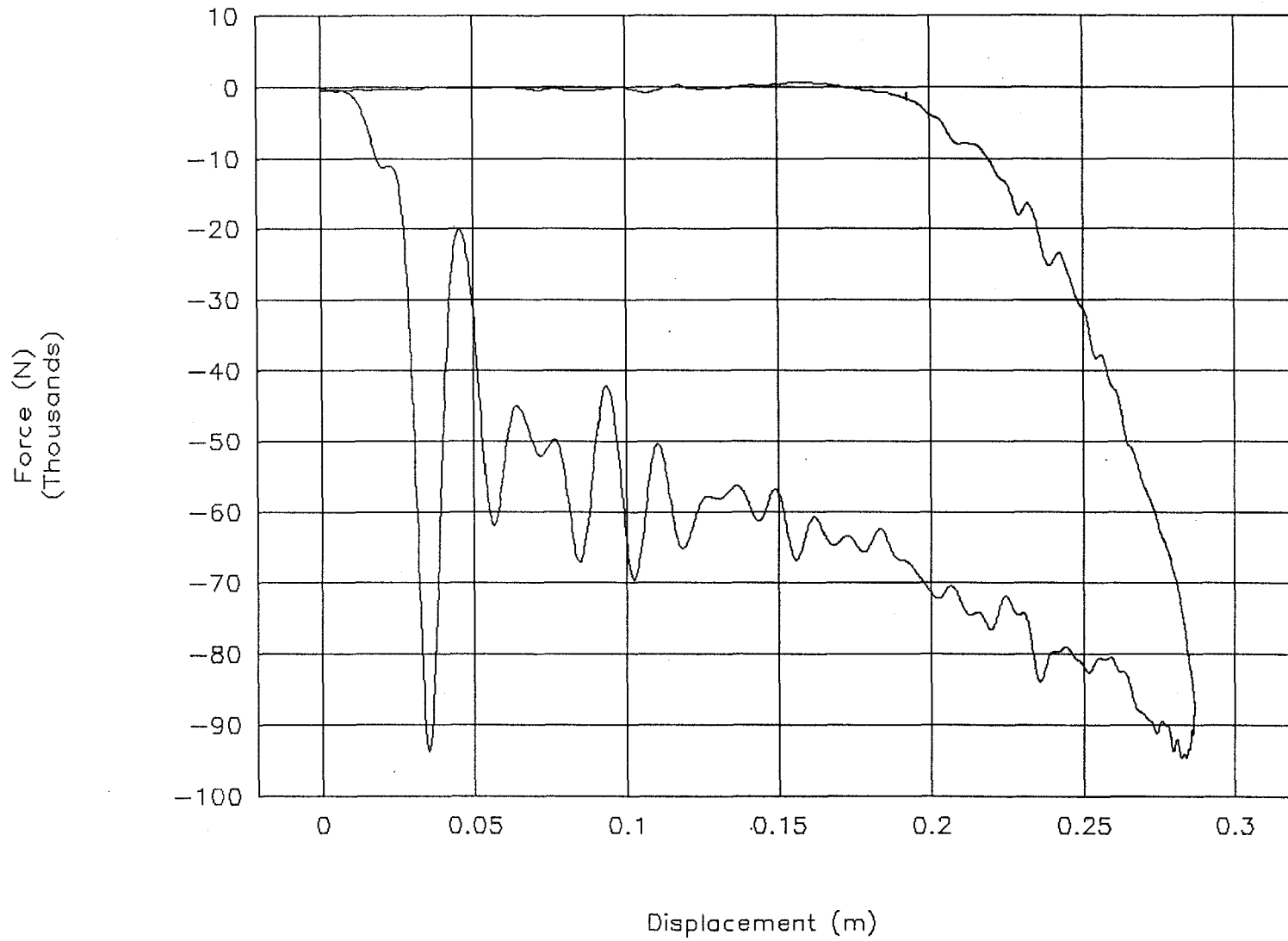


Figure 30. Force vs. displacement, test 00P007.

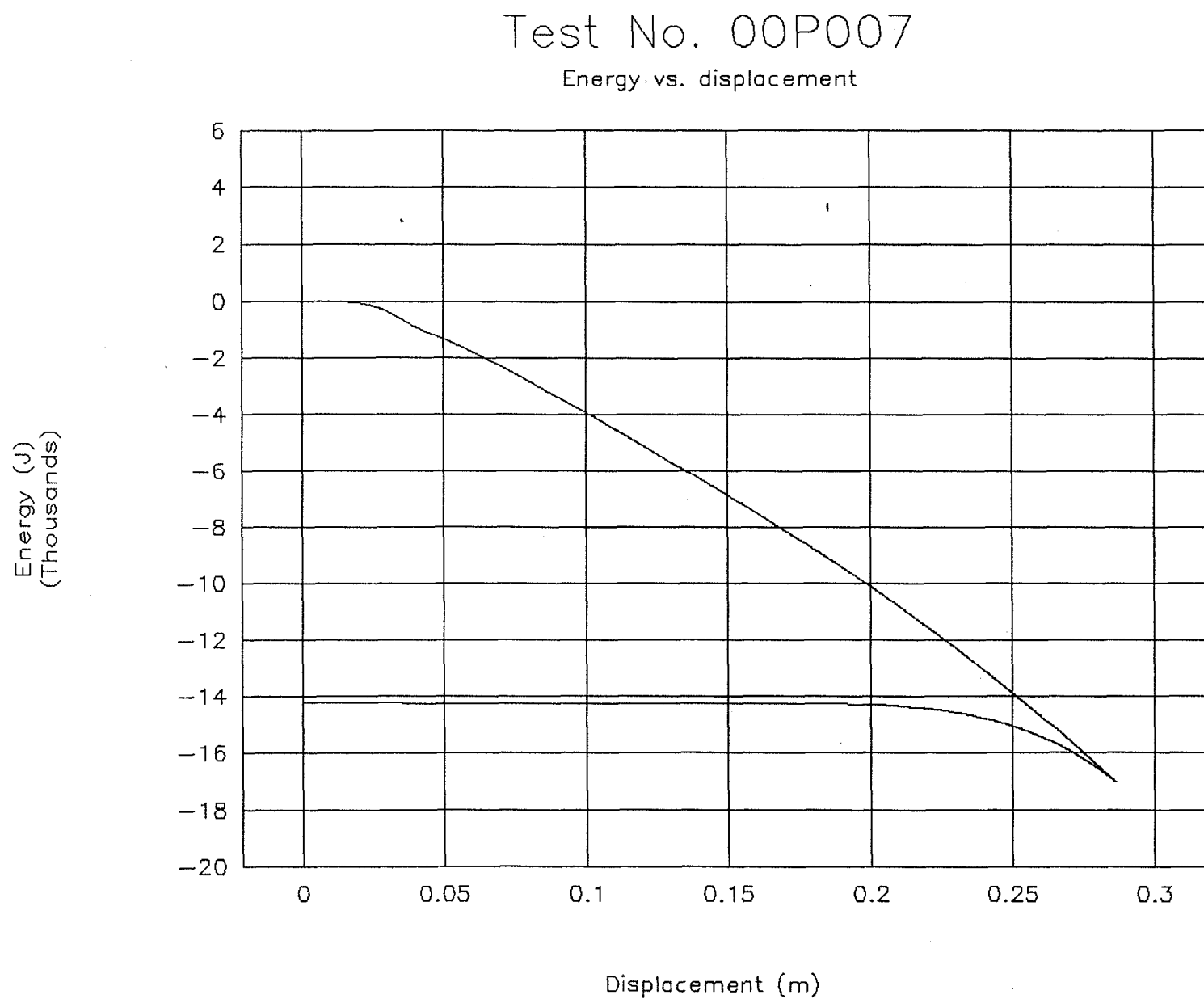


Figure 31. Energy vs. displacement, test 00P007.

Test No. 00P008

Velocity vs. time

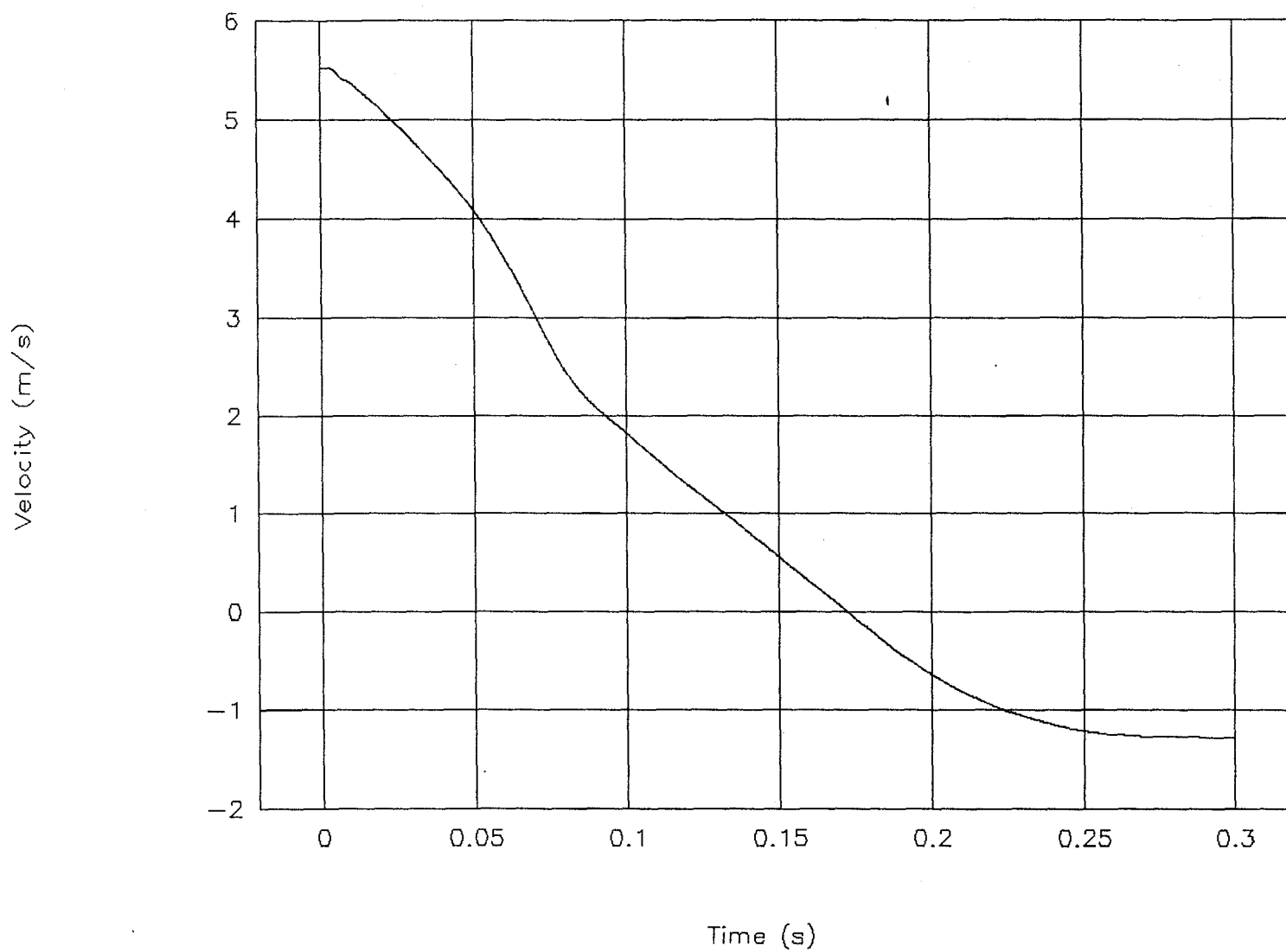


Figure 33. Velocity vs. time, test 00P008.

Test No. 00P008

Displacement vs. time

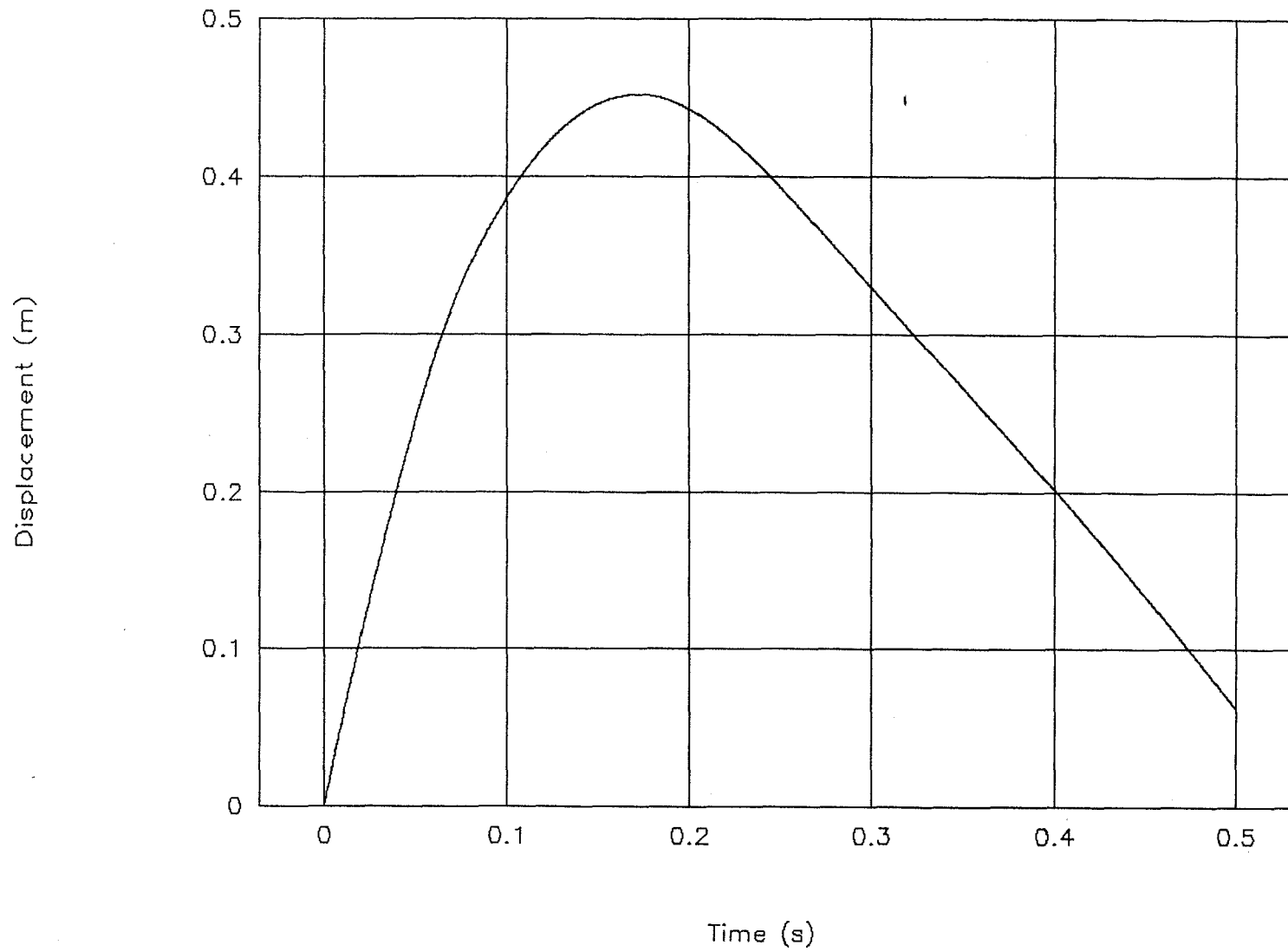


Figure 34. Displacement vs. time, test 00P008.

Test No. 00P008

Energy vs. displacement

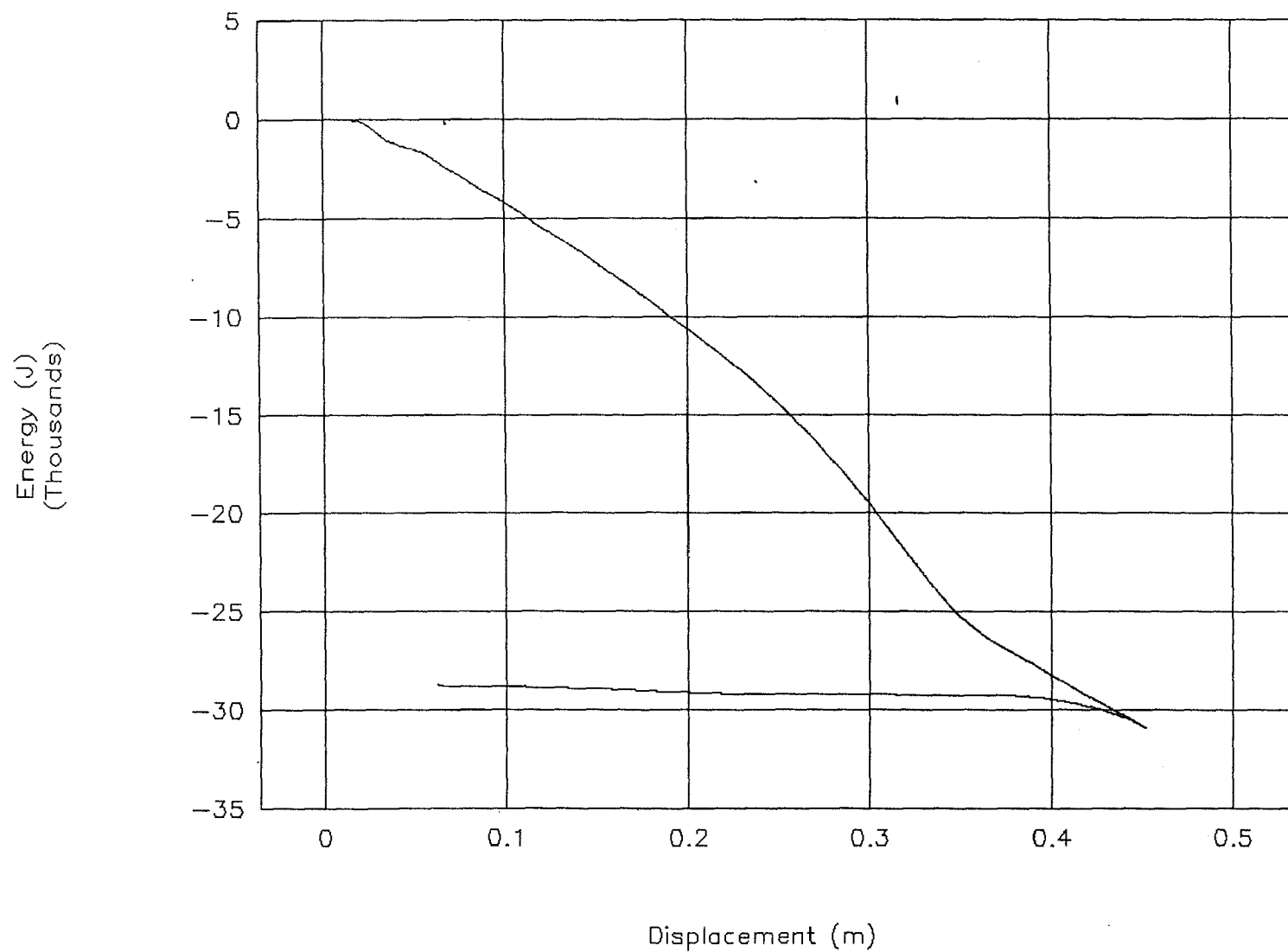


Figure 36. Energy vs. displacement, test 00P008.

Test No. 00P010

Acceleration vs. time (class 60 data)

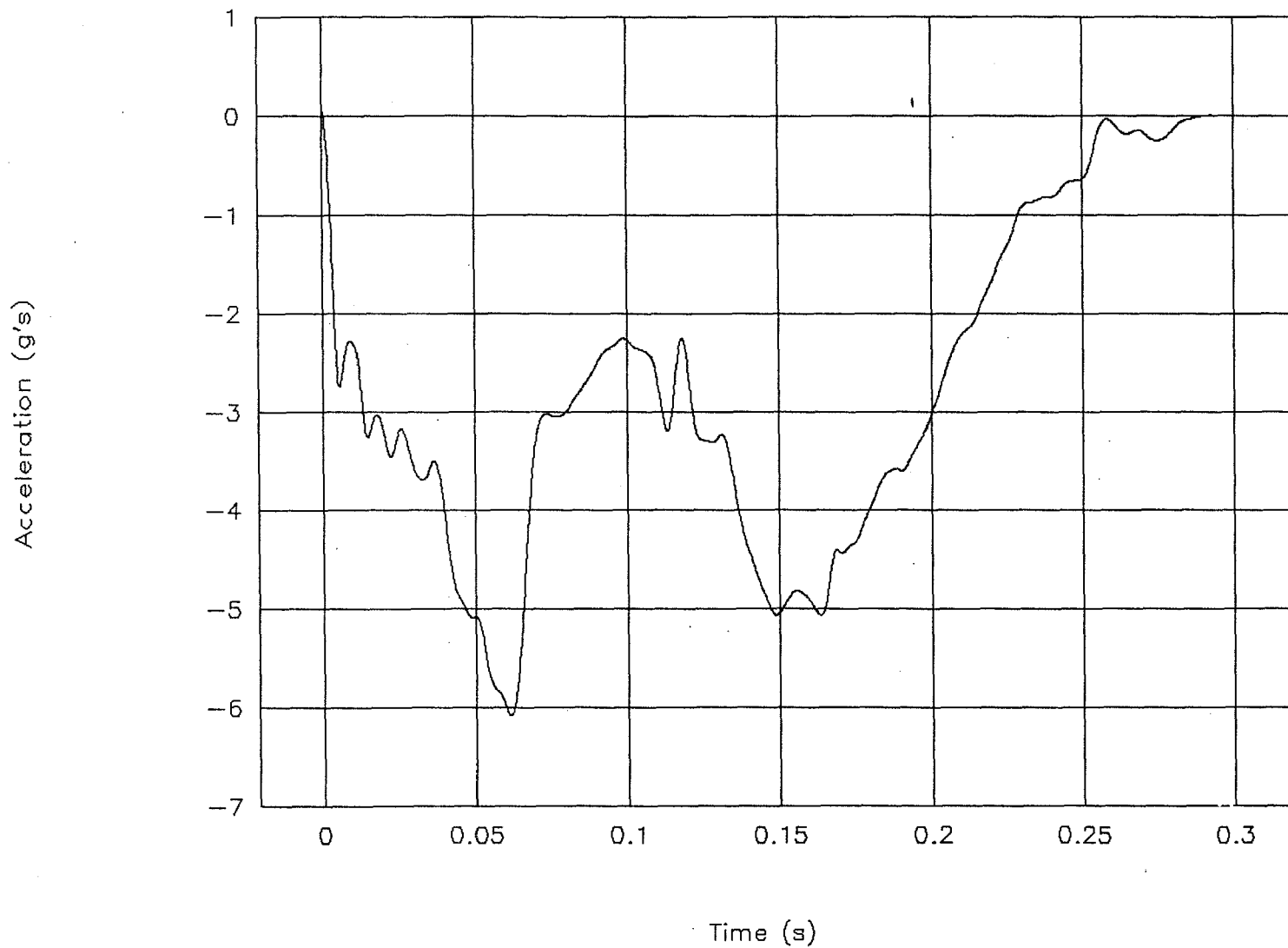


Figure 37. Acceleration vs. time (class 60 data), test 00P010.

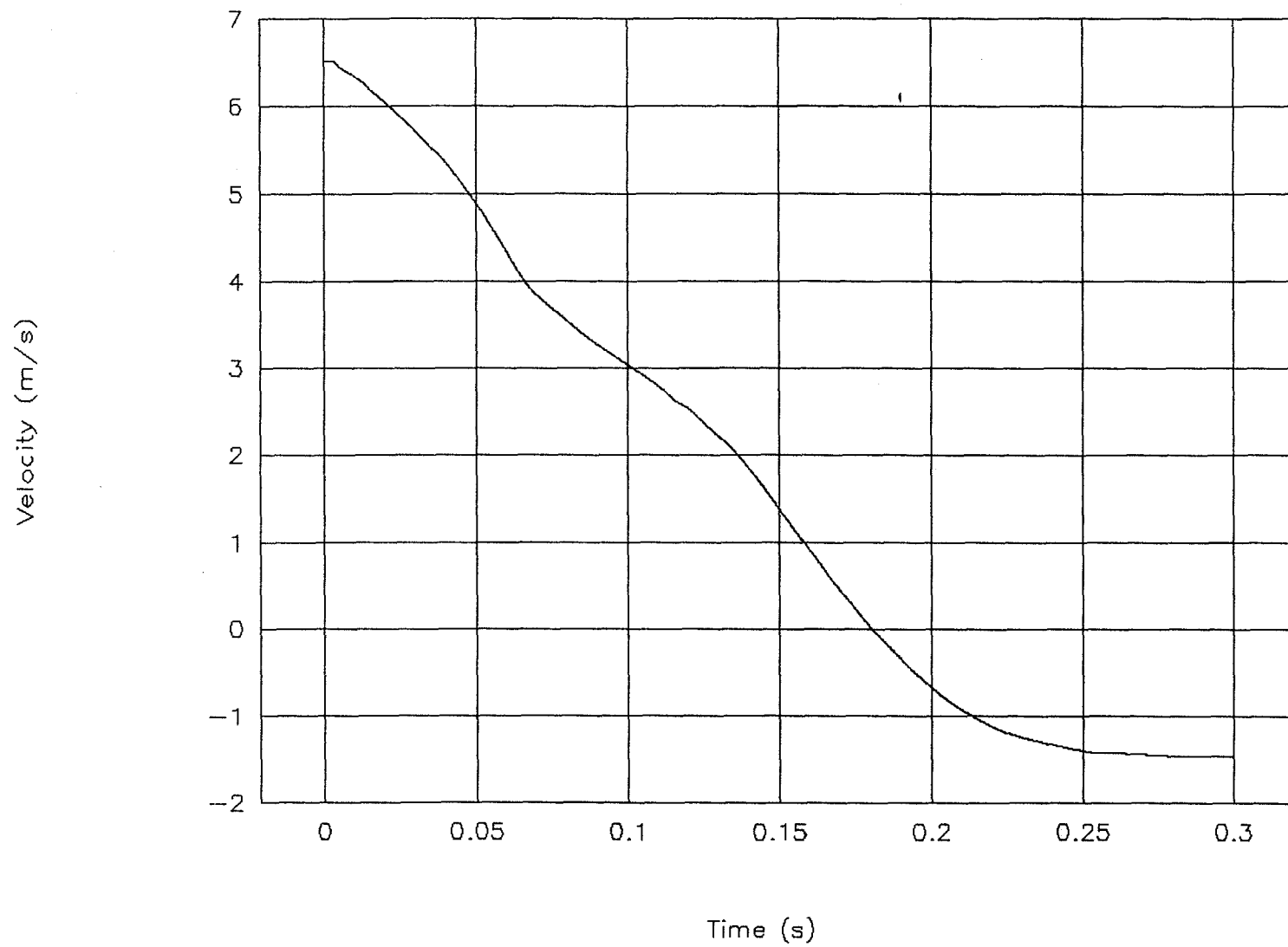


Figure 38. Velocity vs. time, test 00P010.

Test No. 00P010

Displacement vs. time

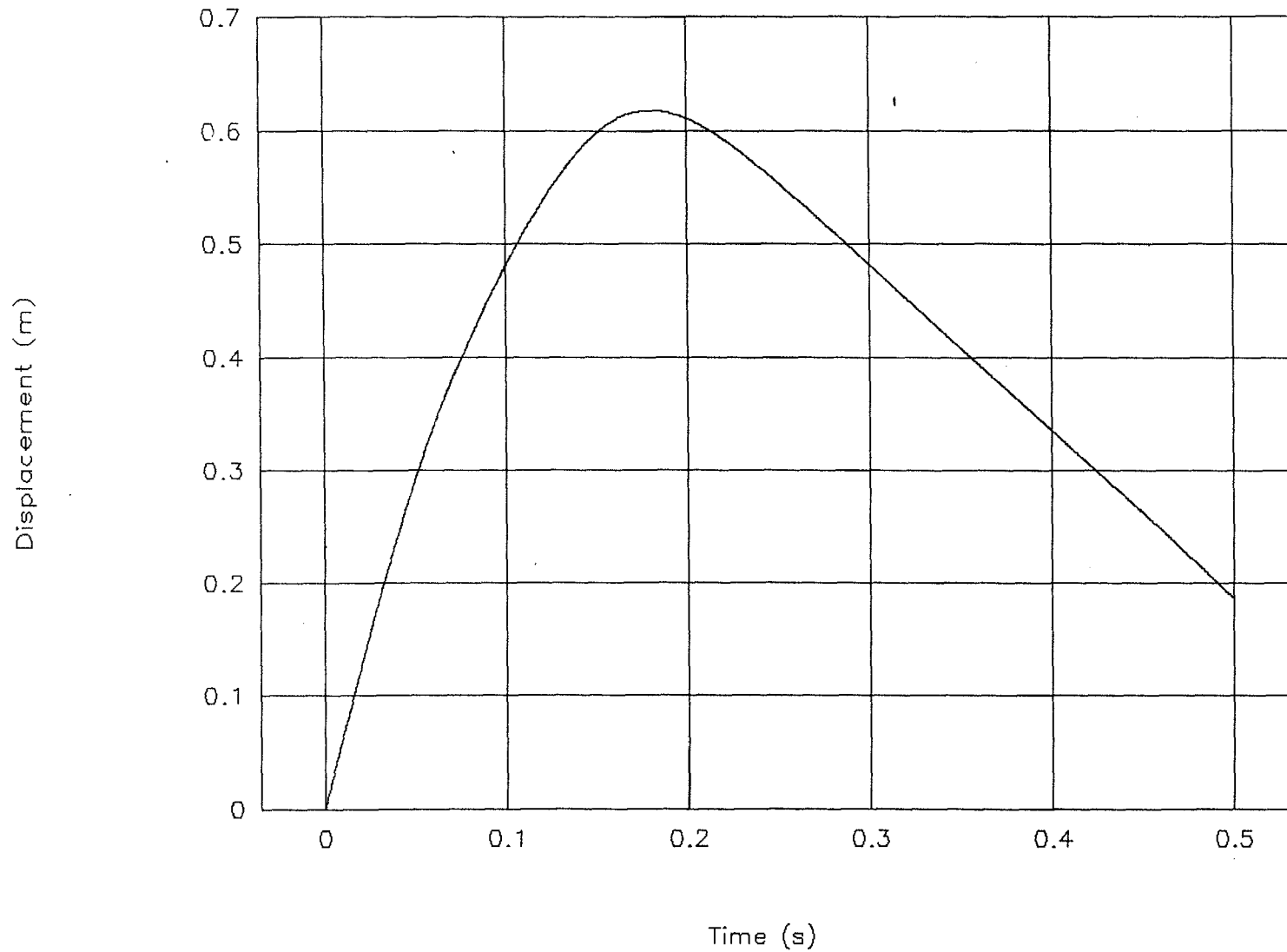


Figure 39. Displacement vs. time, test 00P010.

Test No. 00P010

Force vs. displacement

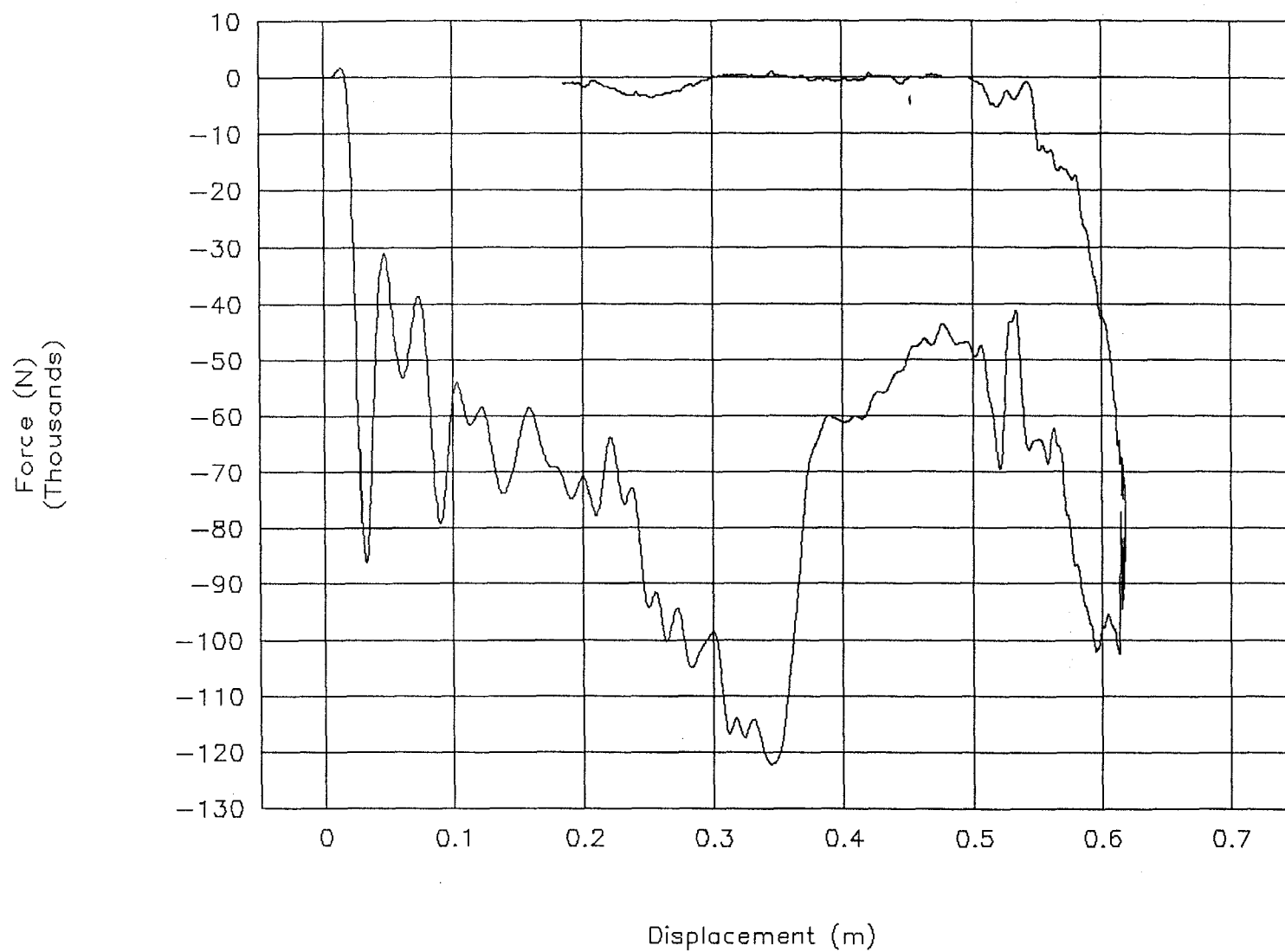


Figure 40. Force vs. displacement, test 00P010.

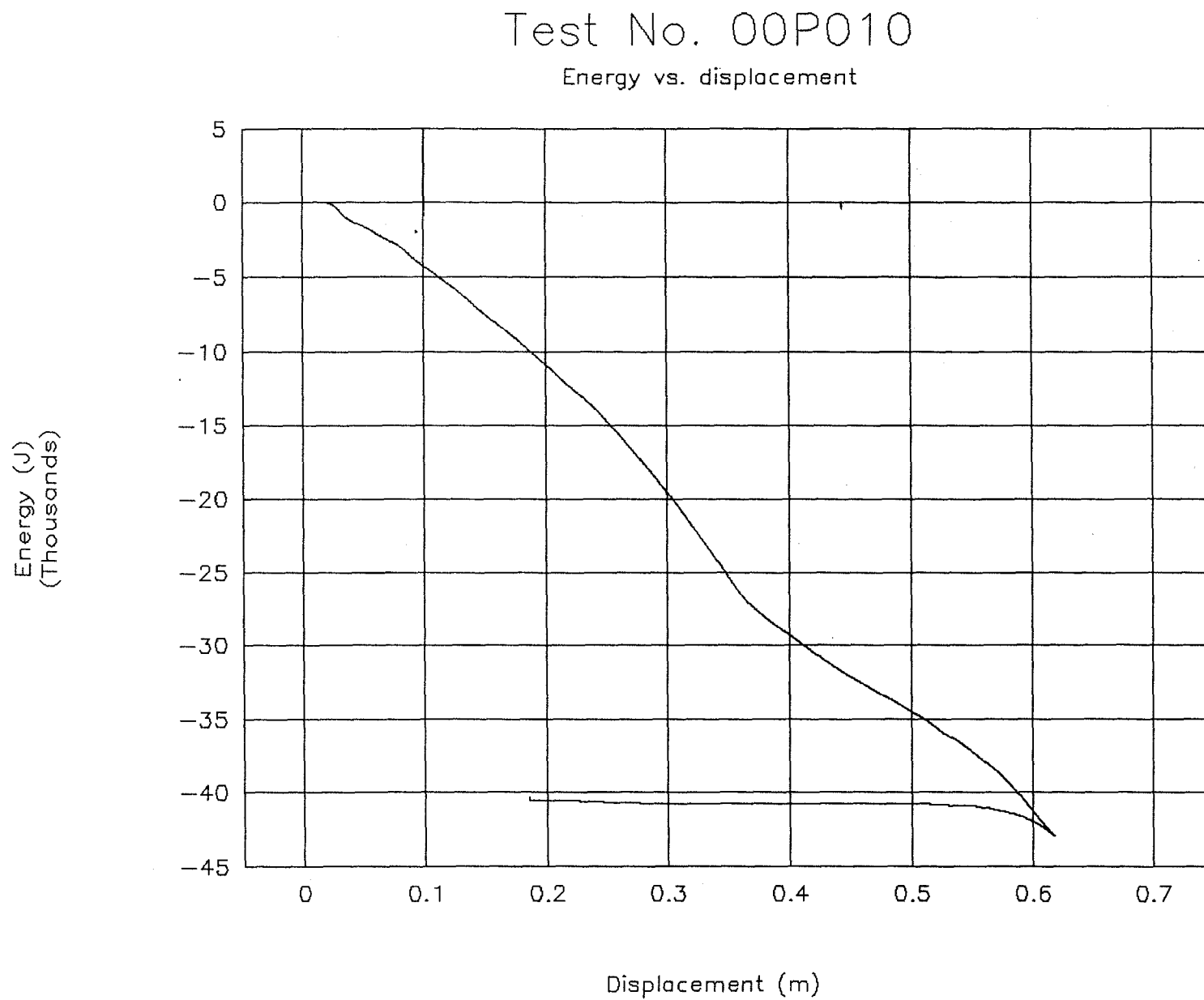


Figure 41. Energy vs. displacement, test 00P010.

Test No. 00P011
Acceleration vs. time (class 60 data)

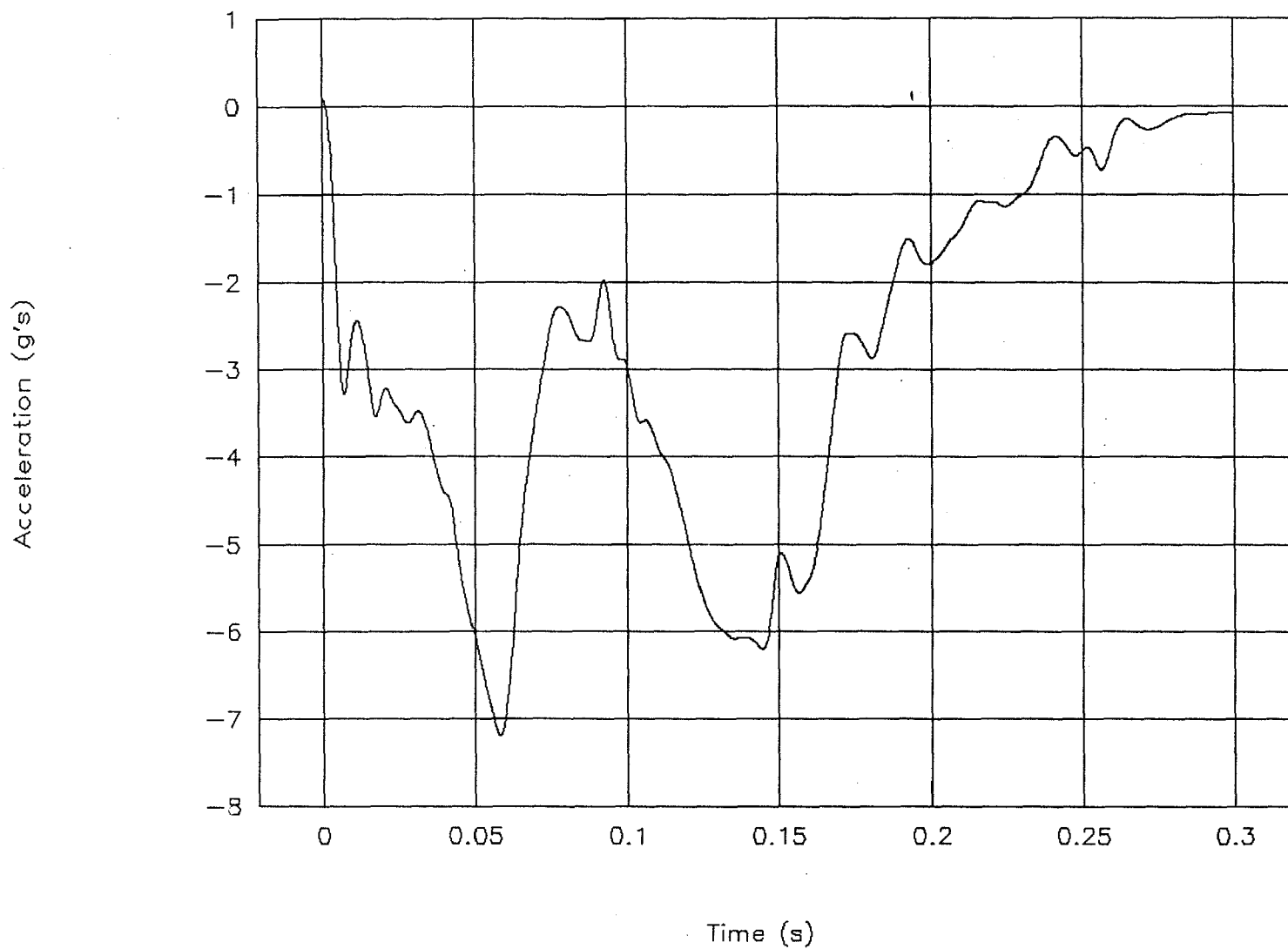


Figure 42. Acceleration vs. time (class 60 data), test 00P011.

Test No. 00P011

Velocity vs. time

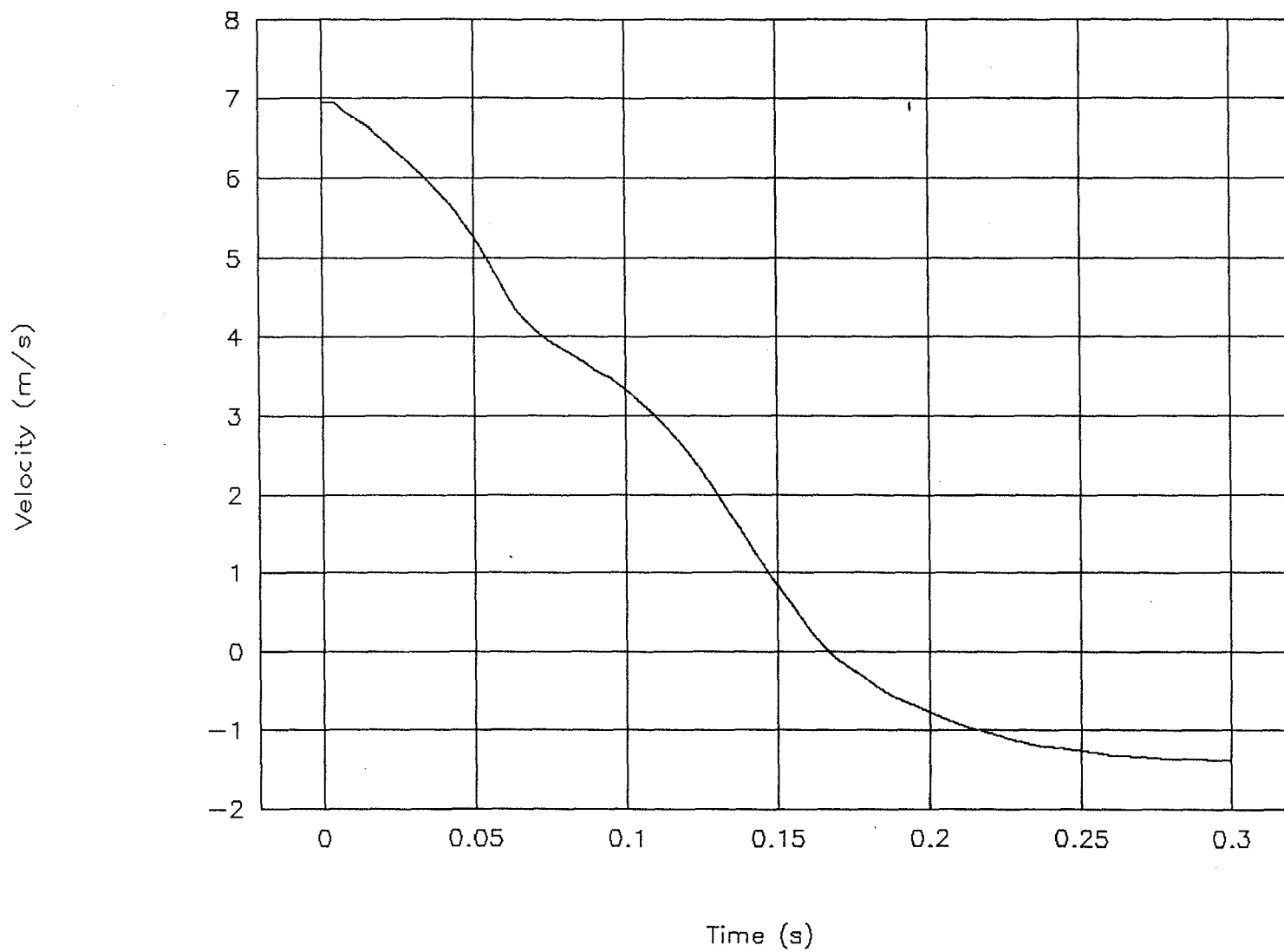


Figure 43. Velocity vs. time, test 00P011.

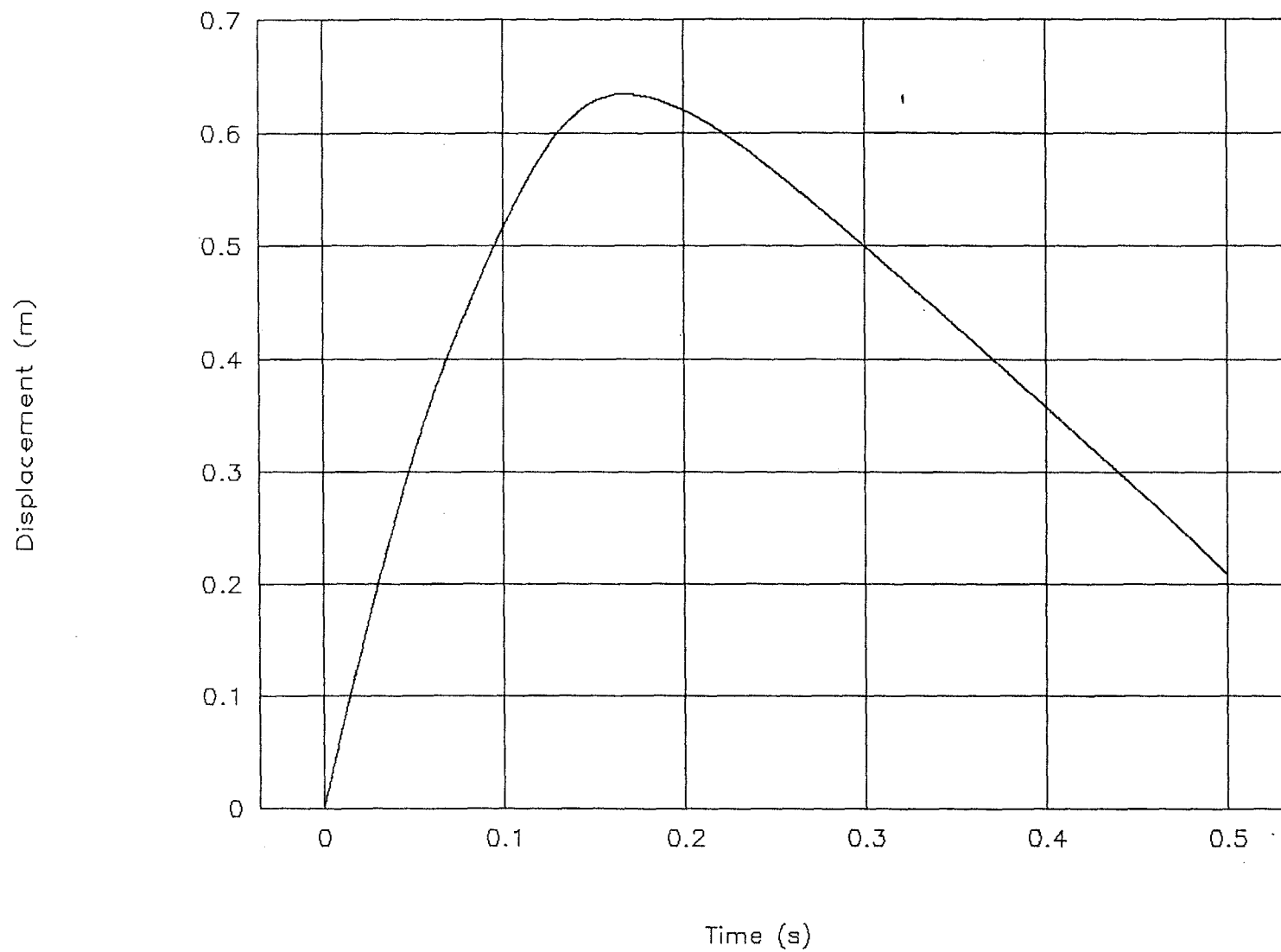


Figure 44. Displacement vs. time, test 00P011.

Test No. 00P011

Force vs. displacement

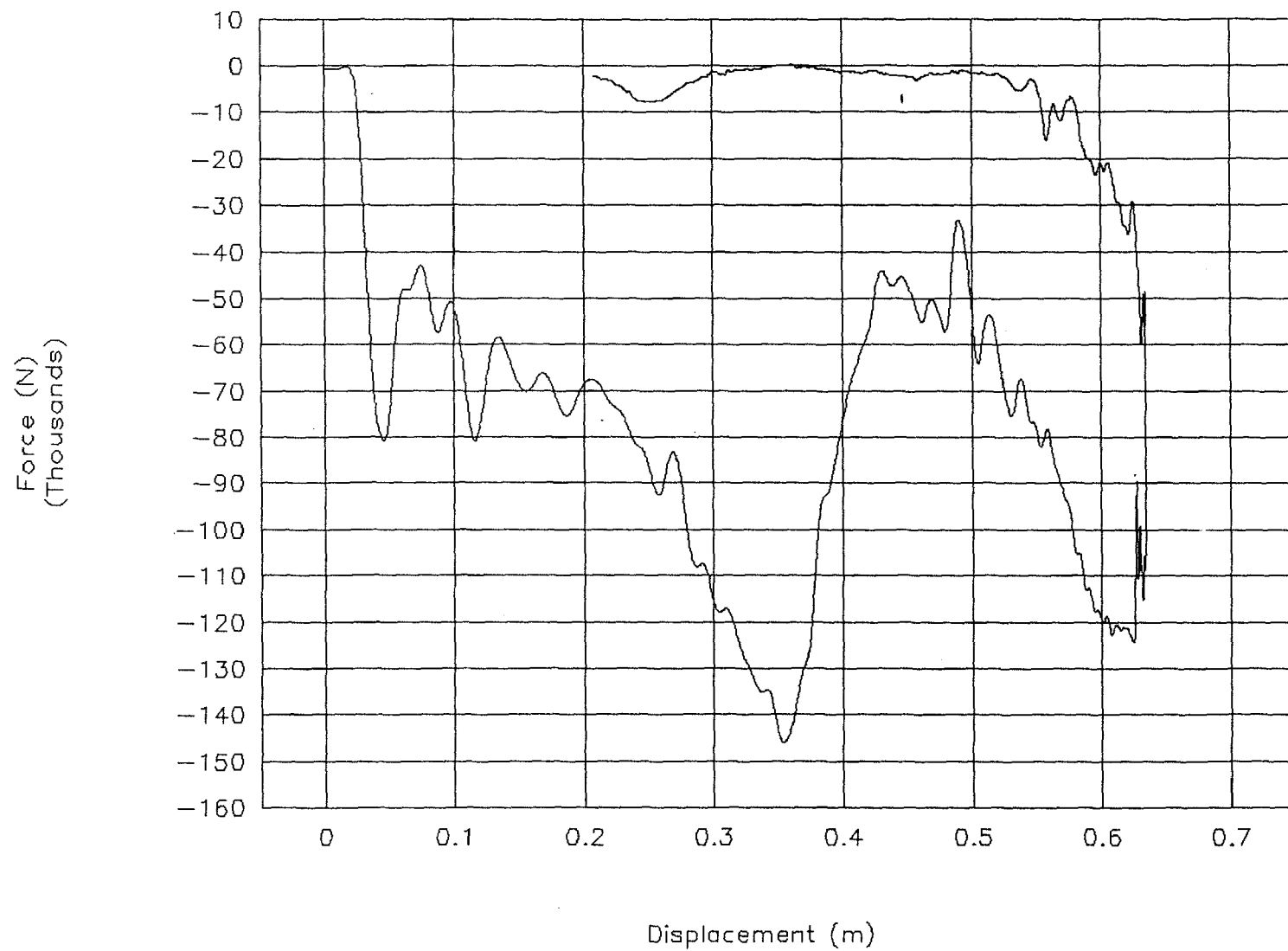


Figure 45. Force vs. displacement, test 00P011.

Test No. 00P011

Energy vs. displacement

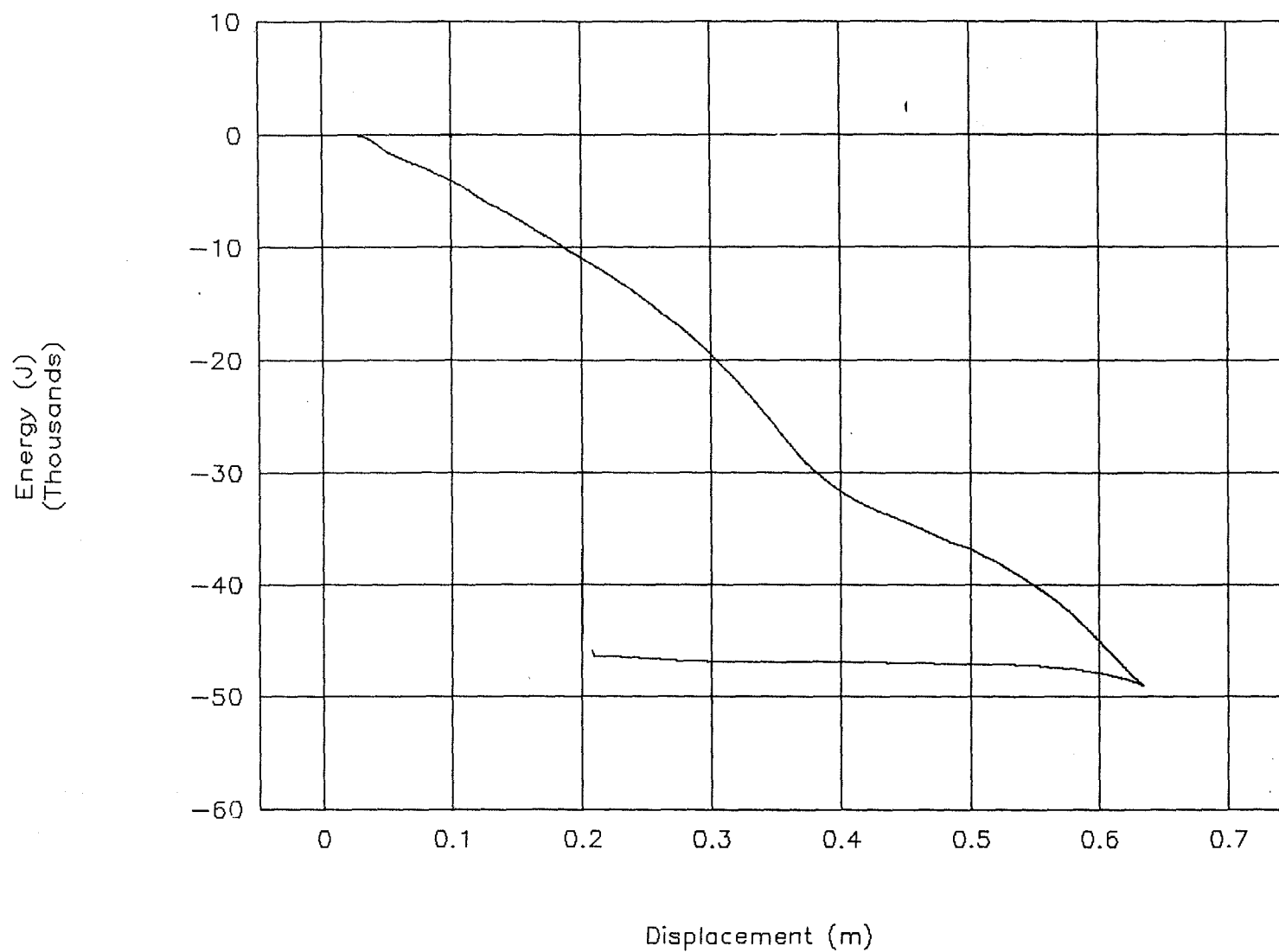


Figure 46. Energy vs. displacement, test 00P011.

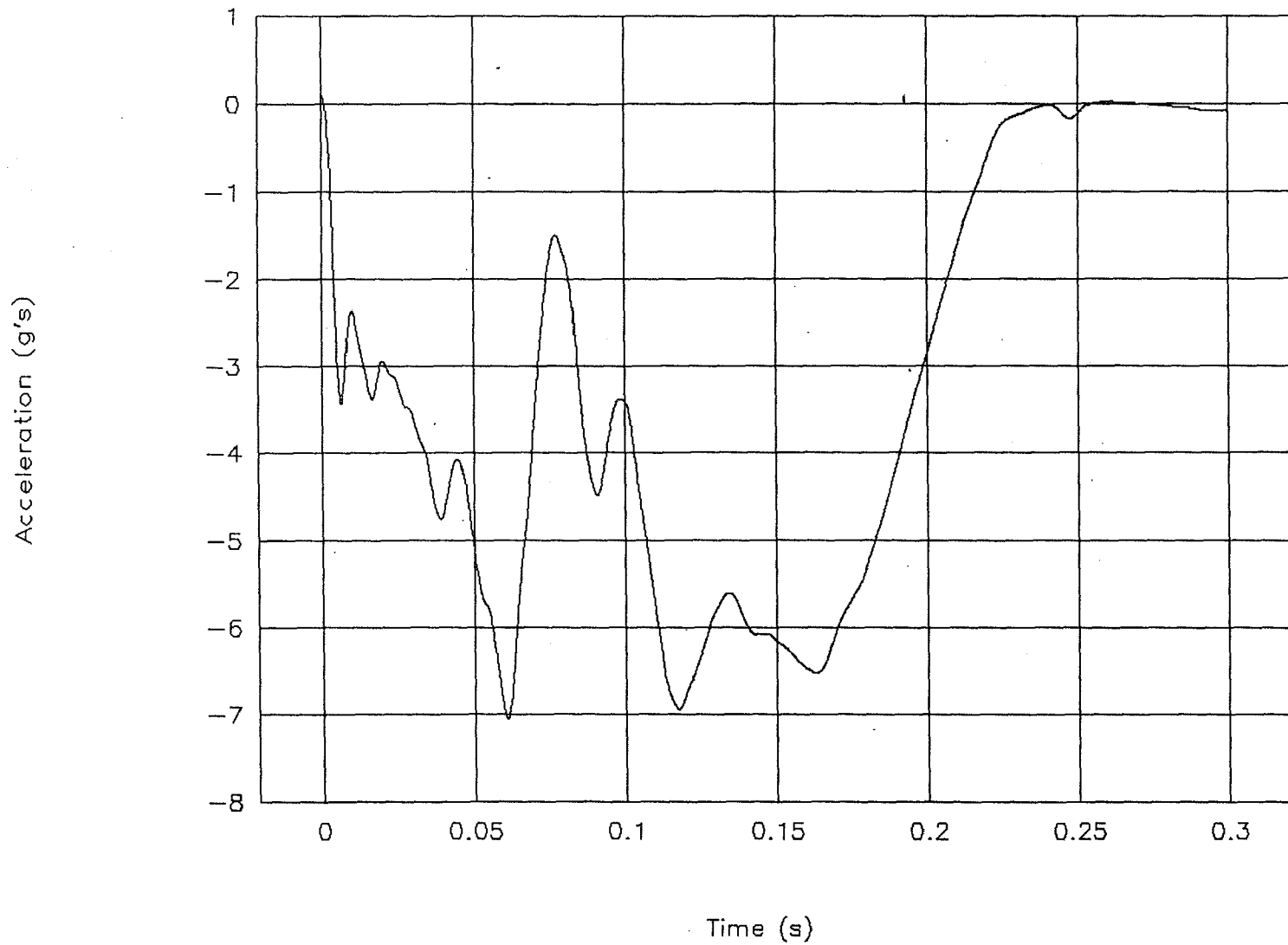


Figure 47. Acceleration vs. time (class 60 data), test 00P012.

Test No. 00P012

Velocity vs. time

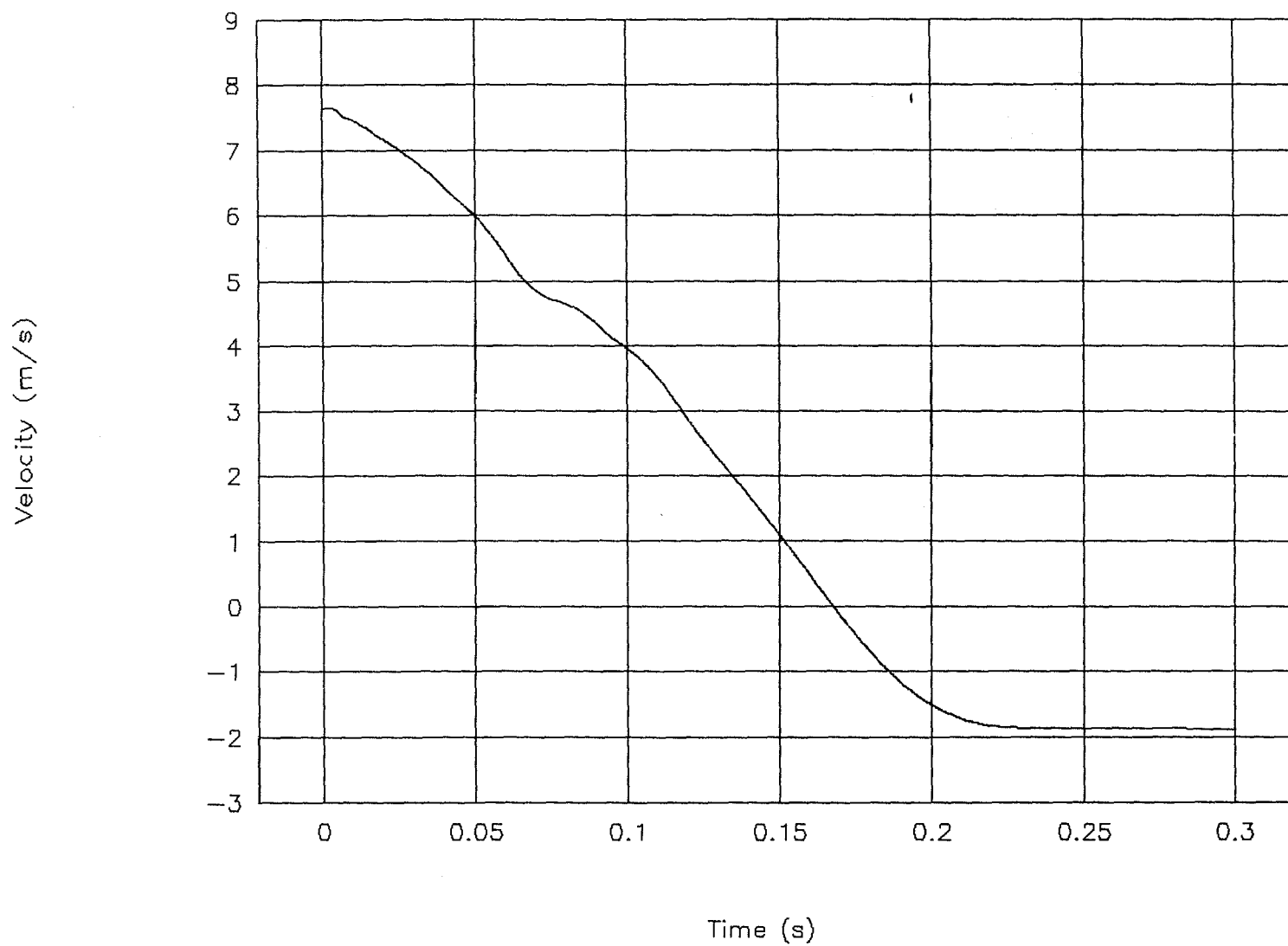


Figure 48. Velocity vs. time, test 00P012.

Test No. 00P012

Displacement vs. time

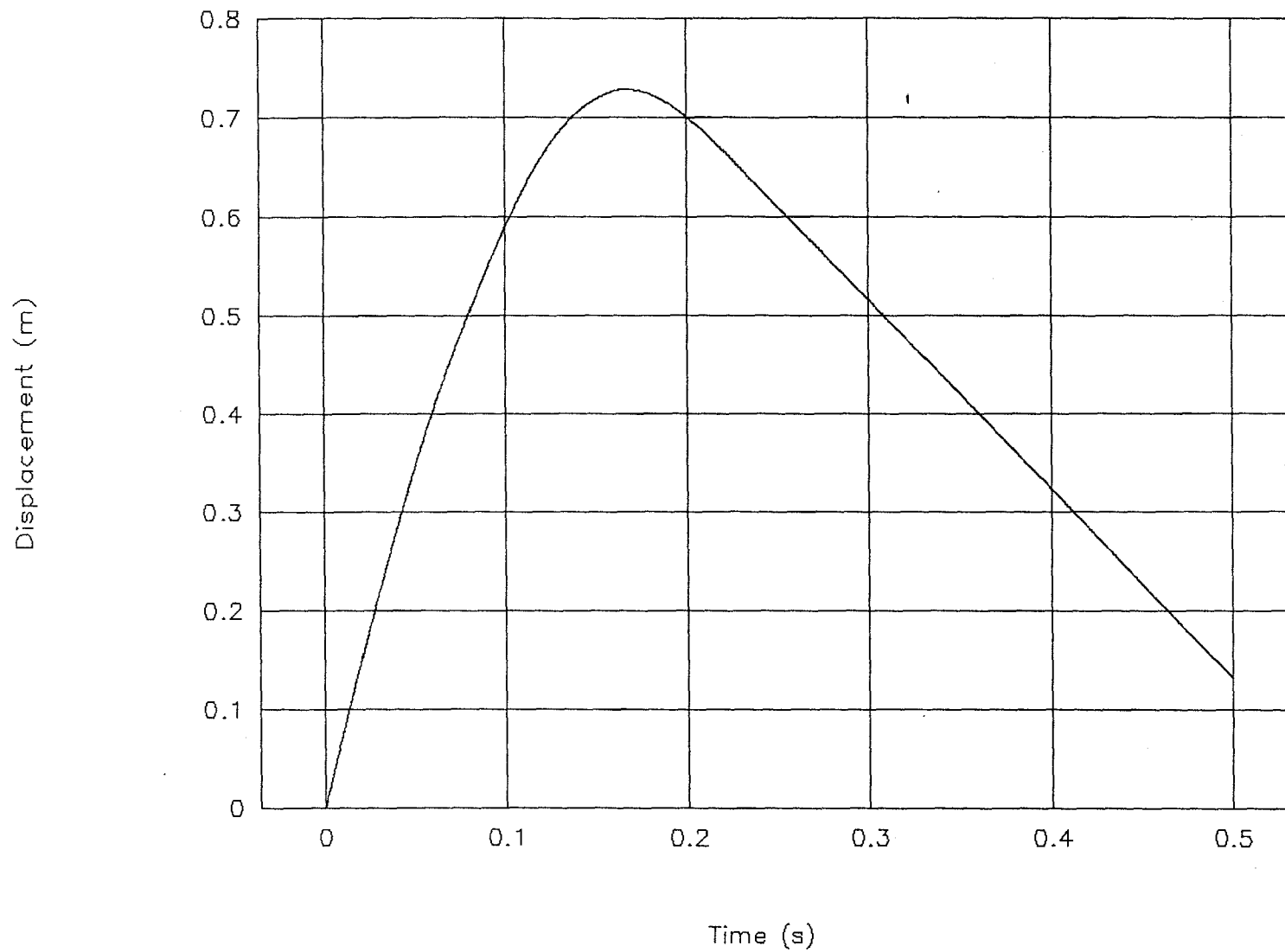


Figure 49. Displacement vs. time, test 00P012.

Test No. 00P012

Force vs. displacement

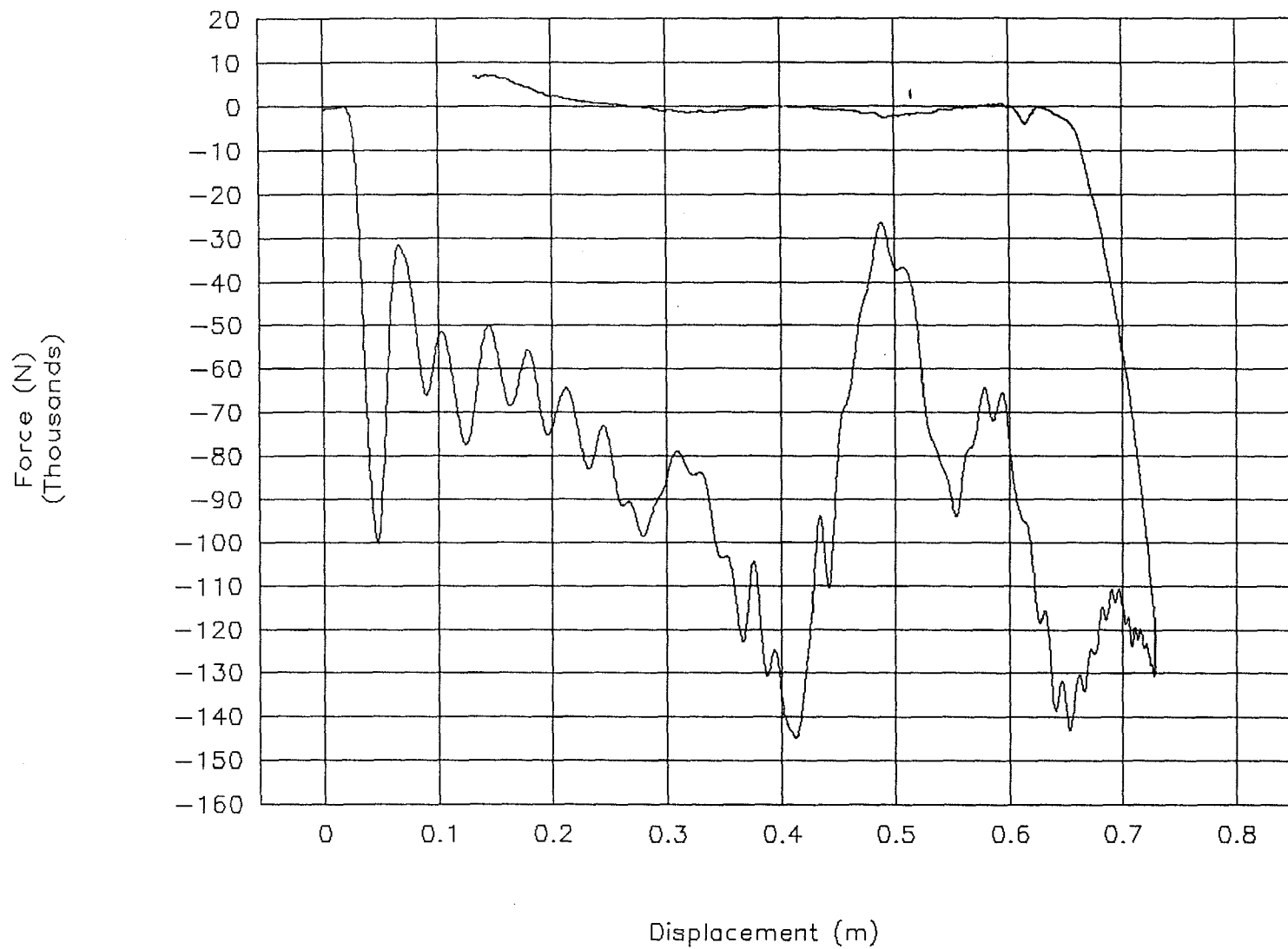


Figure 50. Force vs. displacement, test 00P012.

Test No. 00P012

Energy vs. displacement

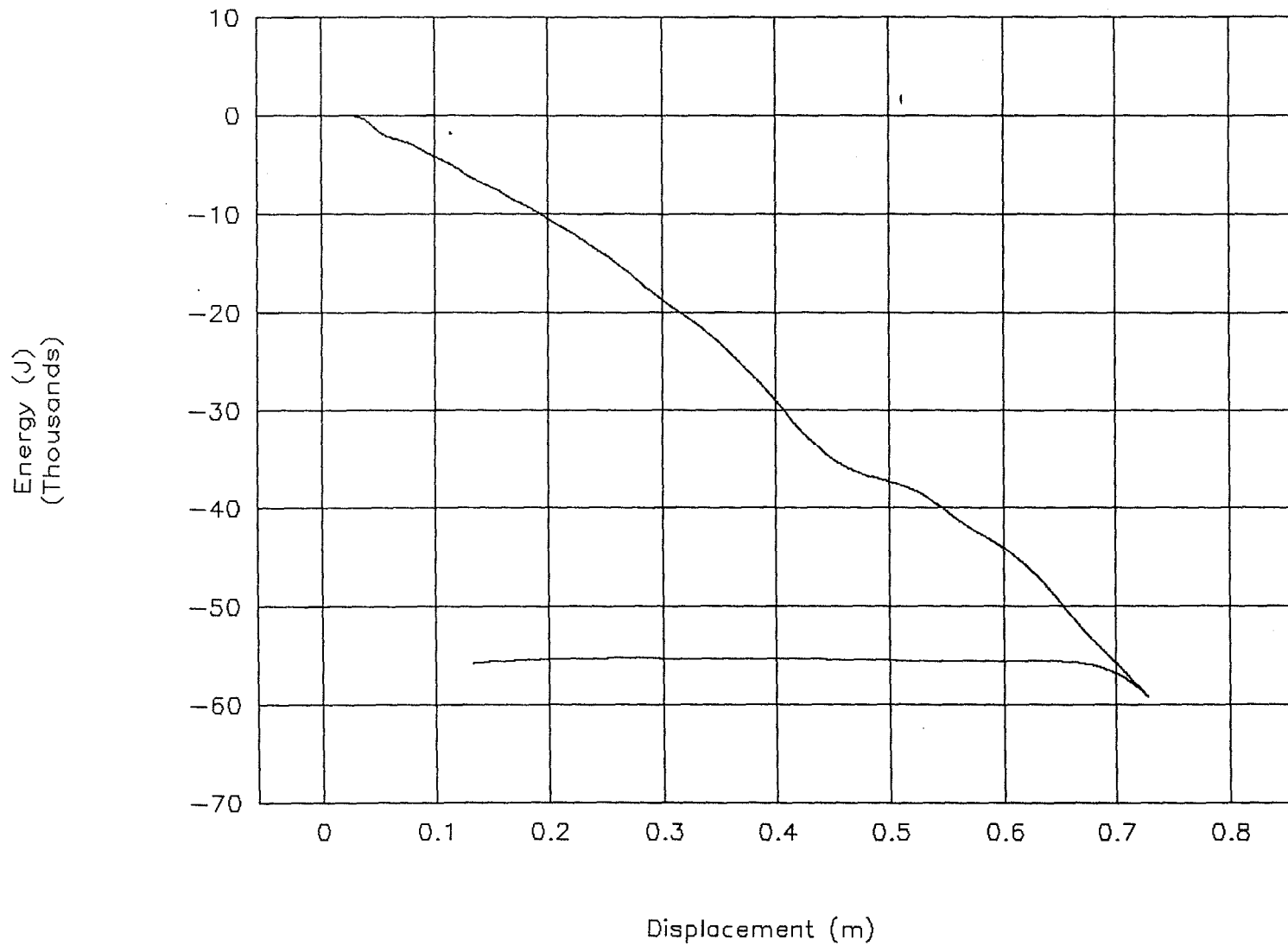


Figure 51. Energy vs. displacement, test 00P012.

Acceleration (g's)

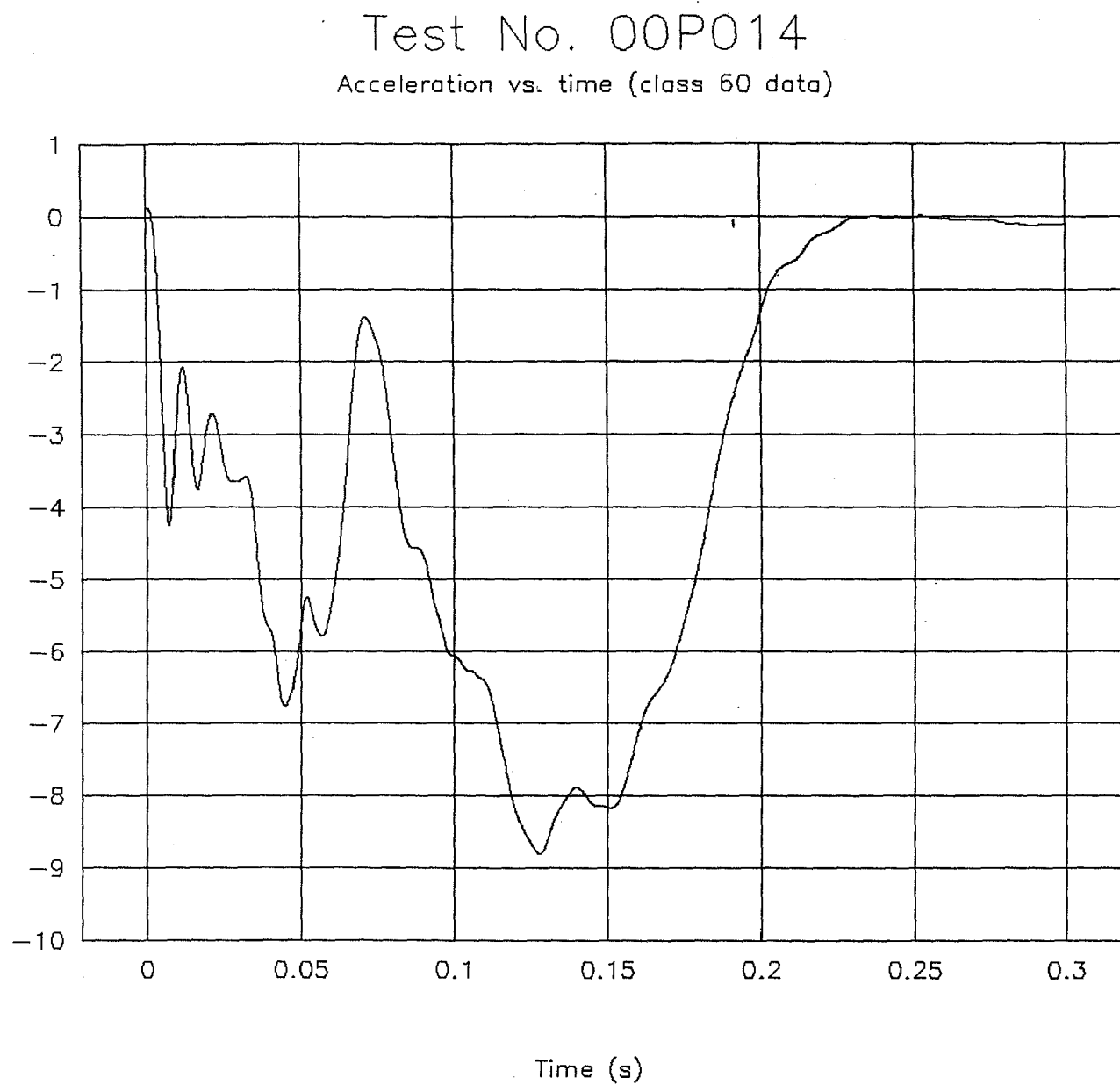


Figure 52. Acceleration vs. time (class 60 data), test 00P014.

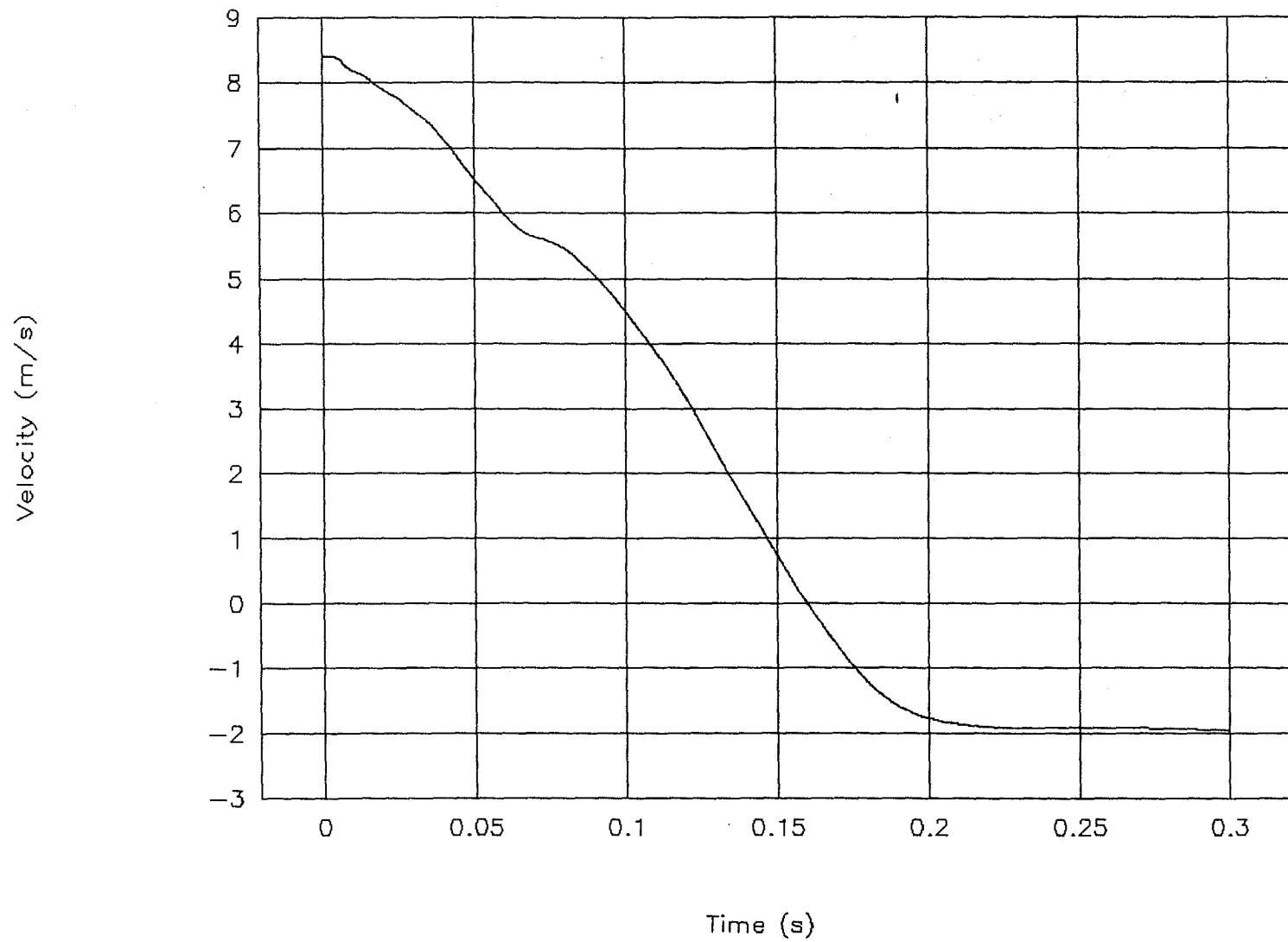


Figure 53. Velocity vs. time, test 00P014.

Test No. 00P014

Displacement vs. time

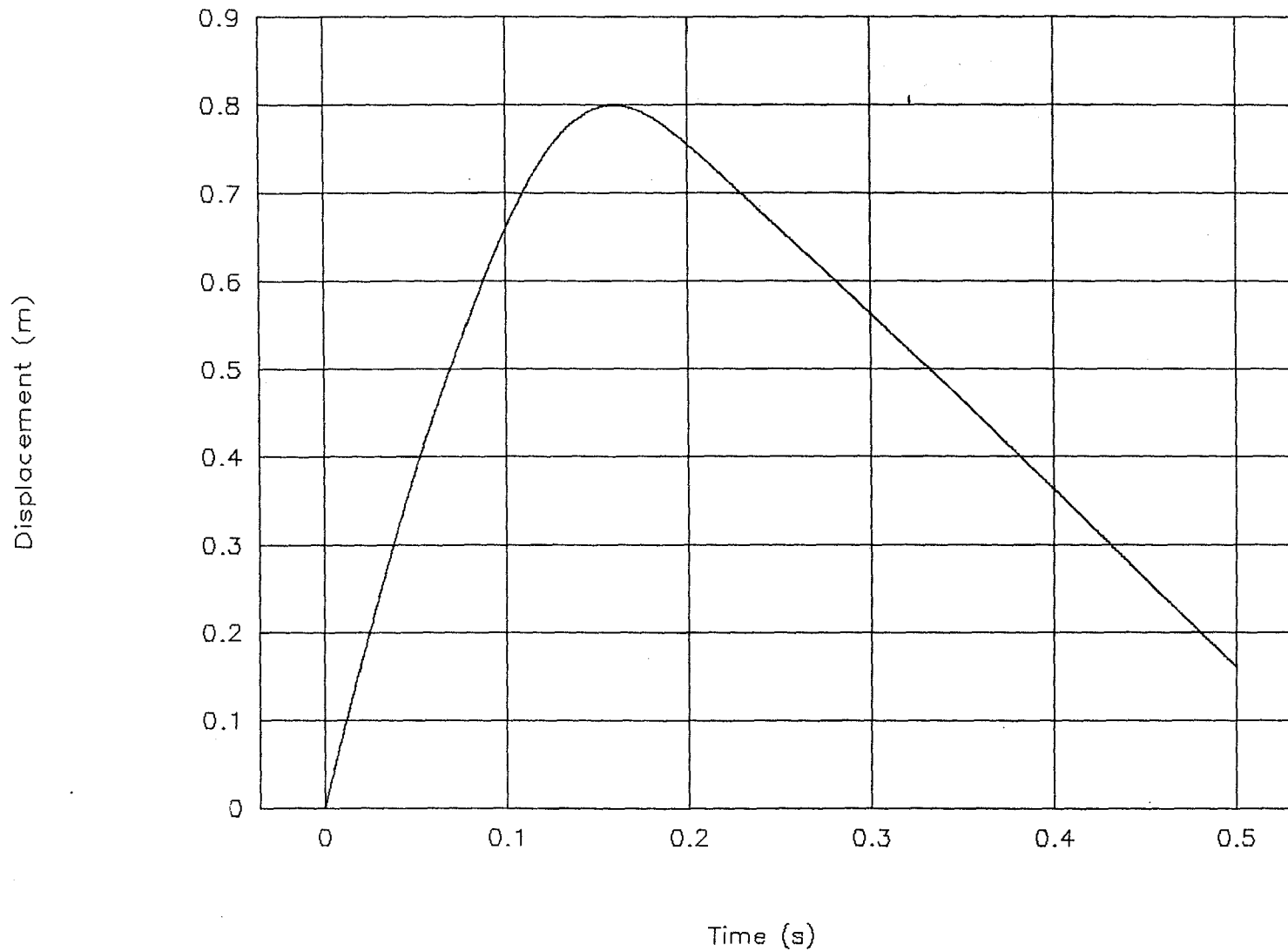


Figure 54. Displacement vs. time, test 00P014.

Test No. 00P014

Force vs. displacement

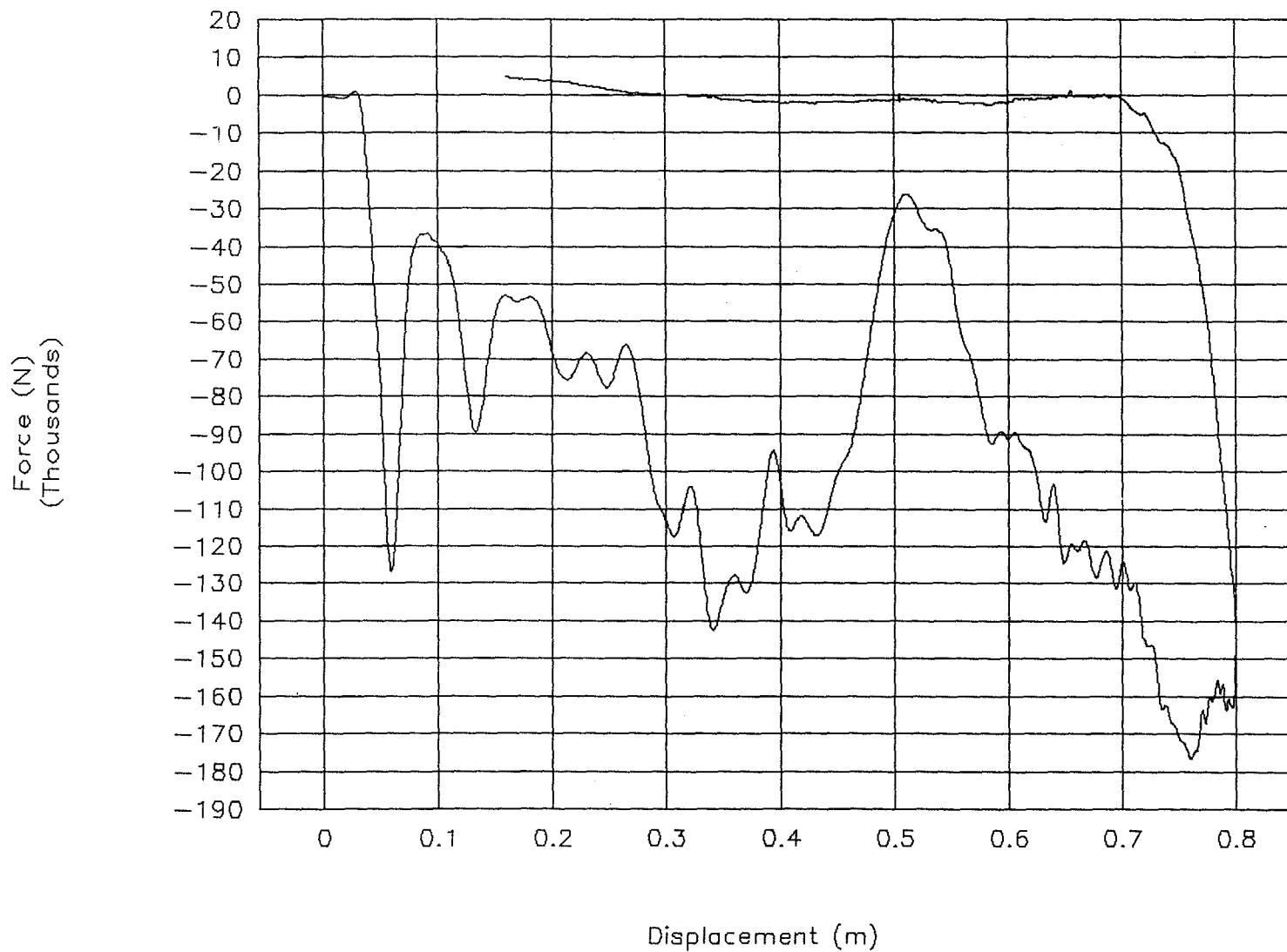


Figure 55. Force vs. displacement, test 00P014.

Test No. 00P014

Energy vs. displacement

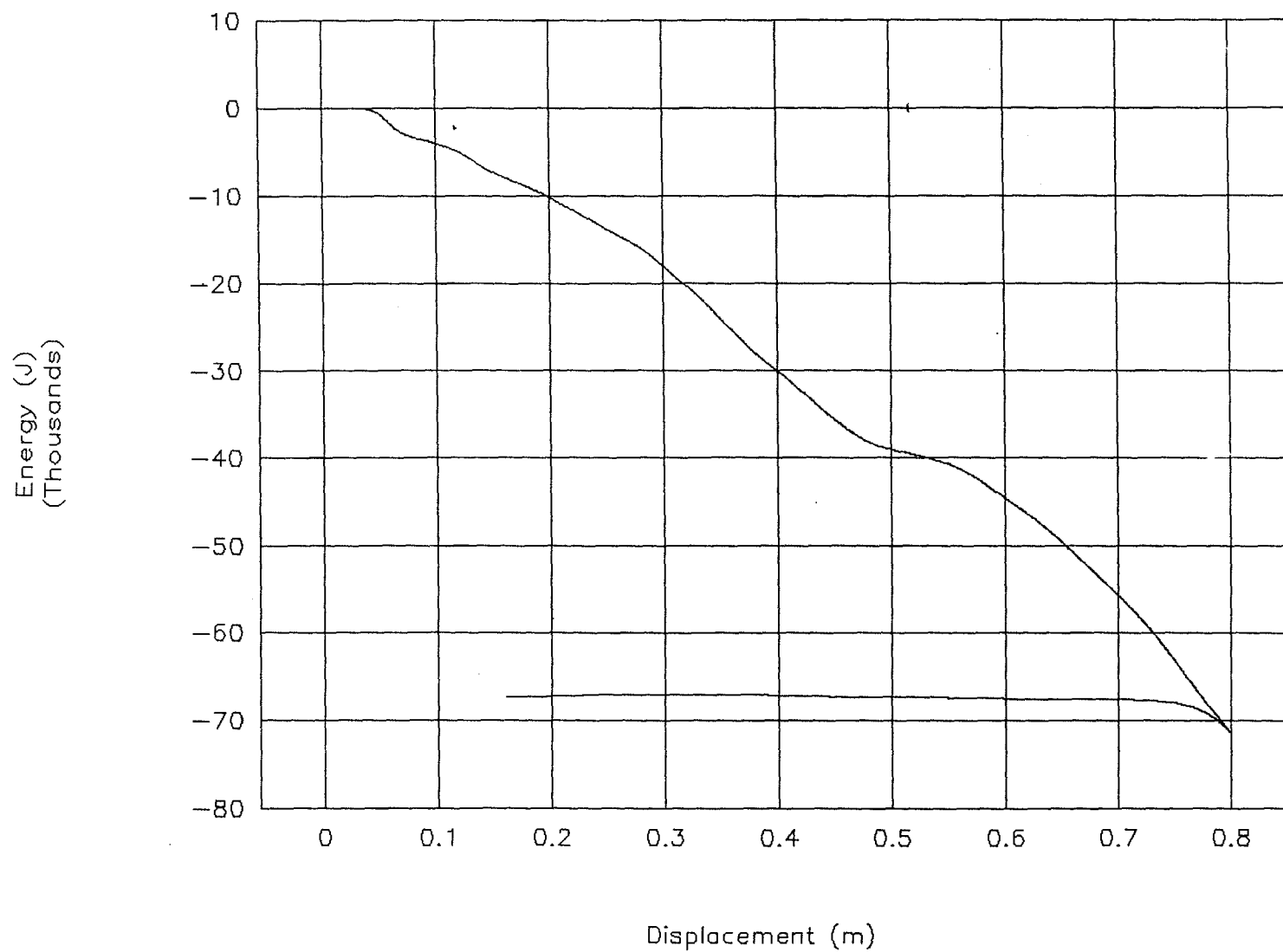


Figure 56. Energy vs. displacement, test 00P014.

Test No. 00P015
Acceleration vs. time (class 60 data)

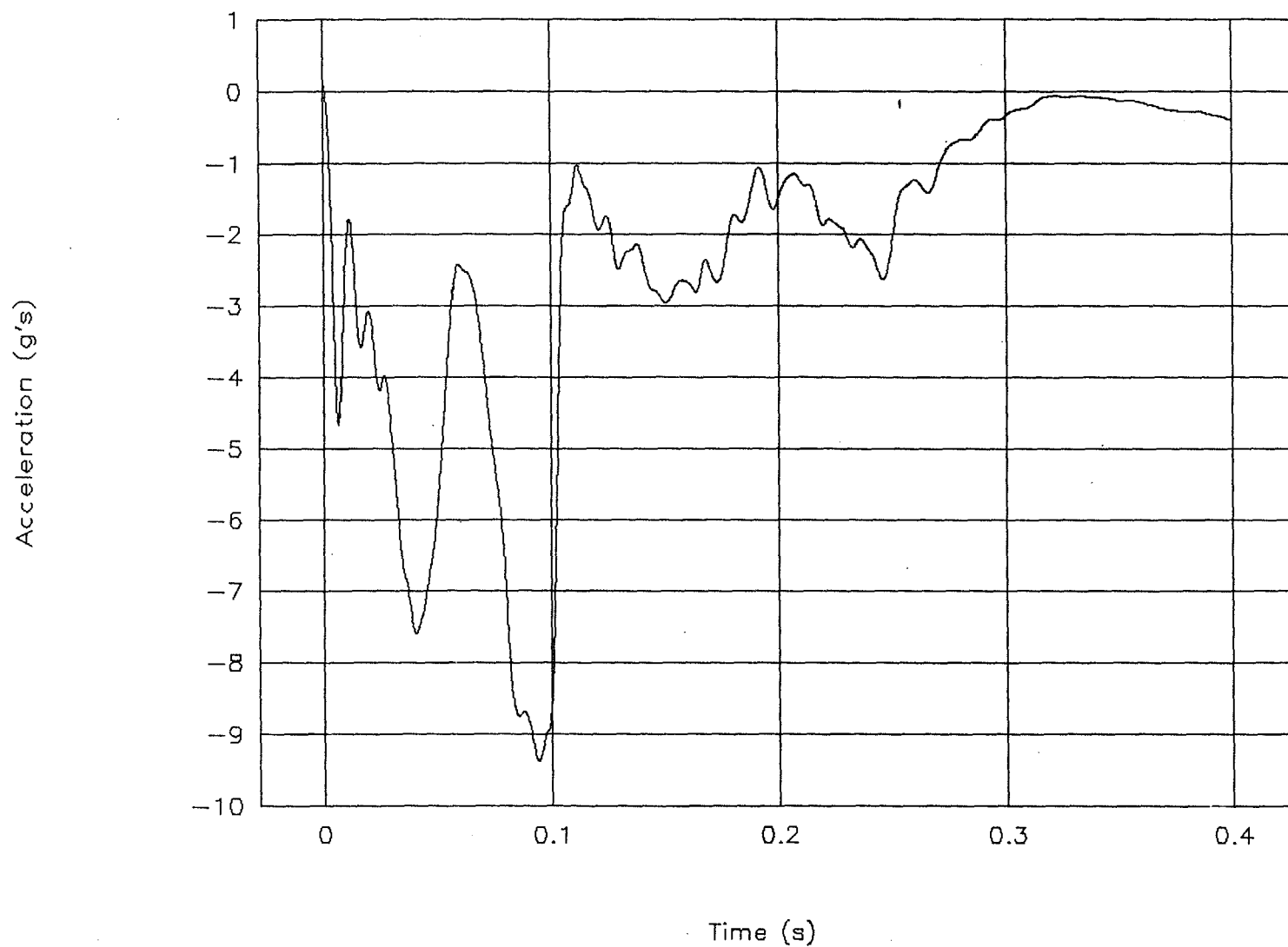


Figure 57. Acceleration vs. time (class 60 data), test 00P015.

Test No. 00P015

Velocity vs. time

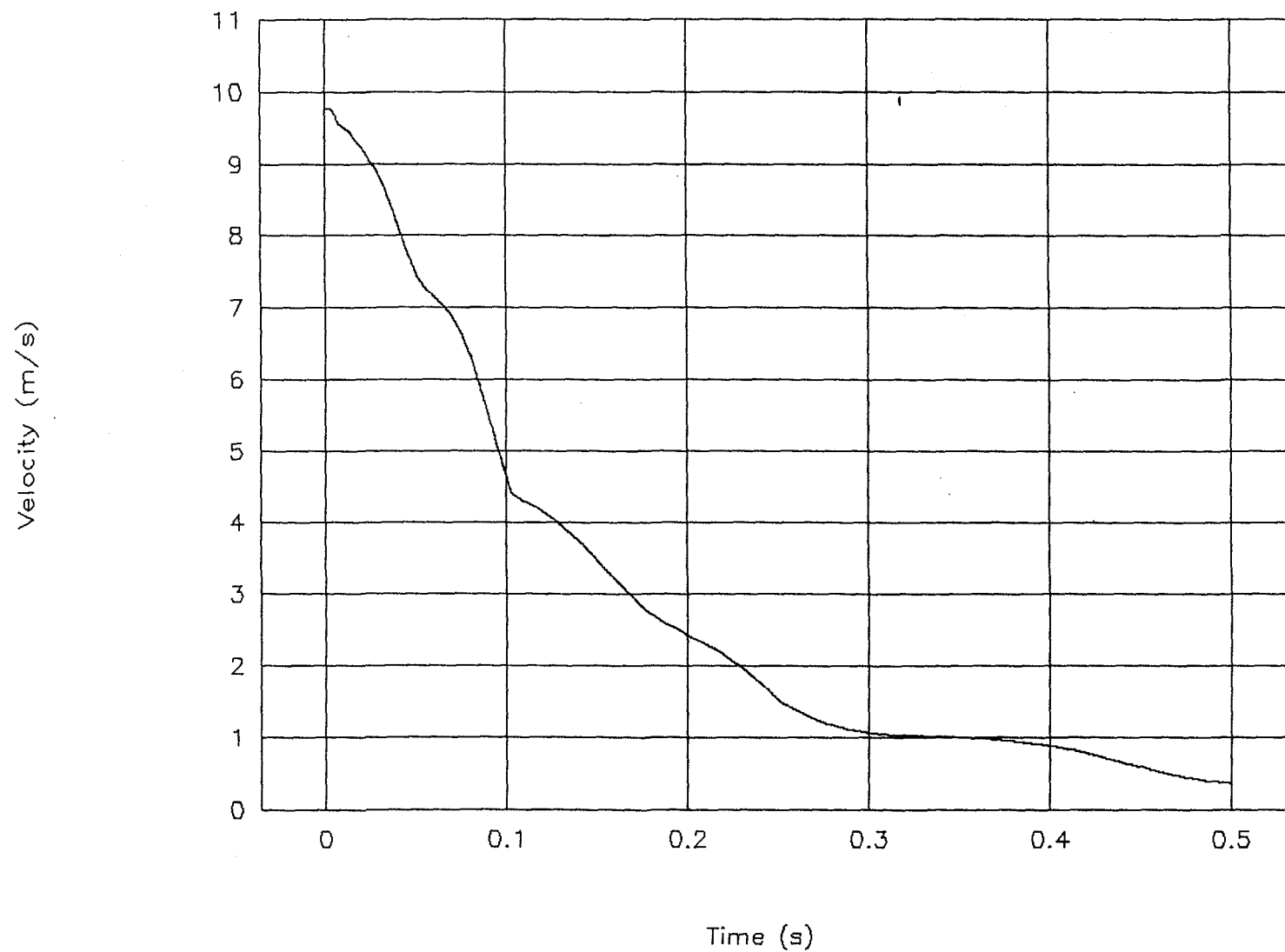


Figure 58. Velocity vs. time, test 00P015.

Test No. 00P015

Displacement vs. time

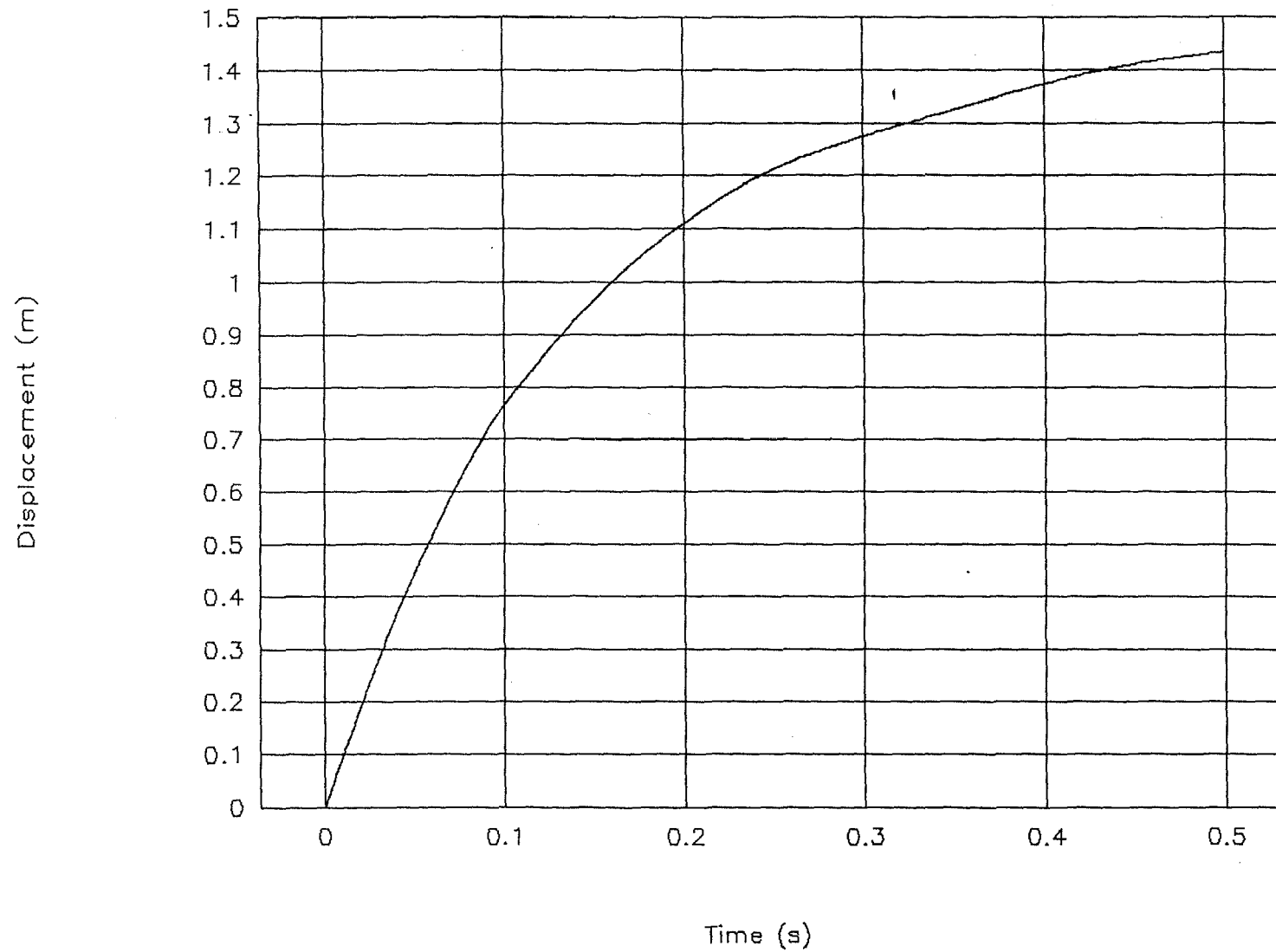


Figure 59. Displacement vs. time, test 00P015.

Test No. 00P015

Force vs. displacement

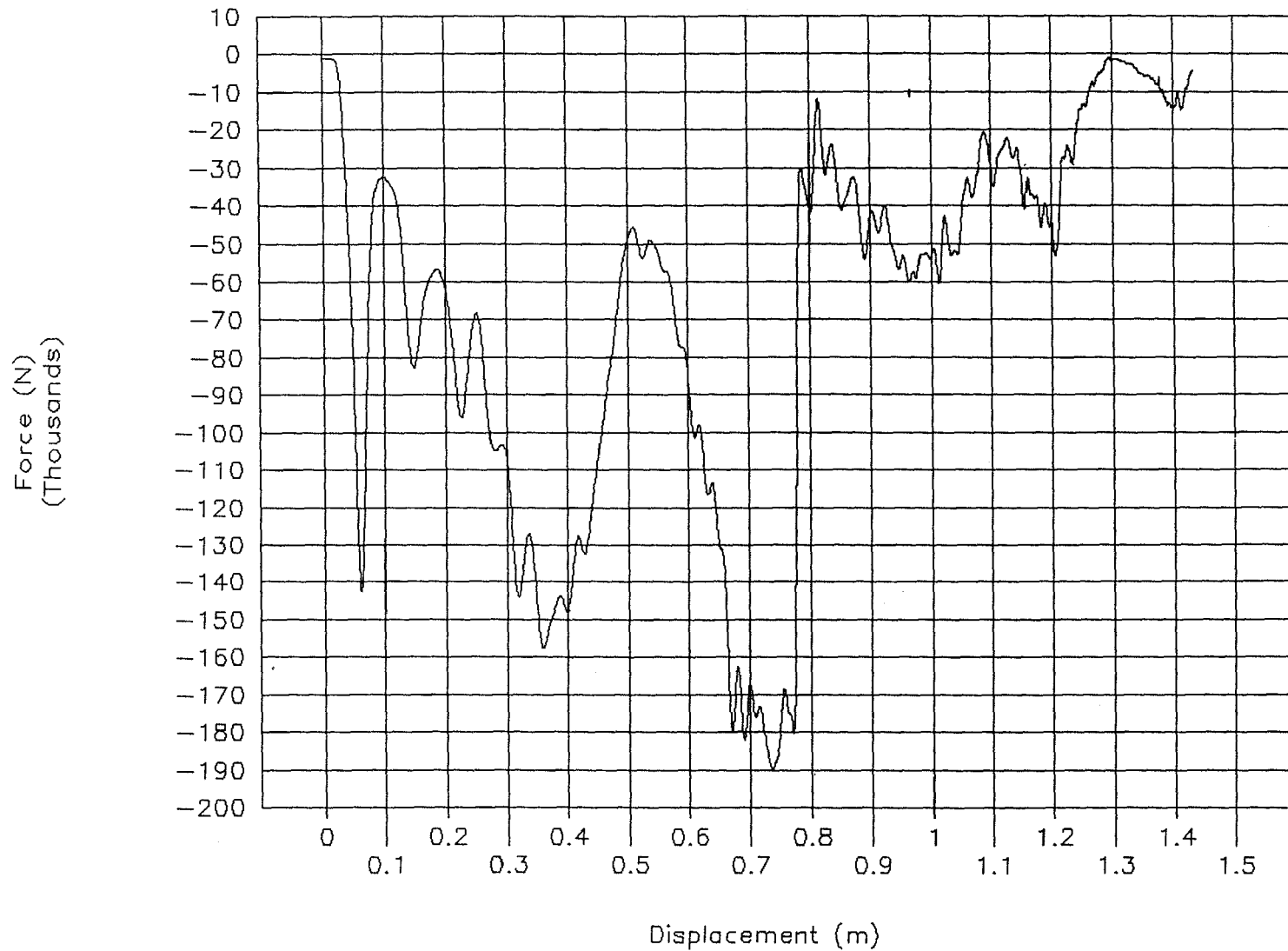


Figure 60. Force vs. displacement, test 00P015.

Test No. 00P015

Energy vs. displacement

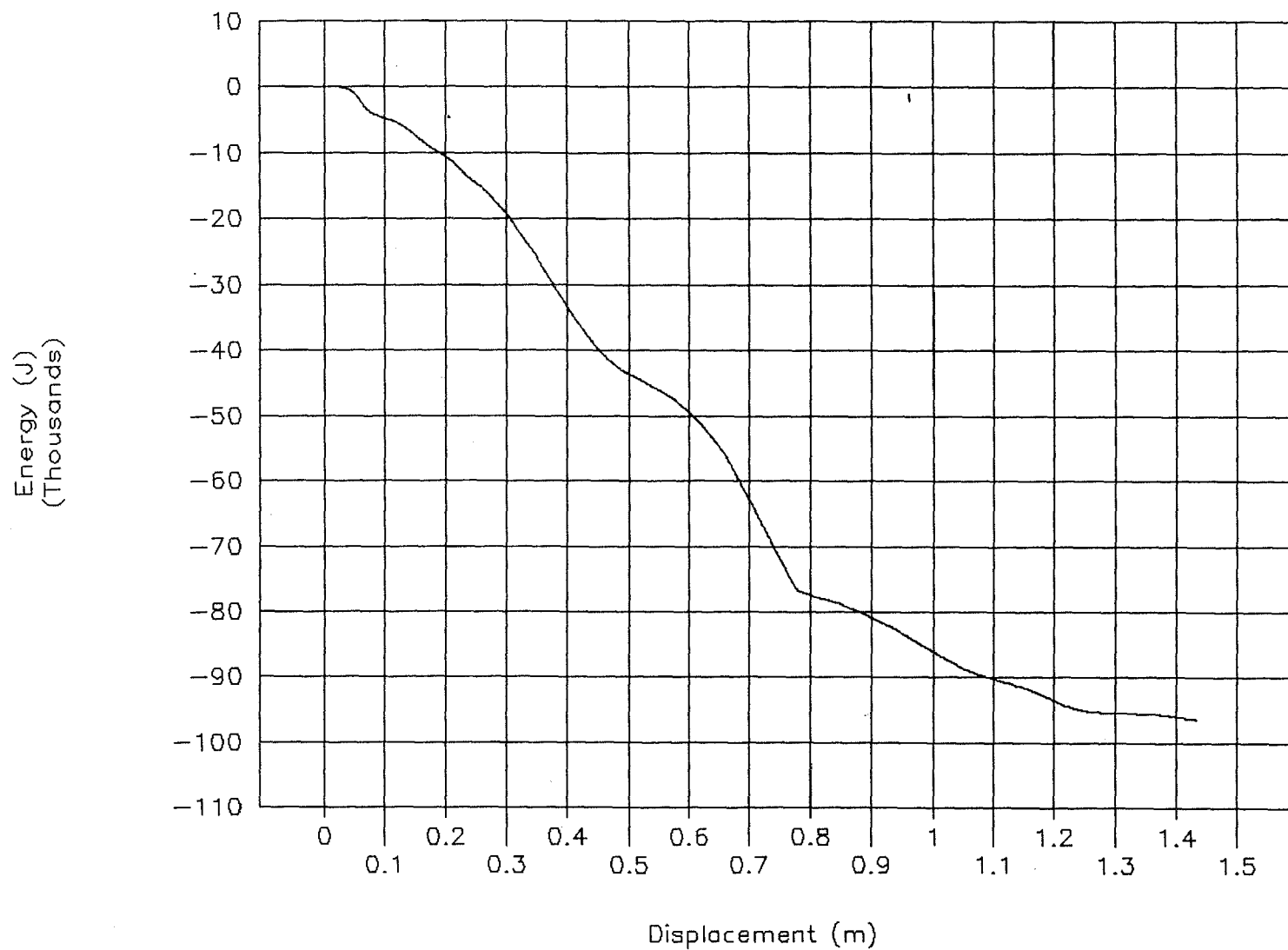


Figure 61. Energy vs. displacement, test 00P015.

Test No. 00P016

Acceleration vs. time (class 60 data)

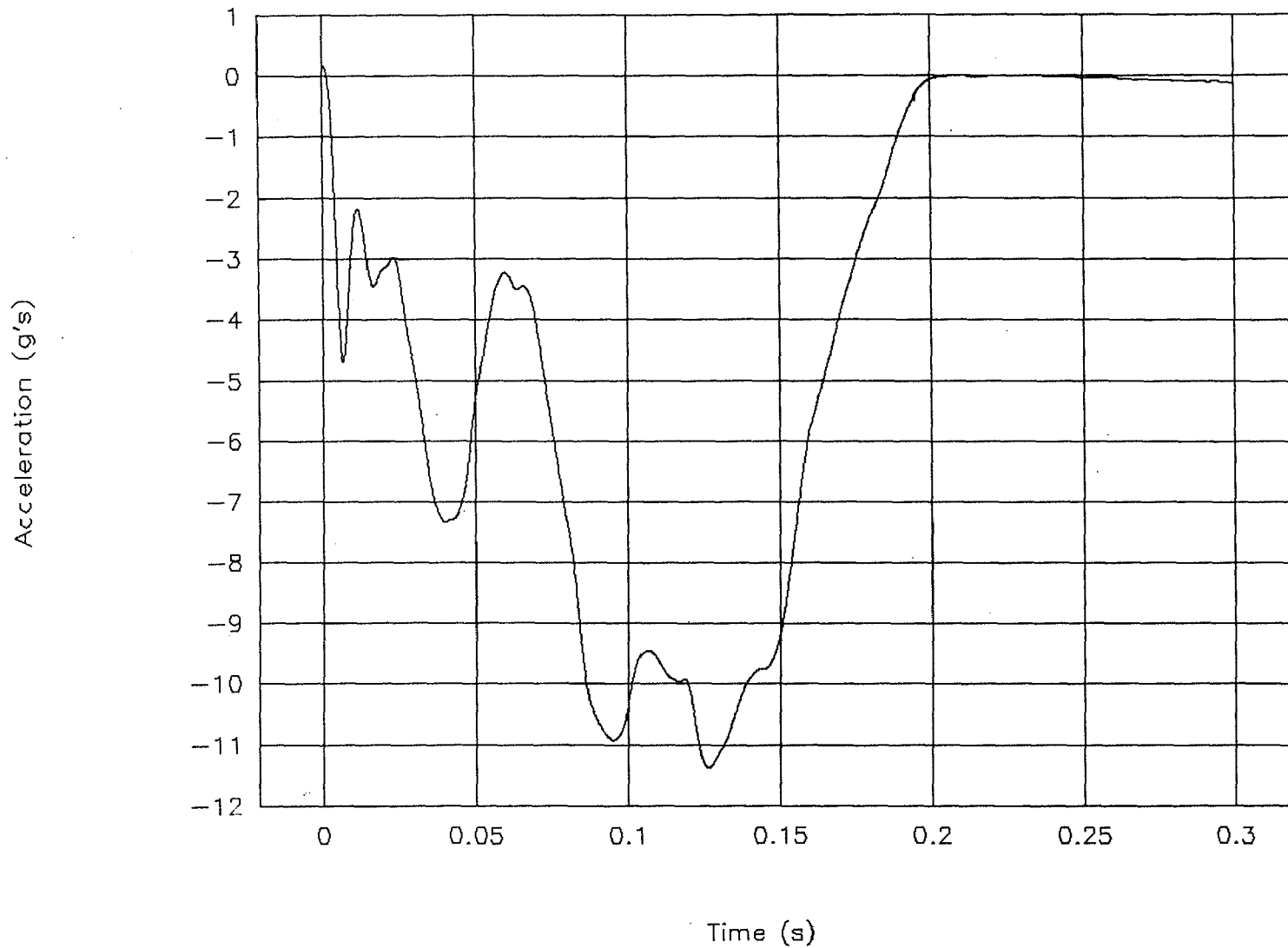


Figure 62. Acceleration vs. time (class 60 data), test 00P016.

Test No. 00P016

Velocity vs. time

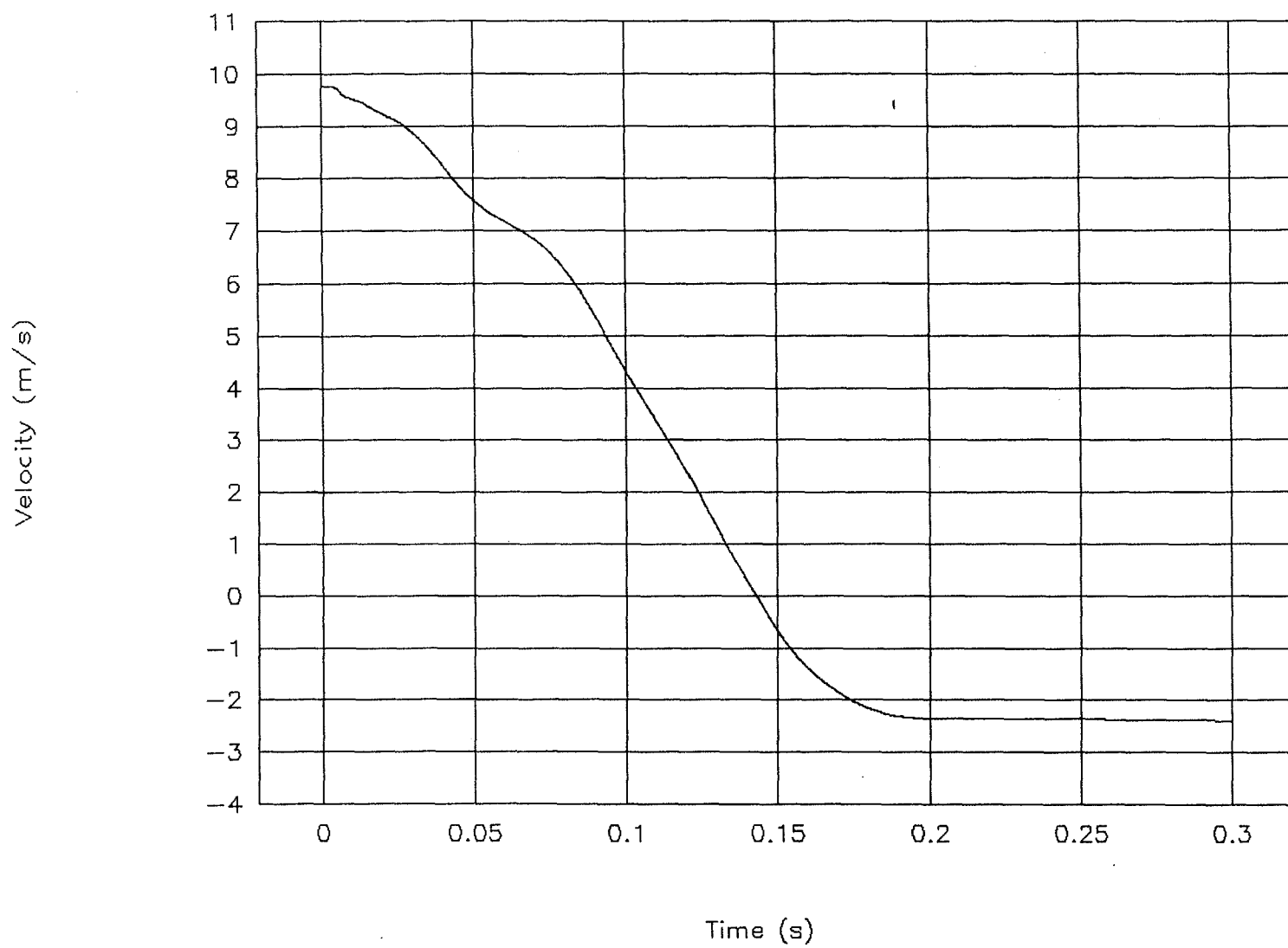


Figure 63. Velocity vs. time, test 00P016.

Test No. 00P016

Displacement vs. time

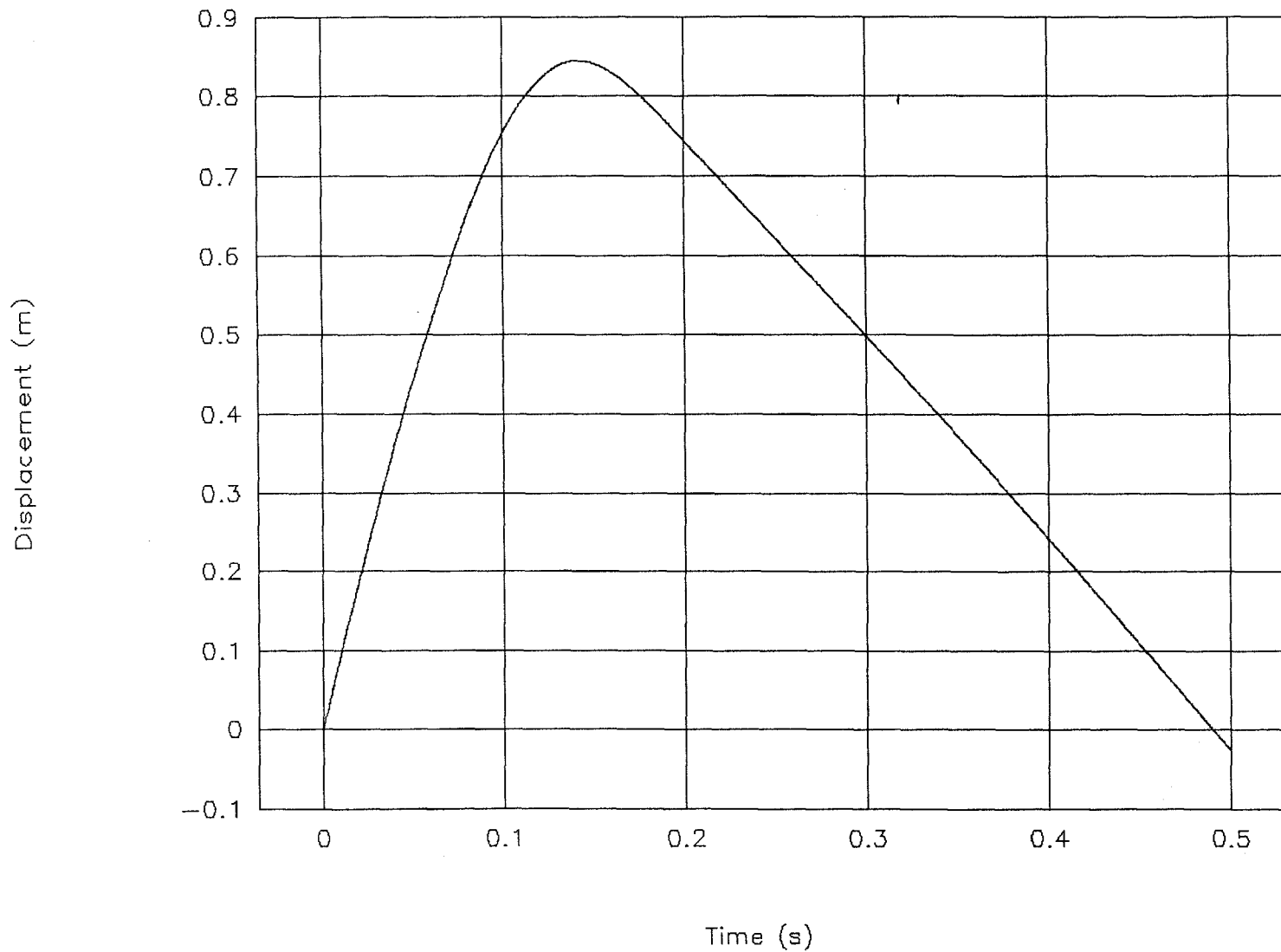


Figure 64. Displacement vs. time, test 00P0016.

Test No. 00P016

Force vs. displacement

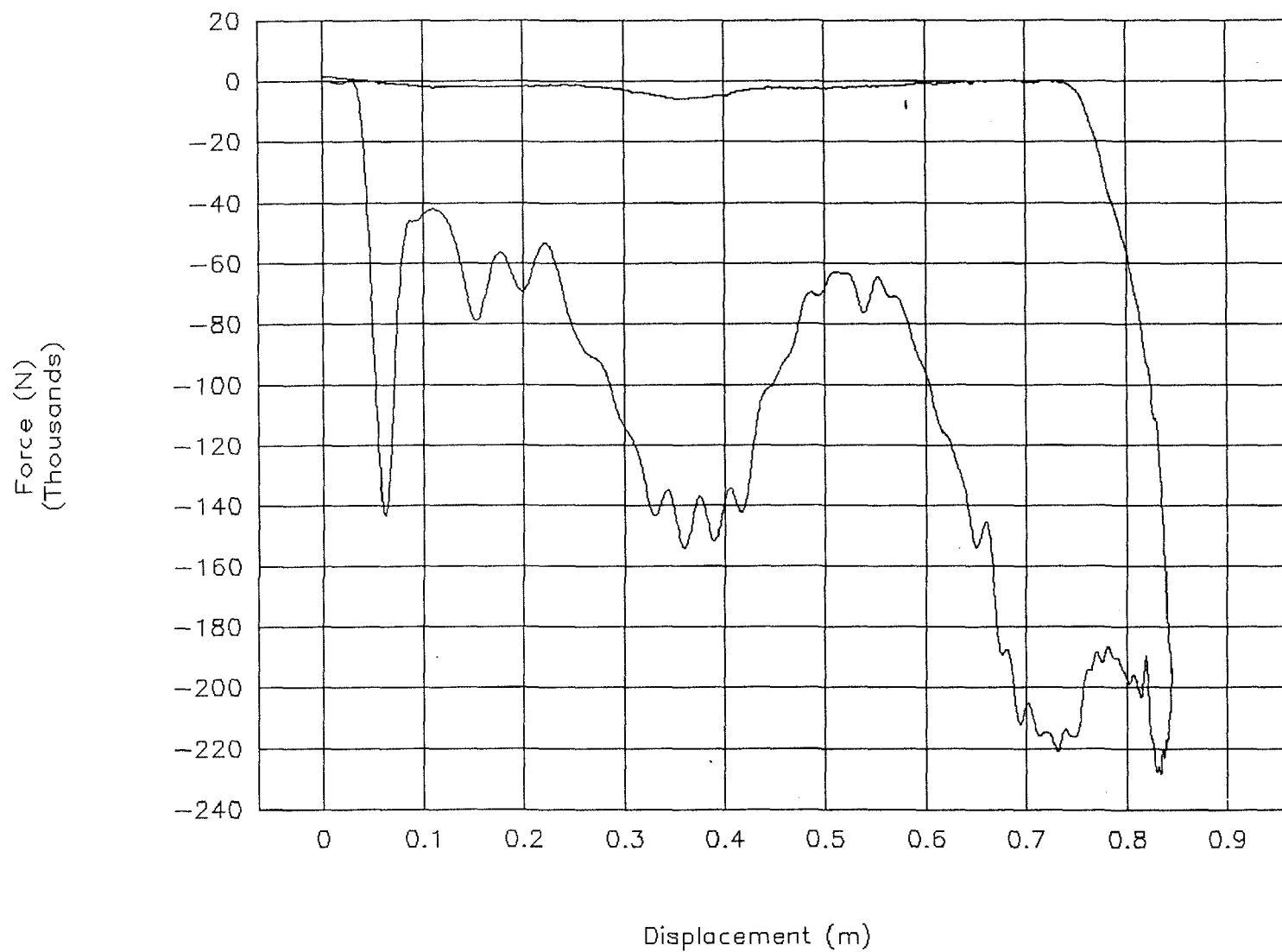


Figure 65. Force vs. displacement, test 00P016.

Test No. 00P016

Energy vs. displacement

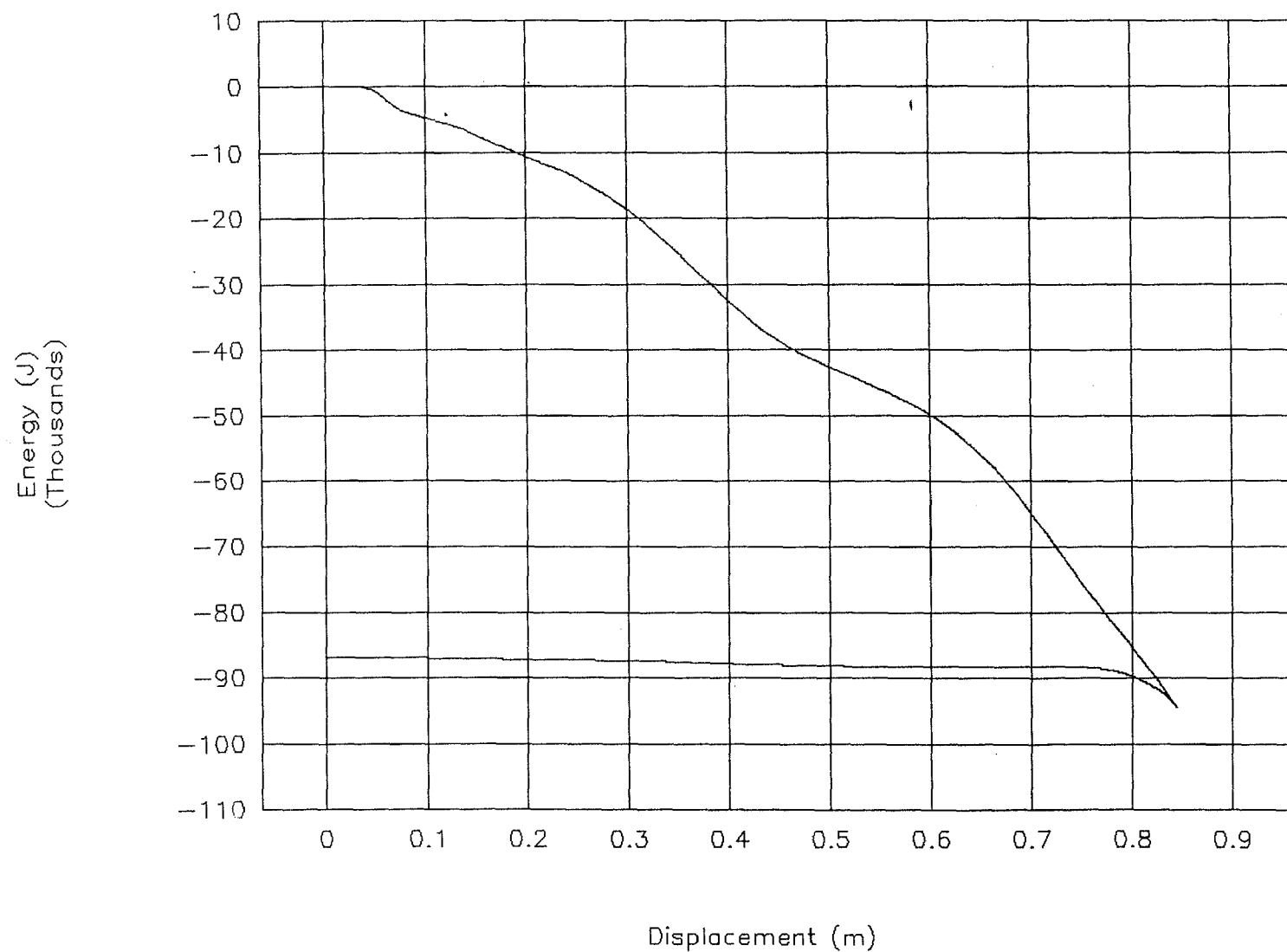


Figure 66. Energy vs. displacement, test 00P016.

Test No. 00P017
Acceleration vs. time (class 60 data)

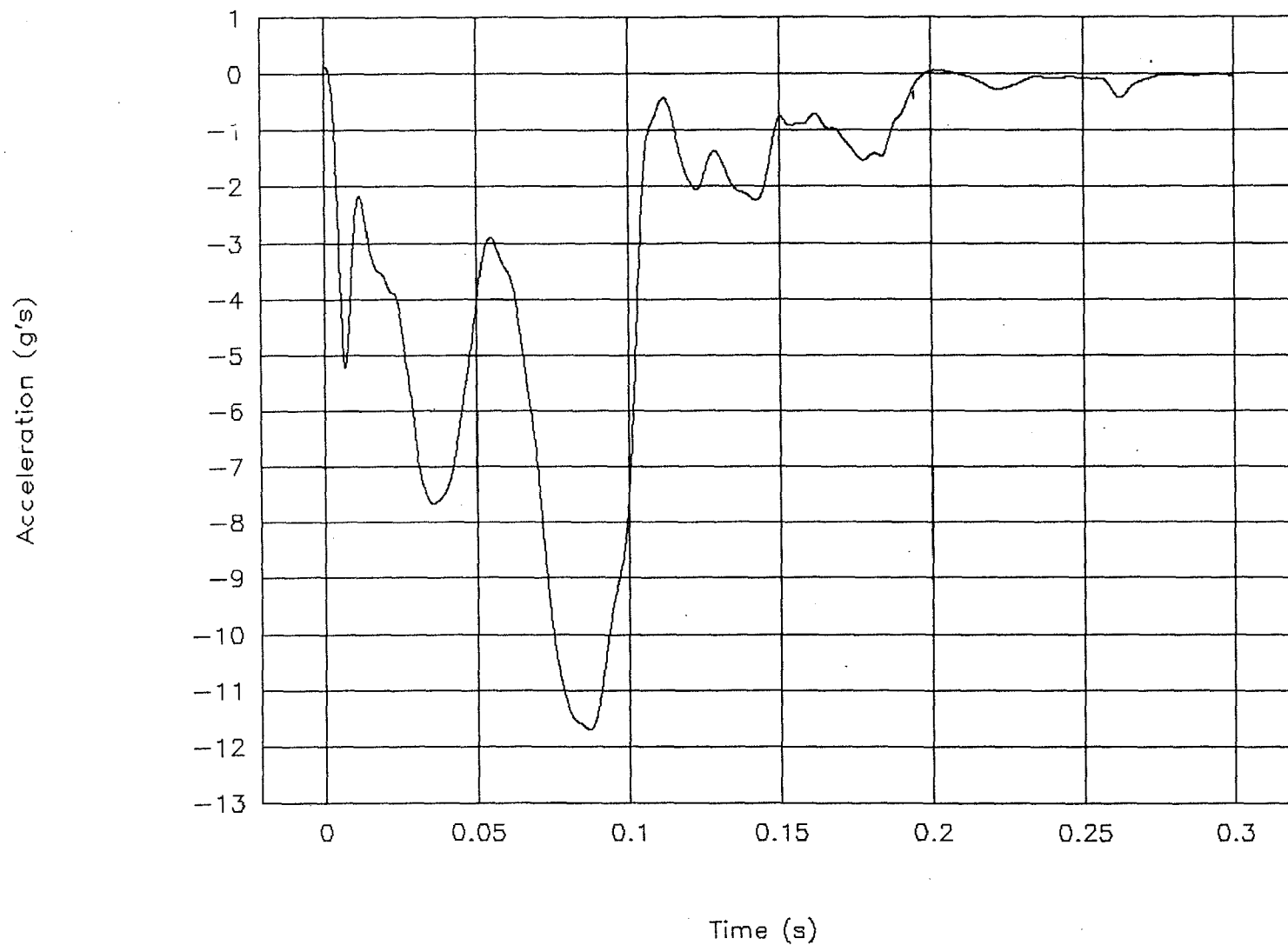


Figure 67. Acceleration vs. time (class 60 data), test 00P017.

Test No. 00P017

Velocity vs. time

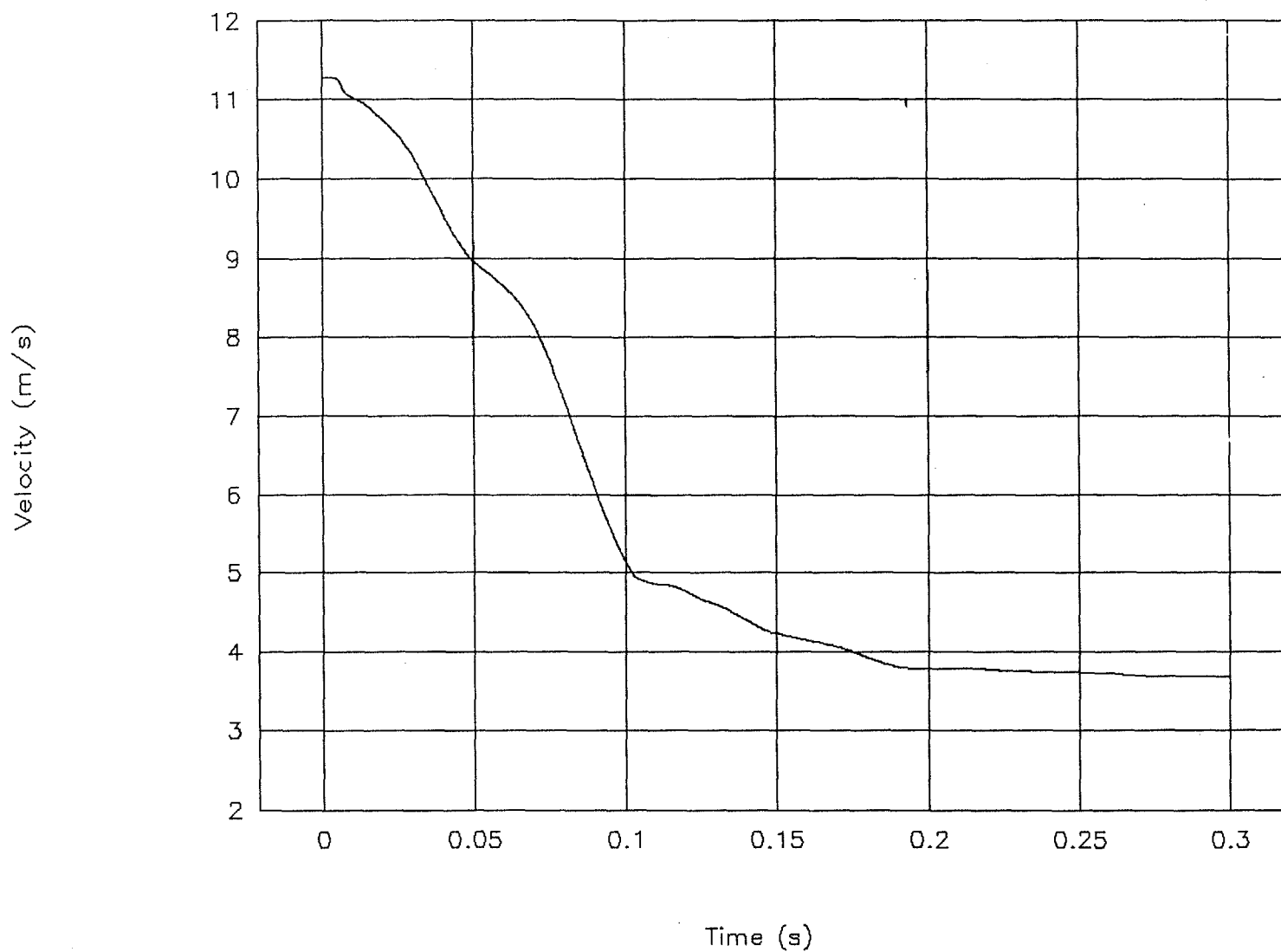


Figure 68. Velocity vs. time, test 00P017.

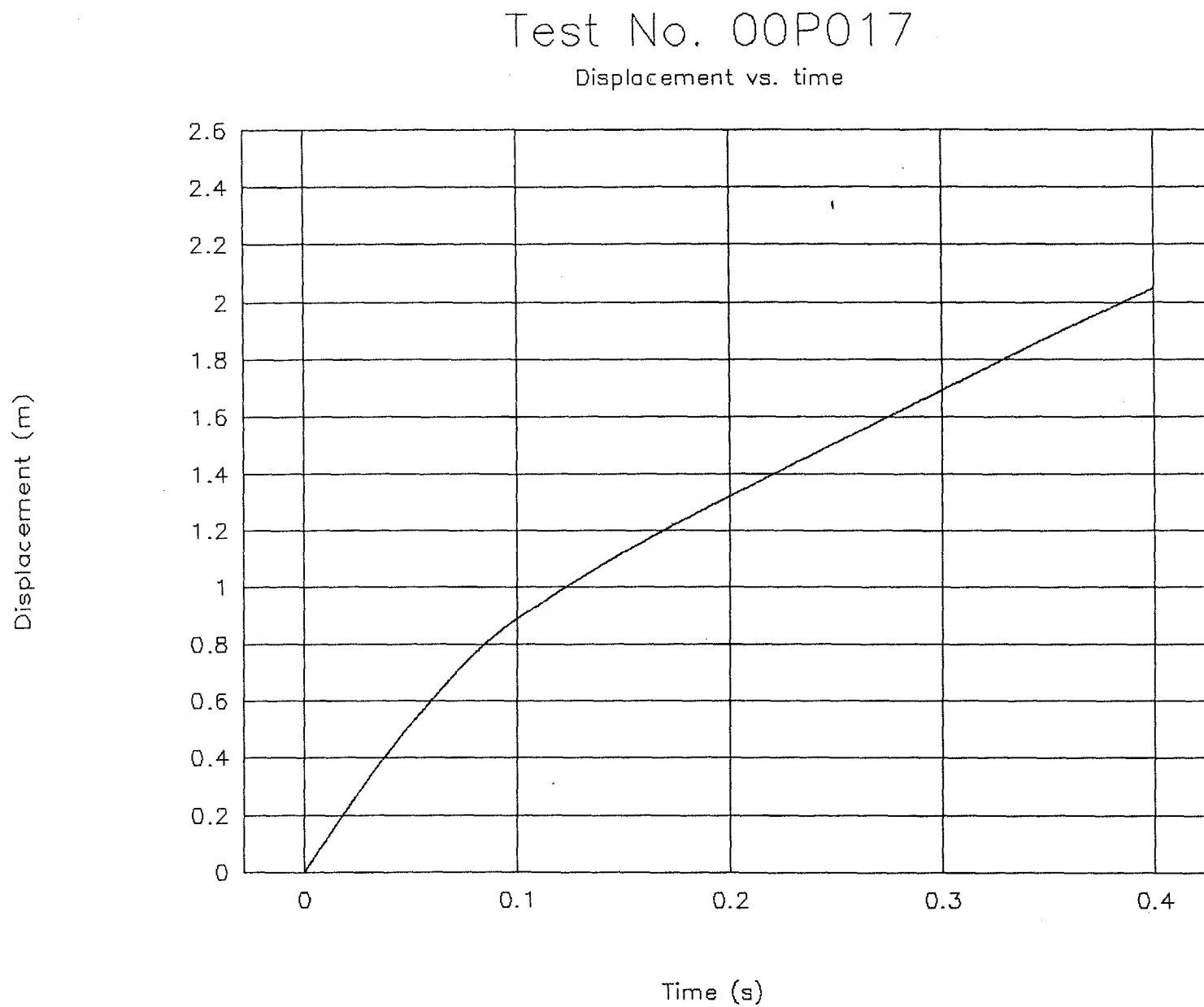


Figure 69. Displacement vs. time, test 00P017.

Test No. 00P017

Force vs. displacement

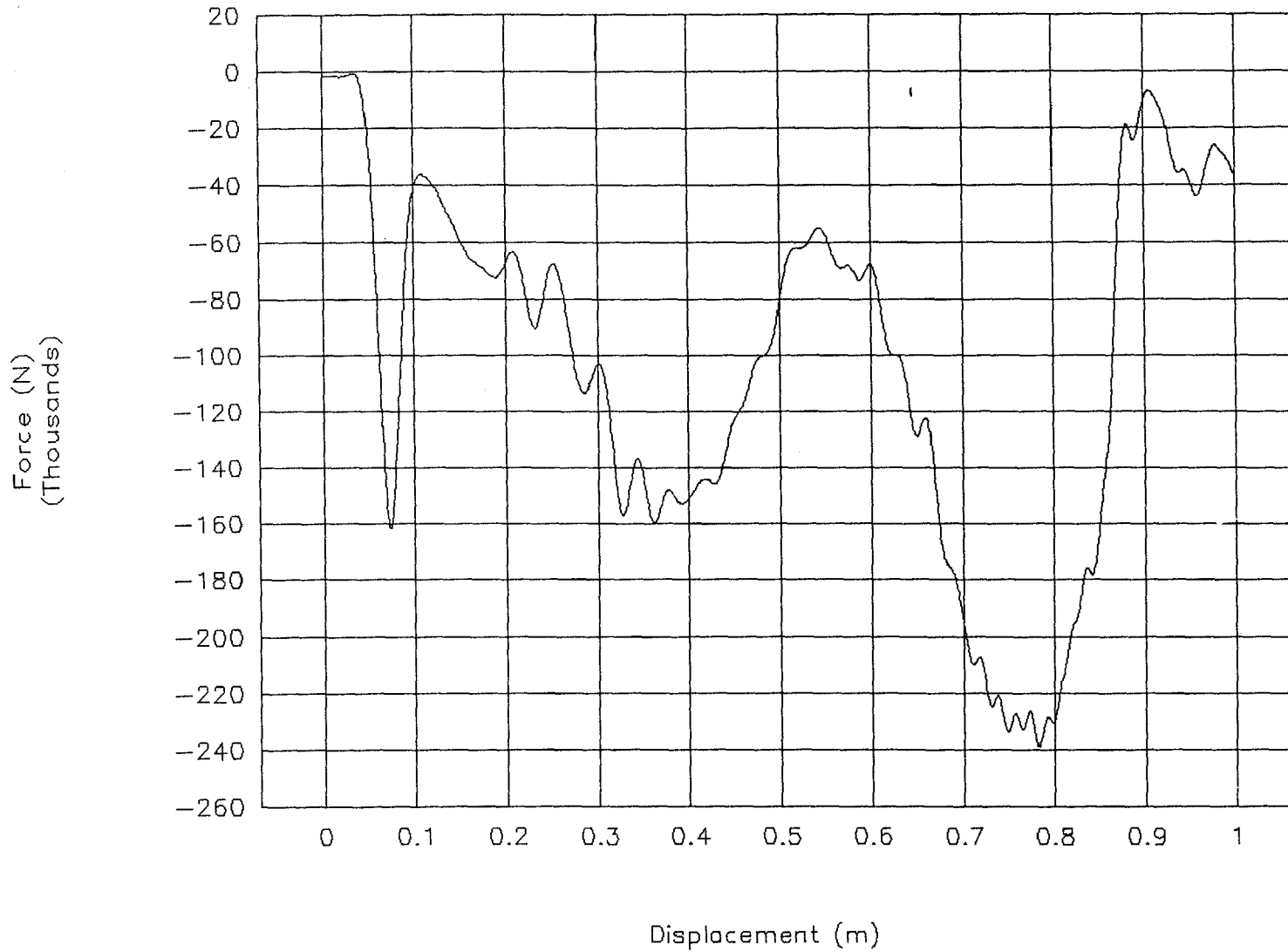


Figure 70. Force vs. displacement, test 00P017.

Test No. 00P017

Energy vs. displacement

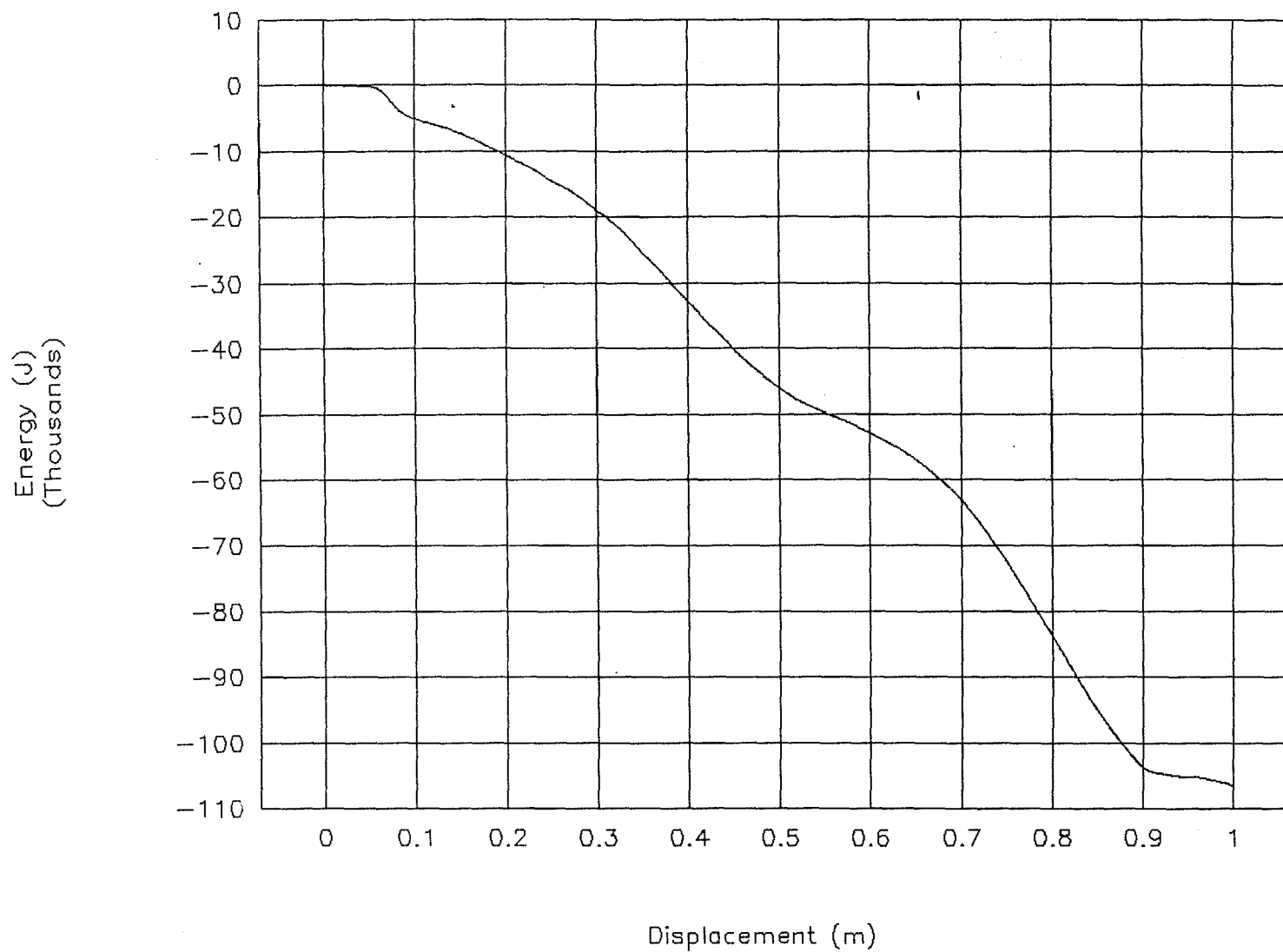


Figure 71. Energy vs. displacement, test 00P017.

